Università degli Studi di Ferrara

High-Yield Cyclotron Production of Metallic Radioisotopes for Nuclear Medicine

Dottorando
Dott. Martini Petra

(firma)

Tutori
Prof. Palmieri Vincenzo

(firma)

Prof. Duatti Adriano

(firma)

Dedicated to my beloved

Nonna Mariuccia

"*Nothing in life is to be feared,*
it is only to be understood.
Now is the time to understand more,
so that we may fear less."

Marie Curie

150 Anniversary (1867-2017)

TABLE OF CONTENTS

INTRODUCTION

The success of Nuclear Medicine in clinics lies in the possibility to develop and employ a wide range of different radiopharmaceuticals (i.e. chemical species labeled with a radionuclide), specific for the tissue biological characteristics or metabolic process under investigation. The use of radioactive isotopes in this medical application has experienced a great development as a result of the increase of technologies for radioisotopes production based on cyclotrons.

At Legnaro National Laboratories of the National Institute of Nuclear Physics (LNL-INFN) a high performance cyclotron has been installed in the SPES (Selective Production of Exotic Species) project context. SPES primary goals are focused on both basic and applied nuclear physics. In particular, the LARAMED project (LAboratoty of Radioisotopes for MEDicine) is the branch studying the cyclotron production of medical radionuclides. While the cyclotron is still not in operation, the LARAMED team started working on the cyclotron production of conventional radionuclides such as Tc-99m (APOTEMA and TECHN-OSP projects), emerging radionuclides such as Cu-67 (COME project), Sc-47 (PASTA project) and Mn-52 (just approved METRICS project) and on the development of high power target (TERABIO premium-project). The collaboration with Nuclear Medicine radiopharmacies holding a PET cyclotron (e.g. Sant'Orsola Hospital, Bologna, IT), national and international research institute, such as JRC-ISPRA (Varese, IT) and ARRONAX (Nantes, FR), made all this possible. A medical radionuclide cyclotron production study involves different interdisciplinary skills ranging from nuclear physics, engineering, material sciences, radiochemistry, biology and so on. Therefore, the team LARAMED has been divided in tasks to accomplish all related skills: target production, spectrometry and imaging, target processing, etc..

The aim of my PhD has been the contribution to all LARAMED's satellite projects mainly in the post-irradiation target processing tasks, one of the most critical steps in the production of radioisotopes. The adoption of target processing is not only mandatory for radionuclides medical applications but it is also advantageous for nuclear data research, such as cross-section studies, preliminary investigation on reactions yields, characterization of reaction products, etc..

In this thesis I'm going to present the work done in the framework of TECHN-OSP (Tc-99m) and COME (Cu-67) projects. In addition, my collaboration experience at

TRIUMF (Vancouver, CA) with the Life Sciences division on two more projects (i.e. Tc-99m cyclotron production and Ga-68 liquid-target cyclotron-production) is here described as well.

The TECHN-OSP project is based on the study of technetium-99m (^{99m}Tc) alternative production routes given that the possibility of a reactor-produced molybdenum-99 shortage, used as parent nuclide of in ^{99}Mo/^{99m}Tc generators, is still a potential scenario. The direct cyclotron-production of Tc-99m through the (p,2n) reaction on a Mo-100 target seemed to be one possible solution. On this topic, the description of TECHN-OSP experiments, performed in collaboration with the Sant'Orsola Hospital, are well detailed. In particular, I developed an automatic separation and purification module, based on solvent extraction, that allowed the recovery in high yield of high purity Tc-99m from the Mo-100 target. This technology was developed together with a designed target, optimized irradiation and target recovery for an in-hospital cyclotron self-production of Tc-99m to afford the availability of the most used radiometal in diagnostic applications in case of shortages.

With the aim to scale-up and validate an alternative Tc-99m production and purification method, the TRIUMF research group is also working on Tc-99m cyclotron-production. When I was there, I had the opportunity to collaborate at the project named "A Trans-regional initiative to achieve large scale production, distribution, supply and commercialization of Tc-99m" by contributing at the optimization and automation of molybdenum target dissolution and purification procedure of cyclotron-produced Tc-99m. A comparison between the two developed, Italian and Canadian, target processing setup is also reported.

The context of COME project is slightly different from the previous one since, even if final purpose is still the radiometal medical application, the state of the project is limited at the evaluation of the cyclotron production efficiency. Cu-67 is particularly interesting for its application in theranostics (a new branch of nuclear medicine joining either diagnostic and therapy). The large scale cyclotron-production of this radiometal is still a poorly studied key point and for this reason we started working on unknown cross-section measurement of nuclear reactions on a Zn-70 target (35-70MeV energy range) to define the best production route of Cu-67, hopefully finding a way to make this radionuclide available in larger amount to the scientific community. Essential for this project was the development and optimization of a

8

high yield separation and purification procedure of Cu-67 from the Zn-70 bulk and the co-produced Ga-67 contaminant that, having the same γ-lines of Cu-67 (both decay to Zn-67 with similar half-lives), poses a serious issue for the determination of the activity of Cu-67. The description of the experiments, performed in collaboration with ARRONAX, is here reported while the cross-section results are still under elaboration.

Finally, the clinical needs of larger amount of the PET radiometal generator-produced Ga-68 prompted TRIUMF Life Sciences division to investigate Ga-68 cyclotron-production from liquid target since it is based on the existing medical-cyclotron network and technology. This technique will improve the availability of Ga-68 in hospitals housing an appropriate cyclotron by making them independent self-producers. Since the major problem affecting liquid targets is the contamination with radioactive/stable metals (e.g. iron) coming from the dissolution of some material from vacuum isolation or target body components during the irradiation, a separation and purification procedure together with a semi-automatic system, particularly focused on the purification of Ga-68 from Zn and Fe, have been developed. The main purpose is to obtain a final product suitable for medical use and to enable radiolabeling and in-vivo imaging studies with cyclotron produced ^{68}Ga-DOTATOC.

1 RADIOMETALS FOR NUCLEAR MEDICINE

Nuclear Medicine is a branch of medicine focused on the use of radioactive substances for diagnostic and therapeutic applications emitting (Qaim, 2001):

- γ or β$^+$ radiation for diagnostic purposes to visualize tissue and anatomic structure displaying functional or metabolic anomalies thanks to the high detection sensitivity;
- β$^-$ or α radiation for therapy through the biological effects of radiation.

Nuclear Medicine, differently from other diagnostic procedures providing morphological information such as Radiography, Ultrasound and Nuclear Magnetic Resonance since, it provides also organ's biochemical and physiological functional information by means of radiopharmaceuticals (Kovalsky & Falen, 2004). Radiopharmaceuticals are medicinal products that combine nuclear properties of a radioactive isotope and pharmacological properties of molecules properly linked to the isotope thanks to special synthesis process called "Labeling".

In this medical field, physics and pharmacology cooperate to provide a wide selection of radiopharmaceuticals. However, the physiological environment in which radiopharmaceuticals shall operate, the human body, foresees rigorous selection criteria making most of them unusable for nuclear medicine application. Moreover, the choice of the proper radioisotope is also based on production easiness, costs, and prompt availability.

In general, nuclides employed for diagnostic purposes should: emit only low energy gamma radiations; have a less than 24 hours' half-life (enough long to allow the radiopharmaceutical preparation but short enough for minimizing the adsorbed patient dose); have a wide chemistry to label carrier molecules to form radiopharmaceuticals stable both *in vitro* and *in vivo*. There are two kinds of radionuclides involved in diagnostic procedure, those that directly decay by emitting gamma rays, involved in Single Photon Emission Computed Tomography (SPECT), and those that decays by positron emission and that subsequently undergoes annihilation with an electron and emission of two gamma ray at 511keV at 180 degrees to each other, involved in Positron Emission Tomography (PET). Longer half-life radionuclides (i.e. Zr-89, $t_{1/2}$ = 78 h, $E_{\beta+,mean}$= 395.5 keV; Mn-52, $t_{1/2}$ = 134.4 h, $E_{\beta+,mean}$ = 242 keV) can be employed in imaging studies with slowly-accumulating

bioactive molecules such as immuno-PET with monoclonal antibodies (Graves, et al., 2015 ; Jauw, et al., 2016).

On the other hand, nuclides employed for therapy should has high energy β^- or α emission able to destroy cells responsible for pathologies (see section 1.2).

Unfortunately, there are no nuclides able to completely satisfy those characteristics and therefore only few radionuclides are routinely employed in nuclear medicine. Those which most closely approximate to the indicated above characteristics are metals. Thanks to their rich coordination chemistry, transition metals offer a wide range of opportunities to link with different ligands in radiopharmaceutical preparations.

New frontier of Nuclear Medicine is the Theranostics that combines, as suggested by the name, therapy and diagnostic at the same time providing a personalized medicine approach. This innovative medical strategy relies on the use of a radiopharmaceutical labelled with a single radionuclide or a pair of radioisotopes whose decay radiation is useful for both diagnostic and therapeutic purposes.

In this work, a radiometal for each kind of nuclear medicine application (SPECT, PET and Therapeutic or Theranostics applications) has been treated and in particular their production by using medical cyclotrons has been reported.

1.1 Radionuclides Applications in Diagnostic

The ability to visualize the anatomic structure and the metabolic activity in vivo is the base of Nuclear Medicine by means of imaging tools such as SPECT and PET.

The principle of nuclear medicine diagnostic investigations is based on the injection of a bioactive molecule into a patient labeled with a radionuclide, γ- or positron-emitters and characterized by suitable half-life and radioactive properties. The γ-radiation exiting the patient body is then detected by SPECT- or PET- cameras respectively and translated into a planar or tridimensional image containing the information related to the clinical conditions of the organ under investigation. In this way it is possible to reconstruct the three-dimensional distribution of the radiopharmaceutical into the patient's body giving not only a morphological

information of the organ or tissue but also functional of the biological activity over time.

1.1.1 The Radiometal Technetium-99m

Nowadays, Tc-99m is the most used γ-emitting SPECT radionuclide (Qaim, 2012) involved in over 85% of all diagnostic procedures. Its employment in routine has risen in the last ten years and it is expected a further 3-5% per year increase, in particular in developing countries (IAEA, 2010).

Its physical and chemical characteristics (*Table 1*) makes it the ideal element for the application in nuclear medicine. Indeed, it decays, with a half-life of 6.02 hours, to Tc-99g for Isomeric Transition (IT) by emitting a 140.511 keV photon (I=89%), causing the least radiation dose to patients. Moreover, thanks to its rich coordination chemistry, the establishment of a wide range of compounds and labeling methods allowed to cover the diagnosis needs for almost all major organs such as brain, thyroid, lungs, heart, spleen, kidney, stomach, liver, bones and so on.

Tc-99m is commonly obtained from the decay of its parent nuclide Mo-99 (half-life 66 hours) by eluting compact and transportable ^{99}Mo/^{99m}Tc generator systems (*Figure 1, 2 and 3*) that makes it almost always available directly in nuclear medicine departments.

Table 1 Datasheet of Tc-99m physical properties (NuDat).

Name	Technetium-99m, ^{99m}Tc	
Neutrons	56	
Protons	43	
Half-life	6.0067 (5) hours	
Parent Isotopes	^{99}Mo (65.976 h)	
Decay Products	^{99g}Tc (2.111 E5 y)	^{99}Ru (Stable)
Decay mode	Isomeric transition (99.9963%)	β- (0.0037%)
Decay Energy [keV] and Intensity (%)	140.5 (98.6%) 142.6 (1.4%)	
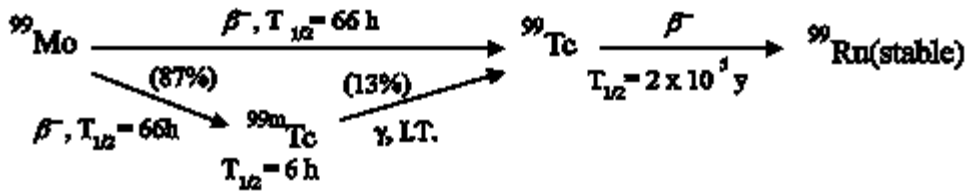
Figure 1 The $^{99}Mo/^{99m}Tc$ decay scheme.

Figure 2 Picture of a commercial $^{99}Mo/^{99m}Tc$ generator.
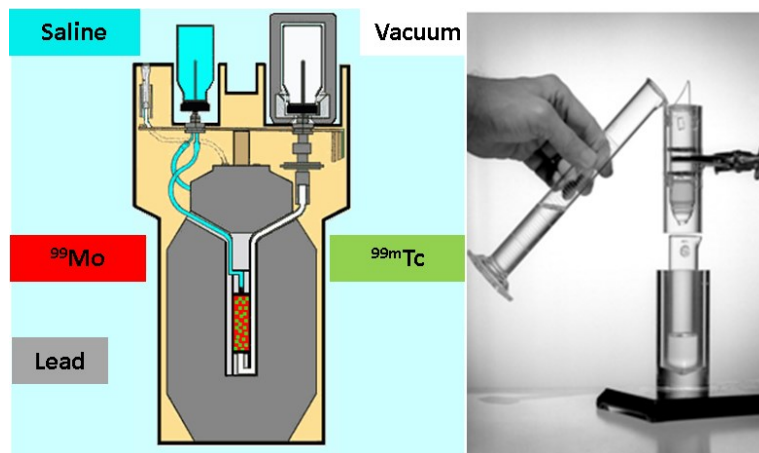
Figure 3 Left: schematic description of a $^{99}Mo/^{99m}Tc$ generator; Right: the first manual generator of ^{99m}Tc, 1958 (Eckelman, 2009).

The generator system is simply composed by an alumina column (Al_2O_3) on which was preabsorbed the Mo-99 as molybdate ($^{99}MoO_4^{2-}$). Once Mo-99 decay into Tc-99m, the thus formed pertechnetate ($^{99m}TcO_4^-$) is less tightly bound to the alumina column, since its single negative charge compared to the double negative charge of molybdate, can be easily eluted from the column with saline solution thanks to the

depression caused by an under-vacuum vial appositely inserted in the pertechnetate collecting area. The so far obtained sodium ^{99m}Tc-pertechnetate is ready for the injection or for the preparation of others radiopharmaceuticals.

The worldwide demand of Mo-99 is actually satisfied by nuclear reactors *via* the ^{235}U(n,f)^{99}Mo fission route on Highly Enriched Uranium targets (HEU, enrichment over 80% in ^{235}U). Nuclear reactors involved in the supply of this isotope are listed in *Table 2*, most of them are going to shut down early since they are over forty years old. In addition, in the last decade they have suffered of planned and unplanned shut down for maintenance or breakdown causing in 2009 a shortage in Mo-99 production and therefore in Tc-99m availability. Several alternative production routes have been evaluated and some of them became reliable thanks to the worldwide research effort of the last 7 years in looking for a solution. A list of different cyclotron and non-cyclotron production routes is hereafter described in *Table 3*.

Table 2 Nuclear Reactors involved in Mo-99 supply for generator medical devices (Esposito, 2011).

Reactors	Place	Start service
NRU	Chalk River (CAN)	1957
HFR	Petten (NED)	1961
BR2	Mol (BEL)	1961
OSIRIS	Saclay (FRA)	1966
SAFARI-1	Pelindaba (RSA)	1965

Table 3 Tc-99m alternative production routes.

Reactor based	Accelerator based
LEU-^{235}U(n,f)^{99}Mo	^{238}U(γ,f)^{99}Mo
^{nat,98}Mo(n,γ)^{99}Mo	^{96}Zr(α,n)^{99}Mo
	^{100}Mo(γ,n)^{99}Mo
	^{100}Mo(p,x)^{99}Mo
	^{100}Mo(p,x)^{99m}Tc

In the framework of LARAMED project (section 1.4.2), a laboratory of radionuclides for medicine under development at Legnaro National Laboratories of the National Institute of Nuclear Physics (LNL-INFN), in 2012 we started investigating cyclotron production routes of Mo-99 and directly of Tc-99m with the three-year APOTEMA

project (*Accelerator-driven Production Of TEchnetium/Molybdenum for medical Applications*). The aim of this project was the feasibility evaluation of cyclotron production of Tc-99m and first production experiments of research amount of Tc-99m for quality assurance.

This interdisciplinary project has involved several INFN sections, universities and research institutes collaborating each for a step in the production chain of Tc-99m such as nuclear simulation, target development, separation and purification procedure studies, products quality evaluation and recovery of the molybdenum target material etc.. Once achieved satisfactory results on the direct Tc-99m cyclotron production, a second project named TECHN-OSP has started in 2015 aimed at the development of a technology, based on the previous studies, for the in-hospital cyclotron-production.

Two schools of thoughts born in the last years on this topic: one based on a centralized production of Tc-99m for national distribution by means of high energy high power cyclotron while the other one is based on in-hospital production of Ci amount of Tc-99m, enough to satisfy the hospital needs by means of the already existing low energy medical-cyclotron network routinely involved in the production of PET isotopes such as F-18 ($T_{1/2}$=109.77 min), C-11 ($T_{1/2}$= 20.334 min), N-13 ($T_{1/2}$=9.965 min) etc..

By considering the Italian reality, the in-hospital Tc-99m cyclotron-production seems to be the most reliable short terms strategy. Indeed, the development of a technology that fits with the existing medical-cyclotron network able to produce Tc-99m sufficient to ensure the daily needs of the hospital and, in case of emergency, of the region needs in case of further shortage of Mo-99.

Our research activity also took part of a Coordinate Research Project (CRP) promoted by the IAEA (International Agency of Atomic Energy, Vienna, Austria) named *Accelerator-based Alternatives to Mo-99/Tc-99m production* at which research groups from all around the world collaborated by sharing their experience on this topic.

State of the art and our experience on direct ^{99m}Tc-cyclotron production is well detailed in *Chapter 2*.

1.1.2 The Radiometal Gallium-68

Positron emission tomography (PET) is a nuclear medicine procedure based on the use of tracer molecules radiolabeled with positron-emitting radionuclides. In some cases, it has been demonstrated that PET is even beyond the most common radiological techniques such as CAT (computed axial tomography) and MR (magnetic resonance) (Pascali, et al., 1999).

PET studies, like all nuclear medicine radioisotope emission procedures, yield images that represent the distribution or the uptake pattern of radiopharmaceuticals depending on the physiologic, pharmacologic, and biochemical state of the individual's body.

Actually, the most common radiotracer used in PET to characterize and localize many types of tumors is ^{18}F-fluorodeoxyglucose (^{18}F-FDG), a glucose molecule labeled with F-18 (Pascali, et al., 1999).

The detection in coincidence of the two diametrically opposite 511keV γ-rays emitted after the positron annihilation with an electron (this phenomenon happens few millimeters from the emission point) provide an increased sensitivity and spatial resolution in the PET imaging acquisition compared to SPET (Rahmim & Zaidai, 2008). Whereas, a limitation in PET arises from the image reconstruction without taking in consideration the positron travelling space before the annihilation event occurs (Bushburg, 2002), leading to the decrease in spatial resolution.

PET Radionuclides can be classified in: biogenic elements (C-11, N-13, O-15, etc.); radiohalogens (F-18, Br-76, I-124, etc.) and radiometals (Cu-64, Ga-66, Ga-68, etc.).

While most PET radionuclides are mainly produced in small size medical cyclotron (10-20 MeV) such as ^{18}F, ^{11}C, ^{13}N and ^{15}O (Pascali, et al., 1999), ^{68}Ga is daily eluted, as $^{68}Ga^{3+}$ in 0.1N HCl, from a compact and transportable generator system, $^{68}Ge/^{68}Ga$. The parent nuclide, Ge-68 ($T_{1/2}$=270.93 d) (*Figure 4*), is commonly produced by the nuclear reaction $^{69}Ga(p,2n)$ using cyclotron at proton energy less than 40 MeV (Roesch & Filosofov, 2010). The current price of a $^{68}Ge/^{68}Ga$ generator is about 30,000-60,000 $ (Gagnon, et al., 2017).
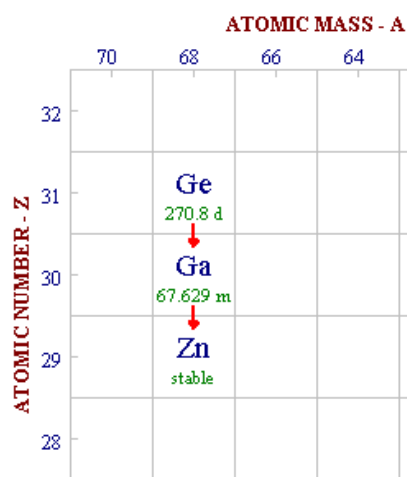
Figure 4 Decay series of Ge-68: tri-linear chart (RadDecay, 2005).

Compared to F-18, generally recognized as the standard PET isotope, Ga-68 may have some disadvantages with respect to production capacity and nuclear decay properties. Its main advantage is the commercial availability by means of generators, a reasonably solution for those centers that do not have access to a cyclotron. Ga-68 has a physical half-life of only 68 min, not suitable for shipping in satellite center. PET radiopharmacies with an on-site cyclotron can produce high activities of F-18 at moderate costs. The physical half-life (110 min) of 18F may also enable centralized production and delivery to distant satellite centers. F-18 also has a lower positron energy than Ga-68 ($E_{\beta+,max}$ 0.65 vs. 1.90 MeV), theoretically resulting in an improved spatial resolution (Kesch, et al., 2018).

Until now the availability independence of Ga-68 from cyclotron was an important characteristic for its early application in Nuclear Medicine. However, now that this nuclide is more widely used in daily diagnostic procedure and radiochemistry research, the need of larger amounts of Ga-68 prompted the study of alternative production routes (*Figure 5*). In particular, the investigation of medical-cyclotron-production from liquid target has taken hold in the radionuclides production research world since it is based on the existing medical-cyclotron network and technology.

Also at TRIUMF, Canada's national laboratory for particle and nuclear physics in Vancouver, the cyclotron production of Ga-68 from Zn liquid target has been investigated as described in *Chapter 5*.
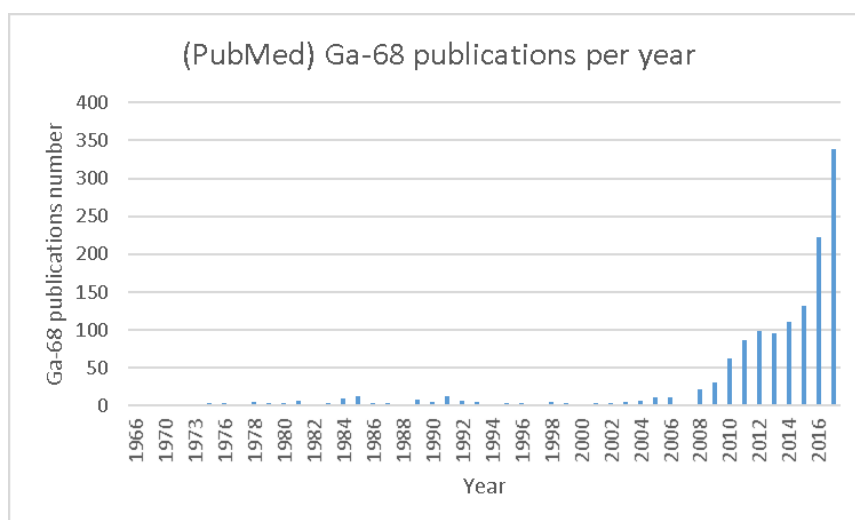
Figure 5 Graphs illustrating the publications increase on PubMed of the past eight years on Ga-68 (PubMed, 2017).

Ga-68 is of particular interest in nuclear medicine thanks to its phisical and chemical properties (*Table 4*). The short physical half-life of Ga-68 is compatible with the pharmacokinetics of peptides making ^{68}Ga-based peptides recognized as a new class of radiopharmaceuticals. Moreover, it is ideal for clinical use since it enables for multiple imaging and improved dosimetry (Banerjee & Pomper, 2013). Ga-68 labeled peptides, somatostatin analogues (Ambrosini, et al., 2010) (Antunes, et al., 2007) (Hofmann, et al., 2001) (Wild, et al., 2005), are widely used in PET diagnosis of various neuroendocrine tumors (NETs).

Table 4 Datasheet of ^{68}Ga physical properties (NuDat, 2.7).

Name	Gallium-68, ^{68}Ga
Neutrons	37
Protons	31
Half-life	67.71 (8) min
Parent Isotopes	^{68}Ge (270.93 d)
Decay Products	^{68}Zn (stable)
Decay mode	β^+ (100%)
β^+ Decay Mean Energy	836.02 (87.72%)
[keV]	352.59 (1.190%)
	107.53 (2.58 E-4 %)
γ Decay Energy	1077.34 (3.22%)
[keV]	1883.5 (0.137%)

1.2 Radionuclides Application in Therapy and Theranostics

Historically, the dermatologist Henri Alexandre Danlos and the physicist Eugene Bloch firstly applied radium for the therapy of tuberculous skin lesion (1901) and later (1913) Dr. Frederick Proescher, director of the Standard Chemical Company laboratory, published the first study on the intravenous injection of radium for therapy of various types of diseases (Proescher, 1913; MacKee, 1921).

Nowadays, Radionuclide therapy is considered one of the most preferred techniques for treating cancer since (Yeong, et al., 2014):

- the radioactivity is delivered selectively on the target tumor saving the surrounding normal tissue;
- minimal radiopharmaceutical administration allows for fast and minimally invasive treatment;
- all organs or tissues are efficiently achievable from the body inside more than whole body irradiation using external beam radiotherapy.

High Linear Energy Transfer[1] (LET) radiations, such as α-, and β-particles are employed in Nuclear Medicine therapeutic treatments since they are fully deposited within a small range of tissue (in the range of mm) ensuring maximum treatment efficiency limited on the malignant area.

The most commonly used therapeutic radionuclides are: iodine-131 (^{131}I) to treat thyroid-related diseases; strontium-89 (^{89}Sr) and samarium-153 (^{153}Sm) labelled radiopharmaceuticals for treatment of bone metastasis; renium-186, -188 (Re-186, -188) and Yttrium-90 (Y-90) for the treatment of a variety of malignancies; lutetium-177 (^{177}Lu) for the treatment of neuroendocrine tumors; radium-223 (^{223}Ra) for prostate cancer treatment etc. (*Table 5*).

---

[1] Linear Energy Transfer (LET): A measure of how, as a function of distance, energy is transferred from radiation to the exposed matter expressed in keV /μm. A high value of LET indicates that energy is deposited within a small distance; protons, neutrons, and α particles have much higher LET than gamma or x-rays.

Table 5 Physical characteristics of commonly available therapeutic radionuclides (Yeong, et al., 2014). RN radionuclide; β- beta electrons; EC electron capture; IT isomeric transition; α alpha particles; * Conversion Electron[2]

RN	half-life	Decay Mode	$E_{Max}^{\beta-}$ (keV)	β- range in soft tissue (mm)		Production Method	Daughter Nuclide
				Mean	Max		
^{32}P	14.3 d	β-	1710	2,6	7,9	$^{31}P(n,\gamma)^{32}P$, $^{32}Sr(n,p)^{32}P$	^{32}S
^{89}Sr	50.5 d	β-	1496	2,4	8	$^{88}Sr(n,\gamma)^{89}Sr$ $^{89}Y(n,p)^{89}Sr$	^{89}Y
^{90}Y	64.1 h	β-	2280.1	3,6	11	$^{89}Y(n,\gamma)^{90}Y$ $^{90}Sr/^{90}Y$ gen.	^{90}Zr
^{117m}Sn	13.6 d	IT	130* 150*	0.22. 0,29	0,27	$^{116}Sn(n,\gamma)^{117}Sn$ $^{117}Sn(n,n',\gamma)^{17m}Sn$	^{117}Sn
^{131}I	8.02 d	β-	606	0,4	2,4	$^{130}Te(n,\gamma)^{131m,g}Te \rightarrow ^{131}I$	^{131}Xe
^{153}Sm	46.5 h	β-	808.2	0,7	3,1	$^{152}Sm(n,\gamma)^{153}Sm$	^{153}Eu
^{169}Er	9.40 d	β-	350	0,3	1	$^{165}Ho(p,n)^{165}Er$	^{169}Tm
^{177}Lu	6.73 d	β-	497.8	0,28	1,7	$^{176}Yb(n,\gamma,\beta-)^{177}Lu$ $^{176}Lu(n,\gamma)^{177}Lu$	^{177}Hf
^{186}Re	3.72 d	EC, β-	1069.5	1,2	3,6	$^{185}Re(n,\gamma)^{186}Re$	$^{168}Os \rightarrow ^{186}W$
^{188}Re	17.0 h	β-	2120.4	2,1	11	$^{188}W/^{188}Re$ gen.	^{188}Os
^{223}Ra	11.4 d	α	5979.2(α)	<10 µm (α)		$^{227}Ac/^{227}Th/^{223}Ra$ gen.	^{219}Rn (unst.)

Some β-emitting radionuclides also present γ-emission of energy intensity suitable for diagnostic purposes. This association of β- and γ-radiation could be advantageous to monitor the radiopharmaceutical distribution and the therapeutic effect with scintigraphy methods (Yeong, et al., 2014). This technique is currently playing a major role in nuclear medicine and it is called Theranostics, the new venture of the personalized medicine. Moreover, the theranostics approach in nuclear medicine couples diagnostic imaging and therapy with the same molecule, but differently radiolabeled.

---

[2] Conversion Electron is an electron released from the atomic shell by transferring the energy of a gamma quantum emitted from the same nucleus to this electron. The kinetic energy of the conversion electron is equal to the energy of the gamma quantum reduced by the binding energy of the electron.

Suitable combinations of molecular targeting vectors and radionuclides for theranostics uses can be:

- a couple of radiopharmaceuticals (bioactive molecules labeled with different nuclide, e.g. Re-188 with Tc-99m, Ga-68 with Lu-177 or Y-90) allowing one for tumor therapeutic treatment and the other for diagnosis and response monitoring

or, even better,

- a single radiopharmaceutical that has both diagnostic and therapeutic properties (bioactive molecule labeled with one isotope whose radiation is suitable for both diagnosis and therapy, (*Table 6*), or a bioactive molecule labeled with a couple of isotopes of the same element (*Table 7*).

Table 6 Theranostics radionuclides (Srivastava & Mausner, 2013). β- beta electrons; C.E. conversion electrons; α alpha particles; Aug. Auger electrons.

Radionuclide	$T_{1/2}$ (days)	Principal γ energy for imaging, KeV (%)	Therapeutic particle(s)
Sc-47	3,35	159 (68)	β-
Cu-67	2,58	186 (40)	β-
Ga-67	3,26	93, 184, 296, (40, 24, 22)	Aug., C.E.
In-111	2,8	171, 245, (91, 94)	Aug., C.E.
Sn-117m	14	159 (86)	C.E.
I-123	13.3 h	159 (83)	Aug., C.E.,
I-131	8	365 (82)	β-
Sm-153	1,94	103 (30)	β-
At-211	7.2 h	79 (21)	α
Bi-213	46 min	441 (926)	β- ; α (from TI-209→Bi-213 decay chain)

Table 7 Theranostics radionuclides pair (Srivastava & Mausner, 2013). β+ positrons; β-beta electrons; C.E. conversion electrons; Aug. Auger electrons.

imaging/therapeutic pair	$T_{1/2}$ (days)	Imaging	Therapeutic particle(s)
Sc-44/Sc-47	3.97/3.35	$β^+$	$β^-$
Cu-64/Cu-67	0.53/2.6	$β^+$	$β^-$
Ga-68/Ga-67	68 min/3.26	$β^+$	Aug; C.E.
Y-86/Y-90	0.61/2.7	$β^+$	$β^-$
I-124/I-131	4.2/8.0	$β^+$	$β^-$

1.2.1 The Radiometal Copper-67

Since the growing interest in the theranostics integrated approach, the production of innovative theranostics nuclide becomes also a priority in the research world.

Among the novel theranostics radionuclides, [67]Cu has recently received the attention of many researchers worldwide (IAEA, 2015).

It has physical characteristics suitable for both therapy and SPECT diagnostic, appropriate β-particle energy and 185 keV γ-radiation respectively (*Table 8*). Moreover, Cu-67 can also be used in combination with another Cu isotope that can improve his diagnostic activity with PET and benefit of the combination of β-particles and Auger-electrons in high dose therapeutic applications, the positron emitter Cu-64 (*Table 9*).

The COME (COpper MEasurement) project, funded by CSN-3 at LNL-INFN, has the aim to study a cyclotron production route for Cu-67, evaluate the optimal irradiation condition to maximize its activity yield and the Cu-67/Cu-64 ratio of co-production (*Chapter 4*). This project participates in a CRP promoted by the IAEA on "*Therapeutic Radiopharmaceuticals Labelled with New Emerging Radionuclides: Cu-67, Re-186 and Sc-47*" with the aim to identify important technical issues related to the radionuclides production and quality control (IAEA, 2015), confirming the recent growing interest on this radiometal.

Table 8 Datasheet of ^{67}Cu physical properties (NuDat).

Name	Copper-67, ^{67}Cu
Neutrons	38
Protons	29
Half-life	61.83 (12) hours
Parent Isotopes	^{67}Ni (21 s) and ^{67m}Cu (ns)
Decay Products	^{67}Zn (stable)
Decay mode	β-
β- Decay Mean Energy [keV]	121 (57%)
	154 (22%)
	189 (20%)
	51 (1.1%)
γ Decay Energy [keV]	184.577 (48.7%)
	93.311 (16.10%)
	91.266 (7%)

Table 9 Datasheet of ^{64}Cu physical properties (NuDat). *ec=electron capture

Name	Copper-64, ^{64}Cu	
Neutrons	35	
Protons	29	
Half-life	12.701 (2) hours	
Parent Isotopes	--	
Decay Products	^{64}Ni (stable)	^{64}Zn (stable)
Decay mode	ec* β+ (61.5%)	β- (38.5%)
β+ Decay Mean Energy [keV]	278.21 (17.6%)	
β- Decay Mean Energy [keV]	--	190.7 (38.5%)
γ Decay Energy [keV]	1345.77 (0.475%)	

1.3 Radiometals Production Routes

As said before, the Nuclear Medicine community is always expanding its applications in diagnostic imaging and therapy of cancer, metastases, arthritis, etc. thanks to the wide spectra of available radiopharmaceuticals coming from the combinations of bioactive molecules and radionuclides. The rapid increase in routine applications of diagnostic, therapeutic and theranostics radioisotopes require reliable availability of the medical-radioisotopes at reasonable costs (IAEA, 2007a).

Research on medical-radionuclide production is indeed an important growing interdisciplinary field with final impacts on Medicine and the routine use of radiopharmaceuticals.

Medical isotopes are commonly produced by nuclear reactors and cyclotrons.

Even if aged, nuclear reactors continue to play an important role in providing radioisotopes for nuclear medicine (Mirzadeh, et al., 2003; Knapp, et al., 1996; Knapp, et al., 2005; Knapp, et al., 1999; Mikolajeszak & Parus, 2005; IAEA, 2003). Most of them are over 40 years old and the announcement of the permanent shutdown of some of them push the radionuclides production research to look for alternative production routes to prevent further medical radionuclide shortages (*section 1.1.1*: Mo-99 production shortages) (IAEA, 2007a; Yeong, et al., 2014).

Nuclear reactors are mainly involved in the production of β-emitting radionuclides directly employed in routine applications or loaded into generator systems waiting for their decay into the daughter nuclides.

Radionuclide generators (*Table 10*) allow daily availability of radionuclides directly in hospital by repeated elution (Roesch & Knapp, 2003). This device is particularly interesting for those nuclear medicine that do not hold a cyclotron or that the radioisotopes distribution from a production site involve long distances and expensive distribution costs (IAEA, 2007a; IAEA, 2004).

Table 10 Some radionuclide generator systems relevant for life-sciences application (f fission; β+ positrons; β- beta electrons; EC electron capture; ERT endoradiotherapy, PET positron emission tomography, SPECT single photon emission computed tomography) (Roesch & Knapp, 2003).

Generator system	Parent nuclide			Daughter nuclide		
	$T_{1/2}$	Main production route	Main decay	$T_{1/2}$	Main emission	Application
^{47}Ca/^{47}Sc	4.536 d	Reactor	β^-	3.341 d	γ, β^-	ERT
^{44}Ti/^{44}Sc	60.3 y	Accelerator	EC	3.927 h	β^+	PET
^{52}Fe/^{52m}Mn	8.28 h	Accelerator	β^+	21.1 min	β^+	PET
^{68}Ge/^{68}Ga	270,8 d	Accelerator	EC	1.135 h	β^+	PET
^{82}Sr/^{82}Rb	25.6 d	Accelerator	EC	1.273 min	β^+	PET
^{90}Sr/^{90}Y	28.5 y	Reactor, f	β^-	2.671 d	β^-	ERT
^{99}Mo/^{99m}Tc	2.7477 d	Reactor, f	β^-	6.006 h	γ	SPECT

Some interesting isotopes for Nuclear Medicine are still not produced in sufficient quantities or not in a carrier free form making their routine application unfeasible. Methods for the production of research quantities of Cu-67, Sc-44, Sc-47, Y-86, etc. have already been studied but more effort are currently dedicated to the development of the technology for production amount for daily use (Huclier-Markai, et al., 2011; Medvedev, et al., 2011; Medvedev, et al., 2012; Srivastava, 2010; Srivastava, 2011).

There are four reaction types for producing radionuclides in nuclear reactors (Srivastava & Mausner, 2013):

- Neutron capture (n,γ), even if this is a high yield production route it presents several disadvantages such as low specific activity[3] (SA) of the final product since the target and the product are the same element making the isolation of the product of interest chemically impossible and the final product not so suitable for nuclear medicine applications (e.g. ^{63}Cu(n,γ)^{64}Cu, ^{88}Sr(n,γ)^{89}Sr, ^{130}I(n,γ) ^{131}I, ^{165}Ho(n,γ) ^{166}Ho, ^{176}Lu(n,γ) ^{177}Lu, ^{187}Re(n,γ) ^{188}Re, ^{185}Re (n,γ) ^{1886}e, ^{187}W(n,γ) ^{188}W)

---

[3] The specific activity (SA) is defined as the activity amount of a sample *per* mass of the sample $A_{sp} = A / m$. Unit: Bq/g or Bq/mol.

- Decay of an intermediate radionuclide produced by neutron capture (n,γ), this strategy is not affected from the same low SA problem as the previous one since the target and the final products are two different elements an therefore chemically separable (e.g. ^{176}Yb(n,γ) ^{177}Yb→ (β- decay)^{177}Lu, ^{198}Pt(n,γ) ^{199}Pt→ (β- decay)^{199}Au). However, the co-production of other isotopes of the same product-element can affect the final Isotopic Purity[4] (IP). This effect can be minimized by using enriched target and use high chemically pure target and processing reagents.
- (n,p) reaction, also in this process target and product are different separable elements (e.g. ^{32}S(n,p)^{32}P, ^{64}Zn(n,p)^{64}Cu, ^{67}Zn(n,p)^{67}Cu)
- Neutron-induced fission of HEU U-235 (n,f), this procedure creates fission products (atomic number Z from 30 to 60) (e.g. ^{235}U(n,f)^{90}Sr→ (β- decay)^{90}Y, ^{235}U(n,f)^{99}Mo→ (β- decay)^{99m}Tc (*Figure 6*), ^{235}U(n,f)^{131}I).
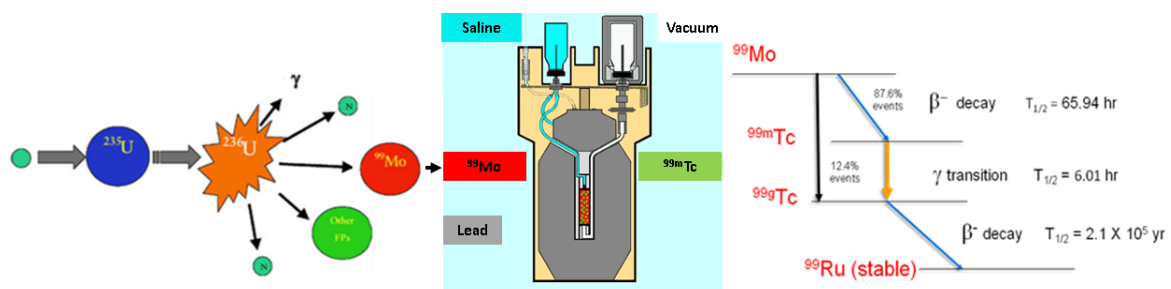
Figure 6 Schematic representation of the generator-production of ^{99m}Tc through the decay of reactor produced ^{99}Mo by ^{235}U(n,f)^{99}Mo neutron fission reaction.

Nuclear reactors planned and unplanned shutdown for maintenance, the announced permanent shutdown of some of them, the use of Weapon-Grade (HEU-WG) target material (^{235}U enrichment > 80wt%), the disposal radioactive waste issue, recent nuclear accidents caused by natural disaster and all others political, economic and historical aspects, pose a challenge to the constant and reliable supply of medical radionuclides globally (Perkins & Vivian, 2009).

The roles of nuclear reactors have not been completely replaced (Qaim, et al., 2011), but further research on alternative accelerator-production routes can result

---

[4] The isotopic purity (IP) of a sample is defined as the percentage of activity coming from the desired isotope in respect to the total activity coming from all the isotopes of the same element as the desired one.

in a transition to a complete, safe, cost-effective, efficient technology able to prevent further medical radionuclide shortages.

The accelerator production of radionuclides is based on accelerated charged particles induced nuclear reactions. Accelerated particles usually involved are protons, deuterons or helium particles. The energy of the "projectile", accelerated particle, covers a wide range from few to hundreds of MeV (Srivastava & Mausner, 2013). Different combination of irradiation parameters (irradiation energy window, irradiation time, target enrichment, etc.) allows to optimize the production of the radionuclides of interest by maximizing the production yield and minimizing the co-production of radioisotopic impurities. High specific activities can be obtained through charged particle induced reactions, e.g. (p,xn) and (p,α), which result in the product being a different element than the target (Siliari, 2010).

A list of the main radioisotopes produced by cyclotrons along with some of the reactions that are used to produce the radioisotopes is reported hereafter (*Table 11*) (Schmor, 2010).

Most of the reactions are proton induced such as (p,n), (p,2n), (p,α), (p,xn) while a lesser extent reactions involves deuterons or alpha particles as projectile.

In a report drafted by the IAEA "Cyclotron produced radio-nuclides: Physical Characteristics and production methods" are collected the measured cross sections for many of these reactions (IAEA, 2009a).

Table 11 List of commonly used cyclotron-produced isotopes, some of possible nuclear reactions.

Medical Isotope	Life-time	Use	Nuclear Reaction
^{11}C	20.4m	PET	^{11}B (p, n) ^{14}N (p,α) ^{10}B (d,n)
^{13}N	9.96m	PET	^{13}C (p,n) ^{12}C (d,n) ^{16}O (p,α)
^{15}O	2m	PET	^{15}N (p,n) ^{16}O (p,pn) ^{14}N (d,n)
^{18}F	109.8m	PET	^{18}O (p,n) ^{20}Ne (d,α)
^{64}Cu	12.7h	SPECT	^{64}Ni (p,n)
^{67}Cu	61.9h	SPECT	^{68}Zn (p,2p)
^{67}Ga	78.3h	SPECT	^{68}Zn (p,2p)
^{82}Sr/^{82m}Rb	25d/5m	PET	^{85}Rb (p,4n)^{82}Sr → ^{82m}Rb
^{99m}Tc	6h	SPECT	^{100}Mo (p,2n)
^{103}Pd	17.5d	Therapy	^{103}Rh (p,n)
^{111}In	67.2h	SPECT	^{112}Cd (p,2n)
^{123}I	13.2h	SPECT	^{124}Xe(p,2n)^{123}Cs → ^{123}Xe → ^{123}I ^{123}Te(d,2n)
^{124}I	4.1d	PET	^{124}Te(p,n) ^{124}Te(d,2n)
^{186}Re	90.6h	Therapy/SPECT	^{186}W(p,n)
^{201}Tl	73.5h	SPECT	^{203}Tl(p,3n)^{201}Pb → ^{201}Tl
^{211}At	7.2h	Therapy	^{209}Bi(α,n)

1.3.1 Radiometals Cyclotron-Production Process

Generally, when facing a new production route of radiometals by means of cyclotrons, several interdisciplinary tasks have to be accomplished. First of all, a deep theoretical studies on nuclear reaction cross-sections involved in the production should be conducted in order to make a first evaluation of suitable irradiation parameters, that usually lies in a compromise between production yield and quality parameters such IP and radionuclidic purity[5] (RNP). Once accomplished this fundamental task, the study and development of a dedicated target (liquid or metals) together with an extraction and purification procedure of the isotope of interest and recovery procedure of the target material need to be carried out. Preliminary experiments with cold material and later by using radionuclides tracers allow for the optimization of the process. Finally, irradiation experiments should be performed by completing the cycle with quality controls, radiopharmaceutical preparation and imaging test to evaluate the injectability and performance of the product. In *Figure 7* the production cycle of Tc-99m as example of the steps for a radiometal cyclotron production.
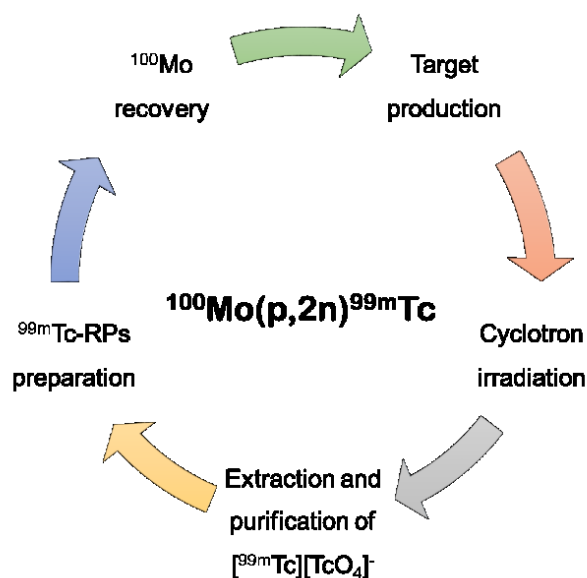
Figure 7 ^{99m}Tc cyclotron production approach based on the $^{100}Mo(p,2n)^{99m}Tc$ nuclear reaction.

---

[5] The radionuclidic purity (RNP) of a sample is defined as the percentage of activity coming from the desired radionuclide in respect of the total radioactivity of the sample.

1.3.2 The Role of Radiochemical Processing in the Cyclotron-Production

Radiochemical processing of activated target is a fundamental step in the cyclotron production cycle to isolate the desired product in a form suitable for its intended application and to recover the enriched target material. The adoption of target processing is not only mandatory for medical applications but it is also advantageous for nuclear data research, such as cross-section studies, preliminary investigation on reactions yields, characterization of reaction products, etc. (Qaim, 2008).

The radiochemical process to be applied for obtaining an injectable medical radionuclide should accomplish different product requirements such as high recovery yield, chemical purity[6] (CP), RNP, SA and sterility. Moreover, the procedure time is a key factor since the speed with which a separations have to be performed depends upon the half-life of the product radionuclide. In this regard, the employment of automatic systems allows for reducing time consuming steps, to minimize human errors and radiation exposure.

The choice of a radiochemical processing method is determined by (Zaitseva & Dmitriev, 1999):

- physical and chemical properties of the target material (e.g. states of matter liquid, solid or gas);
- physical and chemical properties of the desired radionuclide produced in the target during the irradiation;
- quality requirements of the final product for the injectability (ruled by the Pharmacopoeia by means of specific monographs);
- quality requirements of the final product for further radiolabeling process (ruled by pharmaceutical manufacturer in case of kit labeling procedure);
- procedure speed;
- minimization of radiation exposure and contamination;
- avoid the introduction of stable elements that can decrease the SA of the product;
- automation feasibility.

---

[6] The chemical purity (CP) is the evaluation of the chemical compounds in a sample in order to verify the chemical identity of the compound of interest and to ensure the absence of undesired chemical compounds such as residual solvents.

In the case of solid targets (examples described in chapters 2, 3 and 4), usually the radiochemical processing requires first a dissolution step of the target and sometimes chemical treatments need to be carried out to convert the dissolved target into proper chemical species to be efficiently involved in the separation procedure (IAEA, 2008a).

In the case of liquid targets (example described in chapter 5), the target is already in the liquid form and only the chemical conversion to proper species may be necessary. The major problem affecting liquid targets is the tendency of the liquid target to dissolve some material from either the vacuum isolation foil or from the target body results in the contamination with radioactive/stable metals salt, etc. of the target solution. The purification of the desired product also from those contaminants is necessary (IAEA, 2008a).

In the case of gaseous targets, is very important to keep the line free from leaks in order to maintain the purity of the gases and to prevent any contamination of the surrounding area. Moreover, the desired radioisotope may be adsorbed on the walls of the target during irradiation and it should then be removed (IAEA, 2008a).

One or a combination of conventional separation methods such as chromatography, solvent extraction (SE), precipitation, distillation, etc can be selected to isolate the desired radionuclides and eliminate radioactive contaminants.

A brief description of the most used separation techniques in the medical radiometal separations from an activated target is hereafter reported.

Solvent Extraction

This technique is based upon the selective partitioning of solutes between two immiscible solvent phases. It is very effective even on trace level with high selectivity, it is also simple and rapid easily adaptable to automated operation. The SE of complexes by an organic solvent, such as in the case of Tc-99m described in section 2.3, is often followed by further purification step of the product from the solvent (E.g. by means of column chromatography).

K_d (distribution coefficient) represents the equilibrium constant of the process and is defined as the ratio between the total concentration of the desired substance in both phases, usually measured in equilibrium (*Equation 1*).

$$K_d = [C]_{org}/[C]_{aq}$$

Equation 1

The variables that can affect the K_d are: pH; volumes; salt concentration and mixing time.

Chromatography

Chromatography is one of the most commonly used methods for radiometals separation applications in nuclear medicine radiopharmacies since it is readily adaptable to automation. Similarly to SE, it also depends upon the selective distribution of a species between two phases. In chromatography the two phases are a mobile phase (solution in which solutes to be separated are dissolved) and a stationary phase (usually a resin packed in a column). A variety of chromatographic system are actually available such as ion exchange, adsorption, biphasic extraction, size-exclusion, etc..

Ion exchange chromatography is the most used chromatographic technique and is based on the distribution of an element between the mobile and solid phase depending on the ionic form, the solute concentration and the functional group on the resin. Anions are involved in the exchange when the functional groups of the solid phase are positively charged, and conversely, cations are involved when they are negatively charged. Effectiveness of the process can be modulated by variables such as ionic concentration, column volume and diameter, flow rate and eluents.

The distribution coefficient for an element in chromatography is calculated as the ratio between the concentration of the element in both stationary and mobile phases described by *Equation 2*.

$$K_d = \frac{\text{mass of solute per gram of dry solid phase (resin)}}{\text{mass of solute per cm}^3 \text{ of mobile phase (solution)}}$$

Equation 2

The separation factor α between two different elements, A and B, is described by (Equation3) the ratio between the distribution coefficients of the two elements, K_d^A and K_d^B:

$$\alpha_A^B = \frac{K_d^B}{K_d^A}$$

Equation 3

Ion exchange is very useful for separating radionuclides from the bulk target as described in *sections 4.2* and *5.2* in which this technique was applied for the separation of Cu from Zn/Ga contaminants and Ga from Zn/Fe contaminants respectively.

Aqueous Biphasic Extraction Chromatography (ABEC)

ABEC is an alternative to organic-aqueous SE. The partitioning principle is the same of SE but in this method both immiscible components are water-based. A hydrophobic polyethylene glycol (PEG)-based column acts as solid phase in the chromatographic process. This technique was also chosen for the separation of cyclotron produced Tc-99m as described in *section 3.2*.

Automation

The entire automation of a radiochemical separation or radiopharmaceutical synthesis is required when passing from experimental activity levels (few mCi) to clinical production levels of activity (several hundred mCi) (Pascali, et al., 1999). Commercial modules are routinely involved in nuclear medicine radiopharmacies for radiopharmaceutical synthesis. Sector companies provide different customizable modules design suitable for the processing of radioactive materials together with a wide selection of consumables to personalize your own automatic procedure.

Such modules are usually provided with PLC (programmable logic controller), PC and graphical editing software for programming the commands sequence of the procedure together with a scheme of the fluid path as user interface. The building block of the module device provided by the manufacturer usually are

- valves block: valves can be of different type, solenoid, pinch, pneumatic, rotary valves and they can be two or three way valves made of different materials;
- pumps: syringe, peristaltic and vacuum pump are the most used in this field;

- gas flow controller or/and pressure regulator: as alternative way to perform liquid transfer;
- reactor heater and fast cooling feature;
- detection instrumentation: pressure, UV, radiation detectors;
- HPLC, high precision/pressure liquid chromatography;
- all vials, tubing and fittings of different materials to make all the connections for liquid/gas transfer;

The automation process of a separation and purification procedure is the final step of the process optimization. Once defined the proper procedure, usually a combination of separation techniques allowing for both separation of the desired radionuclide from the target and the purification from other contaminants and solvents, at first a semi-automatic module can be designed (e.g. semiautomatic module described in *section 5.2*). This intermediate step is useful when performing low activity experiments to optimize and define a continuity of the operations. Finally, the complete automation allows for the reproducibility of the results and minimization of activity losses and operation time maximizing the final recovery yield. Two examples of radiochemical separation procedure automation are described in *sections 2.3* and *3.2*.

1.4 Cyclotron Production Facilities

As described in the previous section principle advantages of accelerator produced radioisotopes lies in the high SA achievable, the smaller amount of radioactive waste generated in particle reactions compared to reactor produced radioactive isotopes, the cost-effectiveness and tunable on-demand daily availability of the radionuclides.

Among particle accelerators, cyclotron is the most frequent choice for radionuclides production (IAEA, 2009a). The growing number of installed cyclotrons on the territory is consistent with the constant expansion of radionuclides needs for Nuclear Medicine applications. Small cyclotrons (<20 MeV) are the tool of choice for the in-hospital production of most PET isotopes routinely involved in diagnostic procedures (Milton, 1996). Bigger cyclotrons (>20 MeV) are usually installed in institutes for academic research or commercial facilities specializing in producing and selling of radio-isotopes (Schmor, 2010). In 2005, an IAEA report estimated that, worldwide,

there were about 350 cyclotrons that were primarily used for the production of radio-nuclides (IAEA, 2009b) while nowadays the amount of medical cyclotron installed around the world stands at over 950 (Schaffer, et al., 2015b).

Protons accelerating cyclotrons can be subdivided in three categories based on proton energy ranges (IAEA, 2008a): less than 20 MeV, between 20 to 35 MeV and greater than 35 MeV.

Cyclotrons with proton energy less than 20 MeV are located in regional centres/hospitals for the production of short half-life PET radionuclides in sufficient amount to cover the hospital needs. Many of the current cyclotrons have the capability of using multiple targets on each of two or more extracted beams (Schmor, 2010).

Cyclotrons with proton energies between 20 to 35 MeV are generally located in dedicated production facilities for the production of medium half-life SPECT and PET isotopes that can be delivered to hospitals at reasonable distances.

Large multi-purpose research cyclotrons with protons energy greater than 35 MeV and up to 500 MeV are commonly located in academies and governments research institutes consortium and mostly used in the production of radionuclides for therapy, parent nuclides to be loaded onto generator systems and for research.

In the following sections the characteristics of the cyclotrons installed in three facilities: TRIUMF (Vancouver, CA), ARRONAX (Nantes, FR) and the recent SPES (Legnaro, IT) are described.

1.4.1 TRIUMF and ARRONAX Centre

TRIUMF is a centre of particles and nuclear physics owned and operated as a joint venture by a consortium of universities located in Vancouver, Canada (TRIUMF, a).

TRIUMF's Life Sciences program is at the vanguard of scientific innovation on isotope and radiopharmaceutical production. Expertise on particle acceleration, target, radiochemistry, radiopharmaceutical, biology and imaging cooperate for accelerator-based isotope production studies to address the recent medical isotope crisis enhancing the existing isotopes production and exploring new, promising isotopes of the future (TRIUMF, a).

Since the announced permanent shutdown in 2018 of the Canadian Chalk River nuclear reactor NRU, TRIUMF spent much effort to accomplish alternative production of ^{99m}Tc to develop a technology to ensure a supply of non-reactor based technetium-99m for Canada and the world using existing medical cyclotrons to implement its direct production. The research group in the life science division called CycloMed99 is taking care of this topic with the project "A trans-regional initiative to achieve large scale production, distribution, supply and commercialization of Tc-99m" (TRIUMF, b).

The TRIUMF Life Sciences program is also centered around PET novel radiotracer development for neurological applications, for example in Parkinson's disease, as well as applications to cancer detection and treatment, and for other diseases like diabetes. The project "Radiometals Produced by Liquid Targets for Molecular Imaging of Cancer" has in particular the purpose to study the cyclotron-production of PET isotopes such as zirconium-89, gallium-68, yttrium-86 and scandium-44 by irradiating a salt-solution liquid target (TRIUMF, c).

TRIUMF currently operates 5 cyclotrons (*Figure 8*) (TRIUMF, d):
- the world's biggest cyclotron 520 MeV with four independent extraction probes to provide protons simultaneously to up to four beam lines dedicated to different production and experiments on nuclear physics, molecular and materials science (detector tests, strontium isotopes production for medical-imaging generators, radiation testing of electronic circuits, rare-isotope ion beams production, Proton Therapy Program etc.)
- TR-13 cyclotron and three cyclotrons for MDS Nordion[7] CP42, TR30-1 and -2 used to produce medical isotopes.

---

[7] MDS Nordion S.A. is a health science company that manufactures and develops radiopharmaceutical with GMP compliant, steam sterilization, quality control testing, microbiology suite, and sterility. The company also distributes reactor and cyclotron-produced radioisotopes through its multi-reactor partnerships and operates two cyclotrons at its facilities.
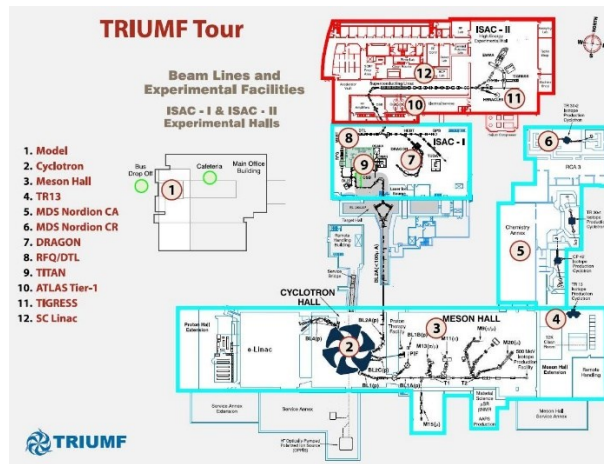
Figure 8 Schematic description of the TRIUMF facility (TRIUMF, e).

Another important cyclotron facility is installed in Nantes (France) called ARRONAX where a dual-extraction multisource 70 MeV high intensity IBA cyclotron is installed (*Table 12, Figure 9*) (ARRONAX; Haddad, et al., 2008).

Table 12 Characteristics of the available beams at ARRONAX.

Beam	Accelerated particles	Energy range [MeV]	Intensity
Proton	H-	30-70	<375
	HH+	17	<50
Deuteron	D-	15-35	<50
Alpha	He++	68	<70

Figure 9 Graphycal representation of the IBA cyclotron instolled in ARRONAX facility.

The cyclotron produces since 2011 Strontium-82 in routine, by the $^{nat}Rb(p,x)^{82}Sr$ nuclear reaction (E=68.7-40 MeV), for the production of Sr-82/Rb-82 generators. Moreover, in tandem with the rubidium target, a Germanium-69 target is co irradiated at energy <40 MeV for the production of the Ga-68 parent nuclide, Ge-68 for generator production as well.

ARRONAX research group is also working on the production of therapeutic isotopes such as ^{211}At, ^{67}Cu, ^{47}Sc, etc., imaging isotopes such as ^{64}Cu, ^{44}Sc and others experiments on radiolysis, radiobiology and physics.

1.4.2 SPES Facility and the LARAMED Project

The SPES project (Selective Production of Exotic Species) is one of the main initiatives of the Legnaro National Laboratories of the National Institute of Nuclear Physics (LNL_INFN) in Italy. Its primary goals are mainly in the field of fundamental physics and applied physics and more specifically the study of highly unstable nuclei and the study and production of medical radioisotopes respectively.

SPES project foresees four phases as suggested by the four-leaf clover SPES logo:

- The α phase includes the realization of the SPES building and the installation, commissioning and acceptant tests at maximum beam power of the BEST 70 MeV high intensity cyclotron (*Figure 10*);
- Phase β, foresees the production of new, extremely neutron-rich nuclei, similar to those generated in advanced stellar stages, for the study of stellar evolution and extending our knowledge of nuclei structure at extreme conditions (PREMIUM-PROJECTS 2011 funded by the Italian government);
- γ phase represented by the LARAMED project *LAboratory of RAdionuclides for MEDicine* (approved by MIUR within the PREMIUM-PROJECTS 2012) is responsible for the study, technology development, and cyclotron-production of radionuclides for medicine;
- phase δ, focused on the development of an intense neutron source.

Indeed, the cyclotron has a simultaneous double beam extraction of accelerated protons with a tunable energy from 35 to 70 MeV, providing a maximum total current of 700 μA.

Moreover, each line will be splitted in more sub-lines for different purposes (*Figure 11*). Two beamlines will be dedicated to the LARAMED project, one for low current cross-sectional studies and the other for high power production studies of medical radionuclides.

Figure 10 Pictures of different moments of SPES realization: from the top SPES building and cyclotron installation phases (LNL-INFN, SPES facility).
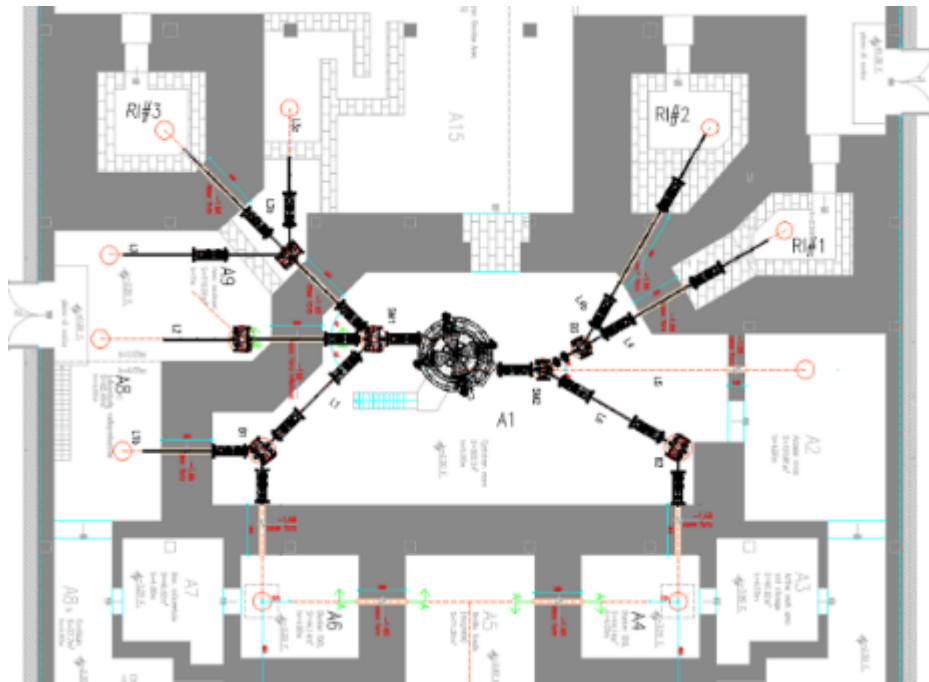
Figure 11 Underground level layout of the SPES building, showing the beamlines distribution: (A6-A4) ISOL bunkers dedicated to the fundamental nuclear physics, (RI#1, 2, 3) LARAMED bunkers dedicated to research and production of medical radionuclides and (A9) neutrons source hall (Maggiore, et al., 2017).

The LARAMED research group, waiting for the realization of the laboratories and the cyclotron operability, has started working on the cyclotron production of conventional radionuclides such as Tc-99m with the two consecutive projects APOTEMA and TECHN-OSP, and of emerging radionuclides, such as Cu-67 with the COME project, Sc-47 with the PASTA project and Mn-52 with the just approved METRICS project. The collaboration with Nuclear medicine radiopharmacies holding a PET cyclotron (Sant'Orsola Hospital, Bologna, IT), with national and international research institute such as JRC-ISPRA (Varese, IT) and ARRONAX (Nantes, FR) respectively made all this possible.

2 Techn-Osp Project: Tc-99m Cyclotron-Production Studies

Technetium-99m (^{99m}Tc; t½ =6h, Eγ=140 keV) still has a fundamental role in nuclear medicine imaging, being the most important gamma-emitting medical radionuclide employed in nearly 85% of all diagnostic nuclear medicine procedures carried out every year around the world (Selivanova, et al., 2017). The possibility of a technetium-99m (^{99m}Tc) shortage at a global scale is still a hot topic and in the last decade it has prompted the study of alternative production routes. Indeed, the conventional supply chain of ^{99m}Tc, generated from the β decay of the nuclear reactor produced ^{99}Mo (t½=66 h), is currently fragile to aging nuclear reactors (see section 1.1.1) and the nuclear weapons' proliferation risk due to the highly enriched uranium (HEU) material involved in the medical radionuclides production (Qaim, 2015). In particular, the unplanned, relatively long term, shut down of some of the few reactors authorized in the period 2009–2010 has forced the scientific community to investigate alternative production routes for this major radionuclide in medicine (Esposito, et al., 2013; Metello, 2015; Pillai, et al., 2013; Qaim, 2012; van der Marck, et al., 2010). One of the most attractive solutions was to consider the direct, cyclotron-based production of ^{99m}Tc as potential replacement of reactor-based technology (Qaim, 2015; Hou, et al., 2016 a; Scholten, et al., 1999; Boschi, et al., 2017; Boyd, 1987; Esposito, et al., 2013; Hou, et al., 2016 b; Manenti, et al., 2014; Pillai, et al., 2013; Ruth, 2009) already evaluated as feasible alternative since 1971 by (Beaver & Hupf, 1971). In contrast, the cyclotron- based production of ^{99}Mo is of limited interest for possible massive production because of the quite low specific activity compared to reactor ^{99}Mo (Esposito, et al., 2013) and low cross section (Scholten, et al., 1999). Accurate calculations and measurements of the cross-section of the ^{100}Mo(p,2n)^{99m}Tc reaction have shown that the most advantageous energy region, where the ^{99m}Tc production is high while the amount of contaminants is minimized, for production yielding ^{99m}Tc in sufficient amounts and while minimizing the amount of contaminants, falls in the range 15–20 MeV (Esposito, et al., 2013; Celler, et al., 2011) although absolute production yields are higher at proton energies of 24 MeV (Celler, et al., 2011). Since this energy range is easily accessible by conventional medical cyclotrons, these results have prompted the scientific community to suggest that the in-house direct production of ^{99m}Tc could make hospital's Nuclear Medicine radiopharmacies, that house a suitable cyclotron, ^{99m}Tc self-manufacturer, as in the case of the local routine production of fluorine-18.

Parallel to in-house ^{99m}Tc cyclotron production approach, the proposal of a centralized production carried out in a professional radiopharmacy, requires a less conventional, high-current cyclotron to ensure a daily production of ^{99m}Tc in amounts sufficient to meet the clinical demand of a metropolitan area (Ruth, 2009; Ruth, 2014; Pillai, et al., 2013; Benard, et al., 2014a).

Tc-99m was the first radionuclide investigated in the framework of LARAMED project, aimed at the study of radionuclides cyclotron production, with two subsequent INFN projects named respectively APOTEMA (Accelerator-based Production Of TEchnetium/-Molybdenum for medical Applications) 2012-2014 and TECHN-OSP (TECHNetium direct-production in hOSPital) 2015-2017. During the APOTEMA project a feasibility study for Tc-99m cyclotron-production has been conducted while in the last three years, the purpose of our work was therefore the development of a technology able to produce GBq amount of technetium-99m by cyclotron in a local nuclear medicine radiopharmacy.

I have reported in this chapter our studies performed and experience related to the proper technology development to provide a routine supply of technetium-99m for a traditional Nuclear Medicine (Esposito, et al., 2013; Manenti, et al., 2014; Martini, et al., 2016; Uccelli, et al., 2013). In particular, after the preliminary theoretical investigation on the most appropriate irradiation conditions (Esposito, et al., 2013), and the development of an efficient extraction and purification procedure (Martini, et al., 2016), we spent our effort in optimizing all the production aspects in order to fit the Nuclear Medicine Hospital Radiopharmacy needs.

2.1 Feasibility Study for Mo-99 and Tc-99m Cyclotron Production

The first objective of APOTEMA project was to define the optimal irradiation conditions in terms of energy, irradiation time, target material, thickness, isotopic abundance, etc. by theoretical investigation of the ^{100}Mo(p,2n)^{99m}Tc and other excitation functions extended up to (p,6n), (p,p5n) and (p,2p4n) levels (TENDL, 2012). Moreover, the reaction yields for each Mo isotope present in the target have been estimated. The isotopic composition of the enriched metallic molybdenum material, chosen as reference for all our studies based on market availability in 2013, is the one provided by the ISOFLEX company (ISOFLEX, 2015): ^{100}Mo

(99.05%), ^{98}Mo (0.54%), ^{97}Mo (0.07%), ^{96}Mo (0.11%), ^{95}Mo (0.10%), ^{94}Mo (0.05%), and ^{92}Mo (0.08%). The nuclear reaction channels opened during the irradiation on Mo-isotopes present in the target brings to the co-production of undesired contaminants such as Nb, and Tc isotopes, such as those listed in *Tables 13* and *14*, and other isotopes of Mo coming from their decay chain.

Table 13 Technetium isotopes expected to be produced in enriched molybdenum-100 targets by Mo(p,xn)Tc reactions (TR-RCM2, 2013; Esposito, et al., 2013). β+ positrons; β- beta electrons; EC electron capture; IT isomeric transition.

Reaction Channels	Produced isotopes	Half-life	Decay mode	Major γ-lines [keV] (Int%)	Stable Daughter
^{93}Mo(p,n) ^{94}Mo(p,2n) ^{95}Mo(p,3n)	^{93}Tc ^{93m}Tc	2.75 h 43.5 m	EC; β+ IT	1362.94 (66%) 391.83 (58.3%)	^{93}Mo
^{94}Mo(p,n) ^{95}Mo(p,2n) ^{96}Mo(p,3n) ^{97}Mo(p,4n)	^{94}Tc ^{94m}Tc	293 m 52.0 m	EC; β+ IT	871.05 (99.9%) 871.05 (94.2%)	^{94}Mo
^{95}Mo(p,n) ^{96}Mo(p,2n) ^{97}Mo(p,3n) ^{98}Mo(p,4n) ^{100}Mo(p,6n)	^{95}Tc ^{95m}Tc	20.0 h 61 d	EC; β+ IT	765.789 (93.8%) 204.117 (63.2%)	^{95}Mo
^{96}Mo(p,n) ^{97}Mo(p,2n) ^{98}Mo(p,3n) ^{100}Mo(p,5n)	^{96}Tc ^{96m}Tc	4.28 d 51.5 m	EC; β+ IT	778.22 (99.76%) 778.22 (1.9%)	^{96}Mo
^{97}Mo(p,n) ^{98}Mo(p,2n) ^{100}Mo(p,4n)	^{97}Tc ^{97m}Tc	4.2·10^6 y 91 d	EC IT	-- 96.5 (0.32%)	^{97}Mo
^{100}Mo(p,3n)	^{98}Tc	4.2·10^6 y	β-	745.35 (102%) 652.41 (100%)	^{98}Ru
^{100}Mo(p,2n)	^{99}Tc ^{99m}Tc	2.1·10^5 y 6.01 h	β- IT	89.5 (0.00065%) 140.511 (89%)	^{99}Ru
^{100}Mo(p,n)	^{100}Tc	15.46 s	β-	539.52 (6.6%)	^{100}Ru

Table 14 Nuclear reaction channels opened during the proton irradiation on Mo-100.
β- beta electrons; IT isomeric transition. *Mo-99 is not stable, it decays to Tc -99g and -99m that consequently decays into the stable Ru-99. (NuDat, 2.7)

Reaction Channels	Produced Isotopes	Half-life	Decay mode	Major γ-lines [keV] (Int%)	Stable Daughter
(p,α2n)	^{95}Nb	34.99 d	β⁻	765.803 (99.808%)	^{95}Mo
(p,αn)	^{96}Nb	23.35 h	β⁻	778.224 (96.45)	^{96}Mo
(p,α)	^{97}Nb	72.1 m	β⁻	657.94 (98.23%)	^{97}Mo
(p,2pn)	^{98}Nb	2.9 s	β⁻	787.4 (13%)	^{98}Mo
(p,2p)	^{99}Nb	15 s	β⁻	137.7 (81%)	^{99}Mo*
	^{99m}Nb	2.6 m	IT	97.785 (6.7%)	

The evaluation of the co-produced unstable technetium isotopes (Tc-xy), other than Tc-99m, plays an important role in the determination of the optimal irradiation conditions. Indeed, Tc-xy are not chemically separable from Tc-99m and therefore contributing to the patient dose during diagnostic activities. Whereas, Nb and Mo isotopes are easily separable from Tc-99m by chemical treatment during the separation and purification step.

It is clear that a compromise has to be found in order to maximize the Tc-99m production yield and minimize the Tc-contaminants (Tc-xy) presence in the final product. The recommended operative irradiation condition for technetium-99m production, from Mo-100 (99.05% enrichment), have been evaluated and summarized in a recent publication by (Esposito, et al., 2013). Taking into account the ^{99m}Tc/$^{99m+g}$Tc and ^{99m}Tc/^{Σall}Tc ratios, the ^{99m}Tc production yield and the nuclides composition during the irradiation time up to the end of bombardment (EOB) and up to 10 h after EOB in the purified product, short irradiation time (i.e. no longer than 3 h) in the energy range between 15 and 20 MeV shall be considered as favorable since the long-lived contaminants ^{99g}Tc, ^{98}Tc, and ^{97g}Tc are mainly produced by nuclear reaction on ^{100}Mo isotope at energies greater than 20 MeV. Although the in-target yields are improved moving towards beam energies higher than 20 MeV, the production of other Tc contaminants starts increasing to levels that are not negligible as described by (Esposito, et al., 2013). Nevertheless, using higher Mo-100 enrichment target material the advantageous energy region rises to 24 MeV.

The ^{99m}Tc production yields estimated at EOB at 20 MeV proton beams on 99.05% ^{100}Mo enriched metallic molybdenum and optimized target configuration, show that is possible to produce from 10.35 to 27.81 mCi/µA for irradiation times going from 1 to 3 h. In such case the SA, IP and RNP are closer to the generator-produced ^{99m}Tc ones (Esposito, et al., 2013). Furthermore, Esposito et al., have calculated the recommended target thickness for an optimized production at different irradiation energies (15, 20 and 25 MeV) (*Table 15*).

Table 15 Integral production yield (normalized per incident proton) estimated on ^{100}Mo enriched target thicknesses for ^{99m}Tc productions and IP quality parameter.

Proton energy [MeV]	Optimized target thickness [mm]	^{99m}Tc/p [adimensional unit]	^{99m}Tc/$^{99m+g}$Tc yield ratio	^{99m}Tc/^{all}Tc yield ratio
25	0.94	$6.70 \cdot 10^{-4}$	0.187	0.117
20	0.57	$5.65 \cdot 10^{-4}$	0.198	0.170
15	0.26	$2.84 \cdot 10^{-4}$	0.235	0.211

2.2 Target Development and Irradiation

High enrichment levels of molybdenum-100 (>99%) are required for high quality ^{99m}Tc production. As described above, the presence of different Mo isotopes affects the IP, SA and RNP of the final product due to the production of unwanted contaminants such as different Tc, Ru, Nb, Zr, etc. isotopes (TR-RCM2, 2013). For this reason, the amount of Mo impurities other than ^{100}Mo should be minimized.

Enrichment in ^{100}Mo up to 99.86% are commercially available in both metal and oxide form (ISOFLEX, 2015). A crucial limiting factor is the thermal power to be dissipated from the target to avoid melting, volatilization or density reduction of the target material reducing drastically the production yield (Beaver & Hupf, 1971; Srivastava & Mausner, 2013). In order to provide a good thermal conductivity and mechanical stability, the molybdenum target should be prepared in the metal form and supported by a back plate that shall meet the requirements of chemical inertness, well heat-dissipation and little activation when irradiated (Gagnon, et al., 2012). The interface between the backing and the target material is a challenging point since it is where many problems arise such as loss of target material or

damage, reducing the heat transfer. The better the connection reached at the interface, the better heat transfer will be (Srivastava & Mausner, 2013).

The Canadian research group at TRIUMF has devoted great effort to the optimization of the molybdenum target as reported in several recent works (Hou, et al., 2016 a; Benard, et al., 2014a; Hanemaayer, et al., 2014; Morley, et al., 2012b; Schaffer, et al., 2015a; Zeisler, et al., 2014; Schaffer, et al., 2015b). Their strategy is aimed at the production of different targets that fit with different cyclotron models able to suit the medical cyclotrons network around the world (16–24 MeV, 100–500 µA). The strategy matches with the optimal irradiation conditions for the ^{99m}Tc cyclotron in loco- and on demand-production. The technology chosen for the high-current target preparation is the electrophoretic deposition on tantalum backing plate, whereas for the low-current target the pressed sintered powder brazed on a copper backing disk is used. Other research groups have developed different manufacturing approaches to the molybdenum target preparation (Thomas, et al., 2014; Matei, et al., 2014) as cold rolling and diffusion bonding proposed by Thomas et al. (Thomas, et al., 2014).

The aim of our work was focused on the development of a technology consistent with medical cyclotrons and able to produce technetium-99m using the already existing PET cyclotron to provide on-site supply for regional radiopharmacies, even in replacement of ^{99}Mo/^{99m}Tc generators. For this purpose, the collaboration with the Sant'Orsola Hospital in Bologna (Italy), their facility and cyclotron (GE-PETtrace 16.5 MeV), has been the key to reach our goals. The design of a target holder able to fit the solid target station of the available cyclotron (16.5 MeV) and different Mo-100 metal target configurations is the starting point. The cyclotron has six target stations, one of them suitable for solid targets (*Figure 12*). The solid target station is equipped with a double cooling system, helium on the front and water on the back of the target, and automatic load, unload and transfer system. The cyclotron is involved in daily production of PET tracers including F-18 and C-11 for routine clinical investigations.

The whole target, composed of a target holder and the target itself (material of interest to be irradiated), was designed in order to fit: 1) the solid target station of the hospital cyclotron involved in the experiments and 2) different target design as thick foil, multi thin targets in stacked foil configuration or thin/thick layer deposited on a backing plate. The target holder consists in two copper pieces clamped

together with the target, in particular the beam-front one was designed with a 12 mm hole for a direct exposure of the target material to the accelerated beam (*Figure 13*).
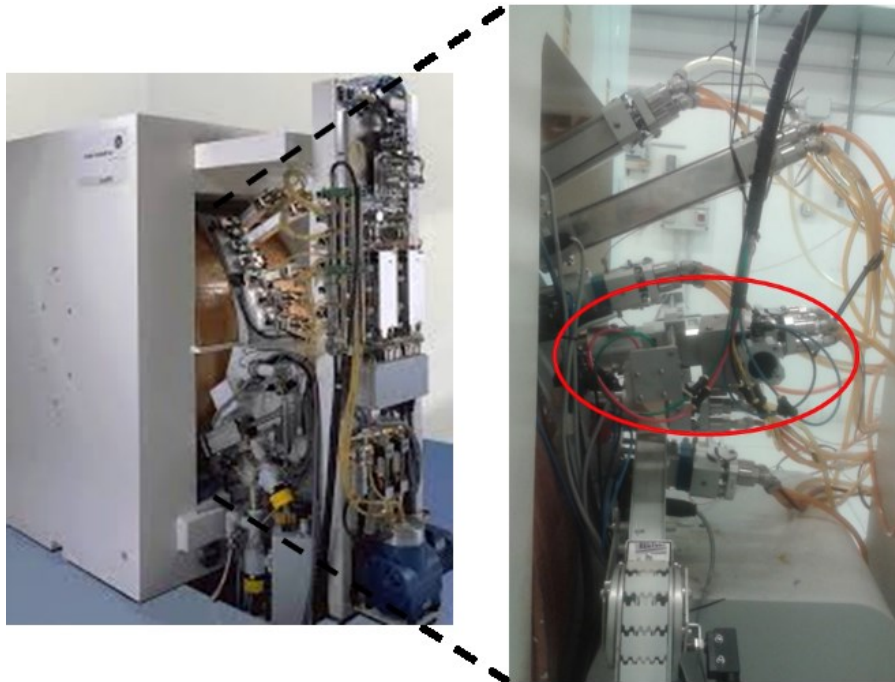
Figure 12 The GE PETtrace cyclotron installed at the Sant'Orsola hospital facility and a zoom on the solid target station.
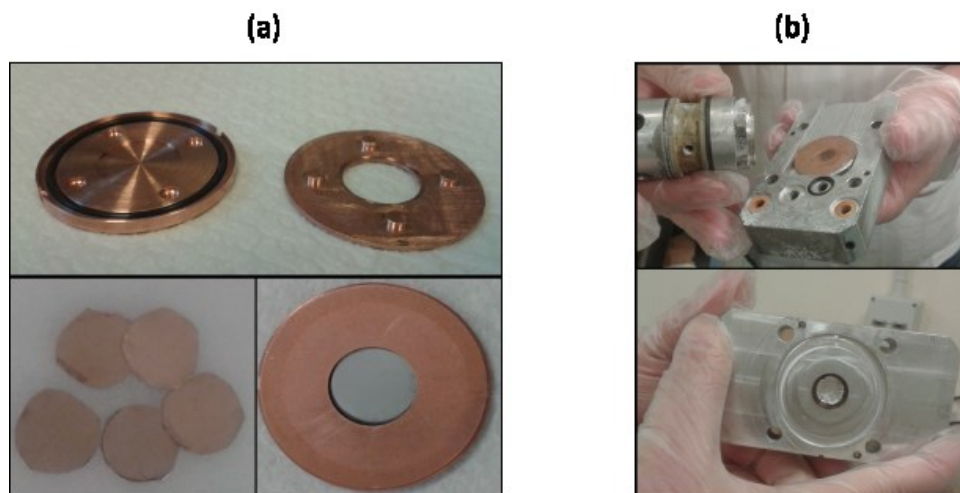
Figure 13 Pictures of the target components: (a) copper target holder, molybdenum metal foils for stacked foils irradiation configuration and the complete assembled target; (b) back and front of the target mounted on the solid target station holding structure (exploded sample for demonstrational purposes only).

For each run, five molybdenum thin metal foils ($\varnothing$ = 0.9 ± 0.2 cm, total thickness = 132 ± 11 µm, total mass = 150.4 ± 25.8 mg), have been produced at the LNL target laboratory by lamination process starting from molybdenum metal powder melted under well-controlled environmental conditions. The isotopic composition of the enriched material, taken as reference in this study, is the one purchased by the ISOFLEX company (San Francisco, USA) (ISOFLEX, 2015): ^{100}Mo (99.05%), ^{98}Mo (0.54%), ^{97}Mo (0.07%), ^{96}Mo (0.11%), ^{95}Mo (0.10%), ^{94}Mo (0.05%), and ^{92}Mo (0.08%).

Several irradiation test were performed beforehand on natural molybdenum foils to test the resistance of the designed target under different proton beam irradiation conditions.

The five molybdenum metal foils were clamped into the target holder in a stacked foil configuration ensuring a good thermal contact between the two materials (*Figure 14*). The targets were irradiated at beam currents of 10 and 20 µA over a period of 60 to 90 min at 15.7 MeV in order to obtain an estimated ^{99m}Tc activity at EOB (End of Bombardment) in the range 1.1-3.7 GBq.
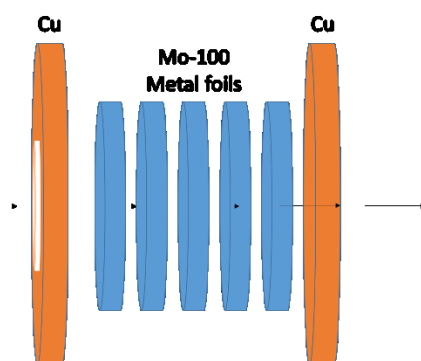
Figure 14 Stacked foil target. Five thin molybdenum enriched in Mo-100 metal foils clamped into the copper target holder.

2.3 Separation and Purification Process ^{100}Mo/^{99m}Tc

An accelerator technology, based on the ^{100}Mo(p,2n)^{99m}Tc nuclear reaction, will always require the application of an effective separation technique to obtain the radionuclide of interest, ^{99m}Tc, in an injectable form and to allow also for recycling of the costly enriched targets, ^{100}Mo, ensuring the economy of the whole production

process. Several separation techniques have been developed, most of which have been listed and assessed by (Dash, et al., 2013), as column chromatography, solvent extraction (SE), sublimation, electrochemical separation, etc. In the closer perspective of a direct ^{99m}Tc cyclotron-production on demand, the focus has turned to the development of automatic modules for the in situ extraction and purification of ^{99m}Tc from the irradiated molybdenum target (Schaffer, et al., 2015b).

My contribution to the Techn-Osp project was mainly the development of a fully automated, remotely controlled module for the fast and efficient extraction and purification of Tc-99m from an irradiated Mo-100 enriched molybdenum metallic target by exploiting the high efficiency of the SE technique. There are two key advantages in using an automated procedure for Tc-99m purification. Primarily, this will sharply decrease the radiation exposure of operators in handling high radioactive materials and, secondly, will definitely contribute to make the whole process much more reproducible and traceable. That is indeed a key pre-requisite for attaining a clinical-grade quality for the recovered Tc-99m. In turn, this may strongly favor a possible approval by regulatory authorities for its use in patients.

2.3.1 Solvent Extraction Automatic System

Several techniques are known for the separation of technetium from molybdenum, the most used are: ABEC (Aqueous Biphasic Extraction Chromatography) technique, the Ion Exchanger Extraction (IEE) method and the SE method with MEK (Dash, et al., 2013; Morley, et al., 2012a). Among them, the SE method with MEK has been proven to be one of the most efficient techniques thanks to the selective affinity of the pertechnetate (^{9x}TcO$_4^-$) for MEK and the affinity of the binegative molybdate (MoO$_4^{2-}$) for the aqueous phase, providing high extraction yield of high quality ^{9x}Tc from molybdenum metal targets (Boschi, et al., 2017; Chattopadhyay, et al., 2010; Dallali, et al., 2007; Noronha, 1986; Novak & Fajgelj, 1983; Martini, et al., 2016; Skuridin & Chibisov, 2010; Tachimori, et al., 1971; Taskaev, et al., 1995; Zykov, et al., 2001). The SE technique in general involves the following procedure steps: (1) dissolution of the irradiated target of molybdenum (VI) oxide (MoO$_3$) in NaOH 5N, (2) extraction of pertechnetate from the aqueous alkaline solution of molybdate into the organic phase (MEK) through the agitation contact between the two phases, (3) separation of the MEK phase from Mo solution, (4) purification of the ^{99m}Tc-pertechnetate/MEK solution by using a silica column in order to remove

traces of Mo, (5) MEK removal by evaporation, (6) reconstitution of Na^{99m}TcO$_4$ from the resulting residue by leaching with saline (Chattopadhyay, et al., 2010; Chattopadhyay, et al., 2012; Novak & Fajgelj, 1983).

Starting from such a method and by applying some improvements to the original procedure, in order to ensure an optimal operator radioprotection and faithful reproducibility of the process, a completely automatic extraction module was thus developed for the ^{9x}Tc separation and purification from ^{100}Mo-enriched molybdenum metal targets.

A first prototype of automatic module, based on SE with MEK was developed in a first step. This first prototype was optimized for preliminary research purposes to deal with thin foils target configuration (5 foils, thickness = 30 μm, mass = 25 mg each). Later, this system has been modified and improved with the aim of enable it to deal with the properly designed target for the hospital-cyclotron's solid target station (*section 2.2*) and a production scale (thick mono-layer deposited on a backing plate 250-350 mg).

Materials and methods

All chemicals and reagents were of analytical grade unless otherwise specified. Hydrogen peroxide (35% w/w) and sodium hydroxide pellets were purchased from Sigma-Aldrich (Milan, Italy). Methyl ethyl ketone (MEK) was obtained from Carlo Erba (Milan, Italy). Sodium chloride was received from Fresenius Kabi (Verona, Italy).

Silica and acidic alumina SepPak cartridges were obtained from Waters Corporation (Milford, MA, USA).

Technetium-99m, as Na[^{99m}Tc]TcO$_4$ in physiological solution, was obtained from a Drytec ^{99}Mo/^{99m}Tc generator (GE Healthcare, UK).

Mo-100 enriched molybdenum powder was purchased from Isoflex (San Francisco, USA) (Isoflex, 2012). The isotopic composition of the batch of the enriched material was: ^{100}Mo (99.05%), ^{98}Mo (0.54%), ^{97}Mo (0.07%), ^{96}Mo (0.11%), ^{95}Mo (0.10%), ^{94}Mo (0.05%), and ^{92}Mo (0.08%).

The prototype was constructed by assembling six prepackaged modular units (Modular-Lab Standard, Eckert & Ziegler, Berlin, Germany) comprising a flow controller module, a heater reactor module (air-cooled), a vial holder module and three connector modules containing two- and three-way switching valves and tubing

for fluid and gas transfer. A control unit, equipped with Modular-Lab Software 4.3.2.0 (Eckert & Ziegler), remotely controlled the various modules. This assembly was customized by adding to the vial holder module a dedicated, handmade glass column vial (length =10 cm, $\varnothing$ =1cm) specifically designed to accommodate the SE step with the highest separation efficiency (*Figure 15*). All consumable and accessories, including PEEK™ tubing for fluid transfer, PTFE tubing for gas transfer, PEEK™ or Teflon connectors flange-type fitting plugs, PEEK™ vial heads for 4 connectors (1/4"-28), glass vials for reagents, pressure sensors (250 bar) and activity detectors, were purchased from Radius, Bologna, Italy.

On the base of the first prototype the new automatic module (*Figure 16*) was improved by the substitution of some components such as the separation column with a longer hand-made glass column vial (length=15cm, Ø=1cm) and the Heater Reaction Module (Eckert & Ziegler) replaced by a home-made reactor heater with a bottom-opened vial and air compressed cooling system especially designed for the dissolution and separation process for an in-hospital high yield production.

Pictures of the two prototypes setup are illustrated in *Figure 17*.
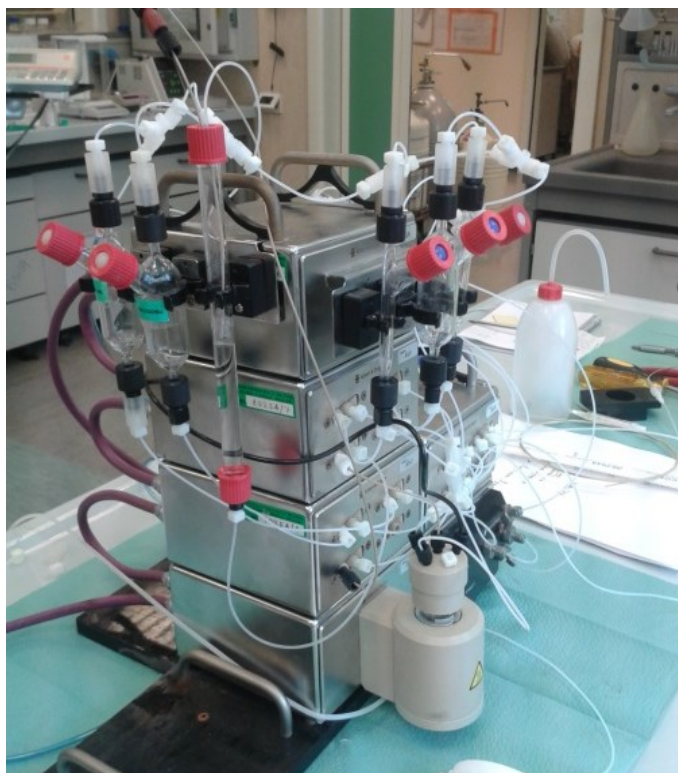
Figure 15 Picture of the first prototype of automatic Tc-99m separation and purification module.
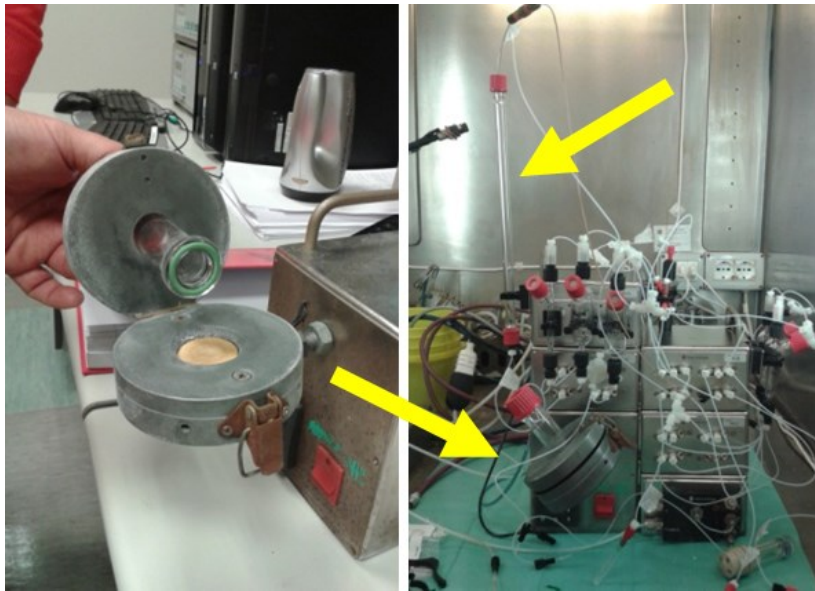
Figure 16 Picture of the second prototype of Tc-99m separation and purification module. The two yellow arrows indicate the home-made reactor heater with bottom opened vial and the separation column.
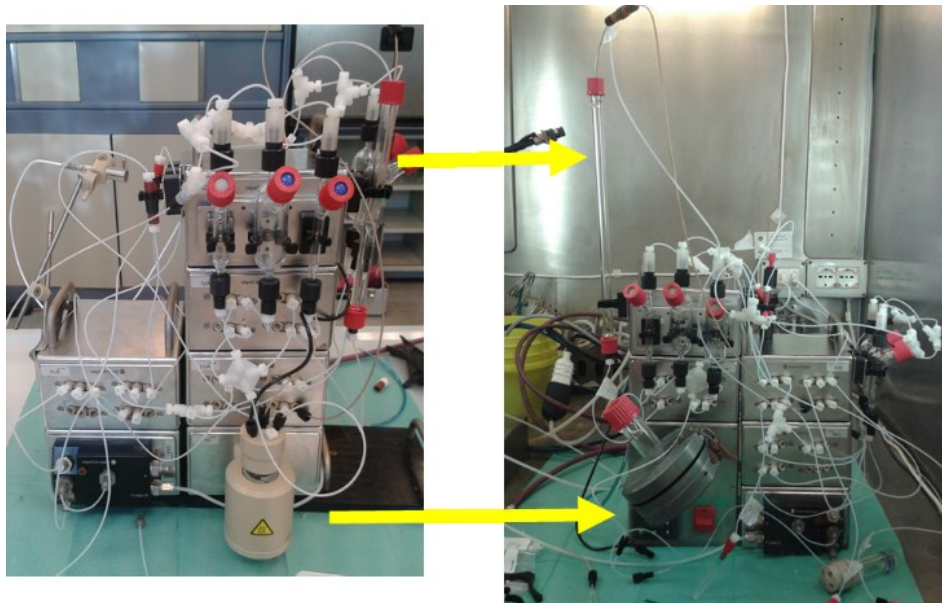
Figure 17 Comparison between the two module prototypes.

A representative description of the whole process and the various steps accomplished by the automated module are reported below.

After irradiation, the target holder was pneumatically transported into a dedicated hot cell through a solid-target transfer system and the five irradiated foils transferred into the reactor vial (1 in *Figure 18*) afterwards. Dissolution of the metallic foils was obtained by addition of 1.5 mL of H_2O_2 (35%) followed by heating at 90 °C for 5 min. After cooling to 50 °C, 5.0 mL of NaOH (6 M) were added to the resulting solution, which was further cooled to 30 °C. After transferring the alkaline aqueous solution to the separation column vial (2 in *Figure 18*), the reactor vial was washed with 4.0 mL of MEK. The organic solvent was then injected slowly from the bottom into the separation column and the resulting mixture vigorously shaken by bubbling helium gas, at a flow rate of 60 mL/min, for 7.0 min in order to maximize the contact between the two phases. Keeping the mixture at rest for 4.0 min resulted in a marked phase separation, the organic solution containing ^{99m}Tc-pertechnetate lying at the top of the column. The organic phase was collected from the separation column, and then passed through a silica SepPak cartridge (3 in *Figure 18*) and subsequently through an alumina SepPak cartridge (4 in *Figure 18*), which immobilized Tc-99m activity. The residual MEK was then sent into the waste vial (5 in *Figure 18*). To maximize the extraction yield, 3.0 mL of MEK were further added to the aqueous phase still present at the bottom of the separation column, and the procedure was repeated. After completing the waste recovery of the second organic fraction, the silica column was washed with 1.5 mL of pure MEK, which was then passed through the alumina column before reaching the waste. Finally, the alumina column was washed with 10.0 mL of deionized water followed by 6.0 mL of saline, thus causing the removal of the adsorbed ^{99m}TcO$_4^-$. The final activity was collected in a sterile vial (6 in *Figure 18*) and the process was completed. The total time to complete the automated procedure was approximately 70 min starting from the introduction of the irradiated foils into the module.
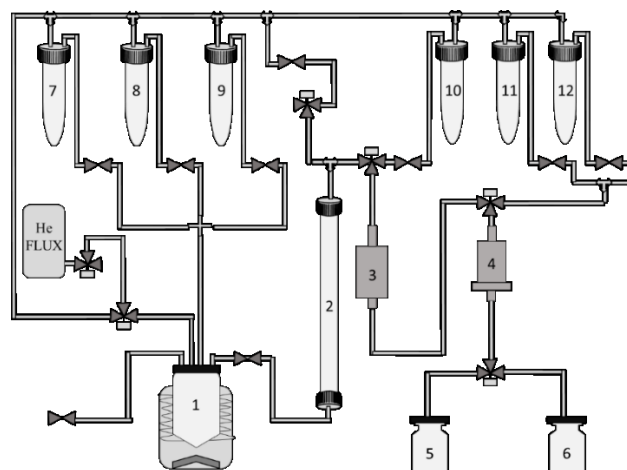
Figure 18 A schematic drawing of the extraction process. (1) dissolution reactor, (2) solvent-extraction column, (3) silica column, (4) alumina column, (5) waste, (6) final Tc-99m solution, (7) H_2O_2, (8) NaOH, (9/10) MEK, (11) H_2O, (12) saline.

Differences in the separation procedure of the second prototype mainly involves (*Figure 19*):

- solvent volumes and processing time, since the mass and target configuration are changed from thin foils to thick monolayer with doubled mass.

- dissolution process, a three step dissolution process, under helium flux and at 90°C was especially optimized. This procedure allows always fresh pure hydrogen peroxide to react and oxidize the metal target, thus avoiding the passivation of the target surface. Indeed, after the reaction occurred, the first amount of solution was transferred to the separation column, leaving the yet still undissolved metal ready to receive fresh hydrogen peroxide, making in this way the dissolution reaction stronger and faster. The resulting solution, collected in the separation vial, was then transferred in the reactor for the subsequent basification with sodium hydroxide.

- extraction with MEK, the addition of MEK to the molybdate alkaline aqueous solution starts the pertechnetate extraction directly in the reactor vial and then greatly increased during the solution transfer and vigorous helium bubbling in the separation column vial, followed by all the other steps unchanged from the previous reported procedure.

56
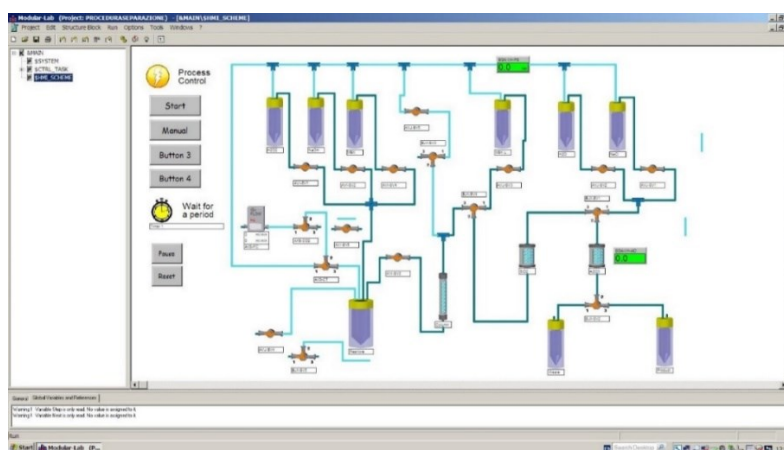
Figure 19 Software control page, fluidic physical layout of the second module prototype.

Results

The optimization of the separation and purification automatic procedures has been conducted with cold materials first (not irradiated molybdenum metal foils), in order to optimize the dissolution step, fluidic path, volumes, temperature and time. Then, the optimization of the extraction yield has been conducted by adding small amount of Tc-pertechnetate eluted from a commercial ^{99}Mo/^{99m}Tc generator. In this way we were able to determine the final recovery yield of ^{99m}Tc and the activity left in all others steps such as in the resins, waste and molybdate aqueous phase. The activity determination has been conducted after each run by measuring it with a Capintec dose calibrator (*Table 16*). Taking into account the different geometry of some solid components (prepacked columns) those activities are to be considered for qualitative and not quantitative purposes. Instead, liquid components have been equally aliquotated and the activity corrected for the total volumes.

Table 16 Percentage and SD of ^{99m}Tc activity (decay corrected) in the different components of the automatic module. n=10

Constituents	% ^{99m}Tc activity
Final solution	93.0±2.8
Aqueous phase	5.3±3.0
Waste	0.7±0.9
Silica column	0.6±0.8
Alumina column	0.4±0.1

The pertechnetate so far obtained from the second module prototype is also, in the final physiological solution, ready to be used. The whole procedure takes about 60 min (10 minutes less than the previous one) and the recovery yield is about 93 ± 3% decay corrected.

The module has been involved in several Tc-99m cyclotron-production. For each run, five molybdenum thin metal foils have been irradiated and then allowed to rest one hour before being processed. The extraction and purification of the Tc from the Mo target and other contaminants has been performed by means of the automatic module. At the end of the purification, the final product, sodium ^{99m}Tc-pertechnetate in saline solution, underwent all quality controls procedures as described in the following *section 2.4*.

After each purification run, the automated module was washed by passing 20 mL of deionized water through the system after removal of the cartridges and of the residual liquid fraction in the reactor. The recovered aqueous waste (washing fraction) and all other components of the module, such as Sep Pak columns waste fraction and residual aqueous solution, were measured for activity and contaminants determination by gamma spectroscopy as detailed below (*section 2.4*).

2.4 Quality Controls and Pharmacopoeia Requirements

The main difference between cyclotron-produced and generator-eluted ^{99m}Tc is that cyclotron-produced ^{99m}Tc is contaminated with other technetium isotopes. As a result of a deep study from world experts, the European Pharmacopoeia has recently adopted a new monograph on sodium pertechnetate (^{99m}Tc) (accelerator-produced) injection to avoid future potential supply problems for the medical world and benefit patients (Ph. Eur. , 2017) keeping high quality of the injectable product. A comparison between fission, non-fission and accelerator-produced sodium pertechnetate (^{99m}Tc) injection is reported in *Table 17*. The main difference with respect to the previous monograph based on generator-eluted ^{99m}Tc, is in the radioisotopic purity. In fact, the presence in cyclotron–produced ^{99m}Tc of other Tc isotopes, coproduced during the irradiation and chemically not separable from ^{99m}Tc, has direct implication on patient dose (Hou, et al., 2012).

The product's IP and RNP are related to the isotopic composition of the target and irradiation parameter; their relationship with patient dosimetry have been deeply

analyzed by (Selivanova, et al., 2015) and (Hou, et al., 2016 a). It is clear by estimation and also by experimental evidences how the IP of the final product decreases by increasing the irradiation energy and time and by decreasing the target enrichment in ^{100}Mo (Cicoria, et al., 2016; Esposito, et al., 2013; Hou, et al., 2016 a; Selivanova, et al., 2015).

In particular, as described by (Hou, et al., 2016 a), the presence of $^{95-97}$Mo should be limited because these radioisotopes generate $^{93-97}$Tc that mostly contribute to patient radiation dose. Moreover, this isotopic contamination may also affect image resolution and contrast. Quality control, on phantom and in vivo imaging acquisition, has been conducted in order to demonstrate the equivalence between cyclotron-produced ^{99m}Tc- and generator-eluted ^{99m}Tc-radiopharmaceuticals (Guérin, et al., 2010; Martini, et al., 2015; Pupillo, et al., 2016).

Moreover, to accomplish the monograph criteria, cyclotron-produced pertechnetate should be evaluated from the Chemical and Radiochemical purity point of view by standard quality controls such as colorimetric and chromatographic.

To check the quality of our product, all quality controls have been conducted after each production following the monograph specifications. Paper chromatography was carried out on Whatman 1 strips using methanol/water (8:2) and Physiological solution as mobile phases, Chromatograph Cyclone Plus Storage Phosphor System and Software Optiquant ™.

Kit Merckoquant Molibdeno 5-250 mg/L was purchased from Merck (Darmstadt, Germany) and Kit Tec-Control Aluminium Breakthru from Biodex (Shirley, New York, USA).

Table 17 A comparison between fission, non-fission and accelerator produced sodium pertechnetate (^{99m}Tc) injection. (RCP: radiochemical purity[8]; CP: chemical purity; RNP: Radionuclidic purity).

Sodium Pertechnetate (^{99m}Tc) injection		
FISSION	**NON FISSION**	**ACCELERATOR-PRODUCED**
Obtained from Molybdenum-99 produced by neutron irradiation of molybdenum	Molybdenum-99 extracted from fission products of uranium	Proton irradiation of highly enriched molybdenum-100
Identification γ-photon at 0.141 MeV	γ-photon at 0.141 MeV	γ-photon at 0.141 MeV
	Chromatogram RCP Retardation factor 0.6	Chromatogram RCP Retardation factor 0.8
^{99}Mo < 0,1 %*	^{99}Mo < 0.1 %*	^{99}Mo < 0.005 %*
^{131}I < 5 × 10^{-3} %*	-	-
^{89}Sr < 6 × 10^{-5} %*	-	-
^{103}Ru < 5 × 10^{-3} %*	-	-
^{90}Sr < 6 × 10^{-6} %*	-	-
α-emitting impurities < 1 × 10^{-7} %*	-	-
-	-	^{96}Nb < 0.005 %*
-	-	^{97}Nb < 0.005 %*
RNP -	-	^{93m}Tc < 0.01 %*
-	-	^{93}Tc < 0.04 %*
-	-	^{94m}Tc < 0.02 %*
-	-	^{94}Tc < 0.04 %*
-	-	^{95}Tc < 0.07 %*
-	-	^{96}Tc < 0.07 %*
-	-	^{95m}Tc < 0.005 %*
-	-	^{97m}Tc < 0.01 %*
Other γ-emitting impurities < 0.01%*	Other γ-emitting impurities < 0.01%*	Other γ-emitting impurities < 0.02%*
RCP Descending paper chromatography Mobile phase: Water:Methanol (20:80 V/V) Retardation factor: 0.6 >95% §	Descending paper chromatography Mobile phase: Water:Methanol (20:80 V/V) Retardation factor: 0.6 >95% §	Ascending paper chromatography Mobile phase: sodium chloride in water (9g/L) Retardation factor: 0.8 >95% §
pH 4-8	4-8	4-8
CP: Al < 5ppm	< 5ppm	< 5ppm

*of the total radioactivity

§of the total radioactivity due to ^{99m}Tc

---

[8] The radiochemical purity (RCP) can be defined as the percentage of the total activity of a specific radionuclide in a specific chemical form.

All measurements in gamma spectrometry were performed by using a High-Purity Germanium (HPGe) detector and reported at the End Of Bombardment (EOB) time. Radionuclides were identified from the acquired spectra by software Genie 2000 (Canberra, Meriden, USA). Efficiency calibration was performed between 59 and 1836 keV through a multipeak certified source (LEA SEARCH Areva, France). Calibration was performed according to the standards IEC 61452 (IEC, 1995) using the Genie 2000 software (Canberra, Meriden, USA), and has been verified on the day before the experiment.

Dose Calibrator Capintec CRC-15R (Ramsey, NJ, USA) was used for generator eluted pertechnetate activity measurements.

Gas-chromatography (GC) was performed using Agilent-Pal H6500-CTC injector, gas-chromatograph Agilent Gc 6850 Series II Network, mass spectrometry detector (MS) Agilent Mass Selective Detector 5973 Network and column Agilent J&W DB-624 UI (20m, 0.18mm, 1.00u) was used for chromatographic separation.

The operating conditions of the headspace were: incubation time: 50 min; incubation temperature: 80 °C; magnetic stirring speed: 250 rpm. The column oven temperature was set at 35 °C and remained constant during 4 min. After this time, the temperature was raised up to 240 °C at 15 °C/min. A constant column flow of 0.7mL/min of helium was used.

Radionuclidic, chemical and radiochemical purity values are reported in *Table 18*. Purity values of final pertechnetate saline solution meet the values requested by European Pharmacopoeia for the generator obtained product (Ph. Eur. , 2016a). In particular, the residual content of MEK in the final Na[^{9x}TcO$_4$] solution, obtained by gas-chromatography, was considerably less than 0.5% v/v (Ph. Eur., 2016c). RNP of the final ^{99m}Tc-pertechnetate solution was higher than 99% as deductible from Table 18, however, a more detailed evaluation of ^{9x}Tc impurities is described hereafter. Traces of other accelerator-Tc nuclides different from ^{99m}Tc were detected and monitored during their decay by a set of gamma spectrometry measurements both at short and long acquisition times in automatic mode. This small amount of ^{9x}Tc isotopes, like ^{93}Tc, ^{94}Tc, ^{95}Tc and ^{96}Tc cannot be chemically separable from ^{99m}Tc and therefore they are selectively extracted by MEK from the aqueous phase. Instead, ^{9x}Mo, ^{9x}Nb and other impurities, co-produced during the irradiation of the ^{100}Mo enriched target, are retained in the aqueous phase as shown in *Figure 20* and *Table 19*.

Table 18 Radionuclidic (RNP), Chemical (CP) and Radiochemical (RCP) Purity values of the [^{9x}Tc]TcO$_4^-$ solution obtained at the end of the automatic procedure. (MDA=Minimum Detectable Activity, ^{9x}Tc not included ^{99m}Tc);* (Ph. Eur. , 2016a; Ph. Eur., 2016b; Ph. Eur., 2016c; Ph. Eur. , 2017); $^¤$ sum of all'Tc-9x isotopes other than Tc-99m detected in the product; § in the European Pharmacopoeia there is no indication on Mo chemical purity evaluation.

Parameter		MEK separation	EU Phar.*
RNP	^{96}Nb	<MDA	<0.005%
	^{97}Nb	<MDA	<0.005%
	^{99}Mo	<MDA	<0.005%
	^{9x}Tc$^¤$	<0,.242$^¤$	<0.265%$^¤$
CP	pH	4,5-5	4-8
	Mo	<5ppm	§
	Al	<5ppm	<5ppm
	MEK	<0.0004% (v/v)	<0.5% (v/v)
RCP	^{99m}TcO$_4^-$	>99%	≥95%

Figure 20 Distribution of radionuclides in the different components of the automatic module. For sake of simplicity, the standard deviation (SD) was not reported.

Quality controls on the final product have always demonstrated high purity levels, in compliance with the limits imposed by the Pharmacopoeia. In particular CP and RCP were found to be respectively Al<5ppm and [^{99m}Tc]TcO$_4^-$ > 99%, while RNP, at the end of the purification process, was evaluated being in the range 99.6 - 99.8 %. An example of qualitative and quantitative isotopes identification in the final product is reported in *Table 20*.

Table 19 Percentage and SD of Tc, Mo and Nb radionuclides activity (decay corrected at the end of the separation (EOS)) in different components of the automatic module. (ND=Non Detectable).

%	^{9x}Tc	^{99}Mo	^{9x}Nb
Final Solution	93.22±0.05	ND	ND
Aqueous Phase	5.75±0.02	97.96±0.04	98.31±0.03
Waste	0.03±0.01	ND	ND
Washing	0.55±0.01	2.04±0.04	1.69±0.05
Silica Column	0.22±0.01	ND	ND
Alumina Column	0.23±0.01	ND	ND

Table 20 Gamma spectra analysis of the radionuclides detected in the final pertechnetate solution obtained from the automatic module (decay corrected at EOS).

Radionuclide	$T_{1/2}$	Activity (Bq)	Uncertainty (Bq)	Activity (Rel.)
Tc-93g	2.8h	1.38E+05	1.41E+04	0.009%
Tc-94g	4.9h	1.38E+06	3.12E+04	0.094%
Tc-95g	20h	1.56E+06	4.61E+04	0.107%
Tc-95m	61d	1.32E+04	9.74E+02	0.001%
Tc-96g	4.3d	4.47E+05	4.72E+03	0.031%
Tc-99m	6.01h	1.46E+09	2.48E+07	99.758%

2.5 Radiopharmaceuticals Preparation

From the radiopharmaceuticals' preparation point of view, there are no differences in the radiolabeling strategy that can be applied for the preparation of cyclotron- or generator-produced ^{99m}Tc- radiopharmaceuticals. The same general procedures for the preparation of generator-produced ^{99m}Tc could be easily applied to the preparation of the analogs cyclotrons produced ^{99m}Tc-radiopharmaceuticals.

Obviously it is necessary to keep in mind the different conditions due to the possible presence of different technetium isotopes in the cyclotron produced ^{99m}Tc, in particular the different SA due to the presence of the co-produced ^{99g}Tc, that is not chemically separable from ^{99m}Tc. As proved by (Uccelli, et al., 2013) the RCP and chemical purity (CP) of some radiopharmaceuticals are not affected by different ^{99g}Tc/^{99m}Tc ratio up to 11.84, corresponding to a generator eluate eluted 72 h after the last elution. This ratio is largely above the expected ratio for cyclotron-produced ^{99m}Tc evaluated by (Esposito, et al., 2013), whose yield ratio was in the range 3.09–4.35 depending on irradiation conditions (considering a Mo-100 enrichment of 99.05%). Moreover, we evaluated that ^{99g}Tc/^{99m}Tc ratio remains below 11.84 up to 5 or 9 hours after the EOB for a 6 hours' irradiation run at 25 MeV or a 1 hour irradiation run at 15 MeV respectively.

The pertechnetate obtained as above was used to assess the efficacy of labelling of selected commercial radiopharmaceuticals kits [HMPAO Hexamethylpropyleneamine Oxime, CERETC^{TM}), ^{99m}Tc-Tetrofosmin (MYOVIEW^{TM}), ^{99m}Tc-methylene diphosphonate ^{99m}Tc-MDP, ^{99m}Tc-L, L-ethylene cysteinate dimer ^{99m}Tc-ECD, purchased from GE HEALTHCARE SRL (Milano, Italy)] and compared with the analogous diagnostic agents prepared using the generator-produced pertechnetate. RCP of the commercial radiopharmaceuticals kits, was performed as requested by the manufacturer.

With the aim to verify the reproducibility of technetium chemistry with medical-cyclotron-produced technetium-99m a preliminary experiment was carried out. The non commercial [^{99m}Tc]TcN-DBODC$_2$ compound was prepared using the same chemical procedure starting from both the cyclotron produced pertechnetate and generator one. The ligand N,N'-bis(ethoxyethyl)dithiocarbamato sodium salt (DBODC) was purchased from Alchemy, Altedo, Italy. Stannous chloride dihydrate, succinic dihydrazide (SDH), and ethylenediaminotetraacetic acid (EDTA) were obtained from Sigma–Aldrich, Milan, Italy. The preparation of [^{99m}Tc] N-DBODC$_2$ was performed as previously reported (Esposito, et al., 2015). RCP of the [^{99m}Tc] N-DBODC$_2$ was determined by thin-layer chromatography (TLC). TLC was performed on silica gel plates (Merck) with ethanol: chloroform: toluene: NH$_4$Ac (0.5 M) (5:3:3:0.5) as the mobile phase (Rf = 0.9) and on reversed-phase C18 plates (Merck) with saline: methanol: tetrahydrofuran: glacial acetic acid (2:8:1:1) as the

mobile phase (Rf = 0.4). The RCP of the cyclotron and generator produced nitride technetium-99m complex was >95% as determined by chromatographic methods.

The stability of ^{99m}Tc-RF was checked for the time of expiry indicated by the manufacturer in the case of commercial radiopharmaceuticals kit and to 6 hours for the [^{99m}Tc] N-DBODC$_2$ compound.

Analogous studies on the preparation of selected cyclotron-produced ^{99m}Tc-RFs are still reported in literature (Chattopadhyay, et al., 2012; Guérin, et al., 2010), but there are no studies that reported indication on the stability of the cyclotron-produced radiopharmaceuticals.

We found that the RCP of cyclotron and generator ^{99m}Tc-RFs were comparable both at the end of the preparation, and at the expiry time (*Table 21*). [^{99m}Tc] N-DBODC$_2$ compounds were found to be stable until 6 hours from the preparation. Additional studies on nitride technetium chemistry (Boschi, et al., 2013; Boschi, et al., 2012) starting from cyclotron produced pertechnetate, not reported in this work, are under investigation.

Table 21 Radiochemical purity of selected 99mTc-labeled radiopharmaceuticals. (G: generator produced; C: cyclotron produced). (n=3)

Compound	RCP at labeling time(%)	RCP at expiry time (%)
[^{99m}Tc]Tc-HMPAO *(G)*	93.02 ± 1.05	87.51 ± 2.42
[^{99m}Tc]Tc-HMPAO *(C)*	94.01 ± 2.11	86.41 ± 1.40
[^{99m}Tc]Tc-Tetrofosmin *(G)*	97.03 ± 0.76	96.07 ± 0.36
[^{99m}Tc]Tc-Tetrofosmin *(C)*	96.73 ± 0.55	95.83 ± 0.50
[^{99m}Tc]Tc-MDP *(G)*	98.22 ± 0.08	97.15 ± 0.17
[^{99m}Tc]Tc-MDP *(C)*	97.22 ± 0.14	96.10 ± 0.65
[^{99m}Tc]Tc-ECD *(G)*	99.01 ± 0.18	98.54 ± 0.12
[^{99m}Tc]Tc-ECD *(C)*	98.87 ± 0.03	97.58 ± 0.33
[^{99m}Tc]TcN-DBODC$_2$ *(G)*	98.51 ± 0.25	97.81 ± 0.35
[^{99m}Tc]TcN-DBODC$_2$ *(C)*	97.99 ± 0.11	96.13 ± 0.09

2.6 Imaging Studies

In order to get a full comparison of imaging performance, between cyclotron produced-[99mTc] and generator-[99mTc], tests were performed on a standard Siemens E.CAM dual-headed gamma camera dedicated to clinical applications. Each head is equipped with sodium iodide crystal (3/8 inches thick) and a Low Energy High-Resolution collimator (spatial resolution nominally 7.5mm @10cm). The gamma camera has wide motion capabilities with flexible patient positioning for planar imaging, whole-body scans, cardiac and general SPECT studies.

An aliquot of pertechnetate sample, either cyclotron or generator obtained, was used for spatial resolution imaging measurements, following standard protocols (according to The Association of Electrical Equipment and Medical Imaging Manufacturers-NEMA guidelines) for control system and quality assurance. In order to assess the planar spatial resolution and tomographic performance of the gamma camera, a 9 point-like sources planar grid phantom and a Jaszczak phantom (IAEA, 2009c) were used respectively (*Figures 21 and 22*).

Figure 21 Planar image of the grid phantom obtained using cyclotron-produced [$^{99m}Tc]TcO_4^-$ 8 hours after EOB.
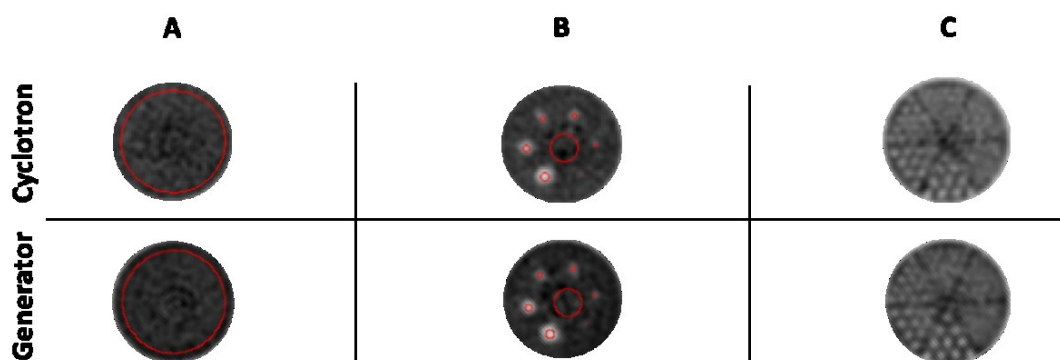
*Figure 22 Tomographic images of the Jaszczak phantom, obtained using generator-
(bottom) and accelerator-produced (top) [^{99m}Tc]TcO4-. A: uniformity zone for the
determination of uniformity and noise values; B: cold sphere zone for the determination of
contrast; C: cold rod for visual quality evaluation (Rod diameters, 4.8, 6.4, 7.9, 9.5, 11.1
and 12.7 mm).*

The planar grid phantom having 9 small holes at a mutual distance of 5 cm in the cross points of a rectangular net, was filled in with 1 µl volume of pertechnetate sample and placed 10 cm distance from the acquiring head of the gamma camera. The initial activity of each point-like source was about 185 kBq (5µCi). The acquisitions times were set at 30 minutes, with 1024 × 1024 matrix (pixel dimensions: 0.6 × 0.6 mm). The first acquisition was made 8 hours after the EOB (see Fig. 5), while the second one 12 hours afterwards. In order to determine the spatial resolution in term of FWHM, both images were analyzed by the Sun-Java-based ImageJ software (Dougherty, 2009), considering profiles with a width of a 1 pixel along the X (horizontal) and Y (vertical) direction profiles. For comparison, the same protocol was applied to both generator-eluted and cyclotron-produced [^{99m}Tc]TcO$_4^-$.

The comparison between the tomographic imaging performance of the gamma camera obtained with cyclotron and generator technetium-99m, was performed by using a Jaszczak Flangeless Deluxe SPECT Phantom (Biodex). The phantom was filled with 259 MBq (7 mCi) ^{99m}Tc and 5650 ml H$_2$O. The tomographic acquisition was performed by using the following parameters: duration 60 minutes, angular step 3°/frame, time 60 s/frame, angle of rotation 180°, matrix dimensions of reconstructed slices 128 × 128. The image reconstruction was performed using the Filtered Back Projection method (FBP), considering a slice thickness of 4.795 mm, and was corrected for attenuation by using Chang method with linear attenuation value µ=0.11 cm^{-1}. Images of Jaszczak phantom, obtained using accelerator-produced

[^{99m}Tc]TcO$_4^-$ are shown in *Figure 5*. The spatial uniformity and noise, calculated as standard deviation of counts, were evaluated by considering a Region Of Interest (ROI) in the upper uniform region of the phantom. The contrast resolution was calculated by considering 6 different ROIs centered on the 6 spheres, located in the upper sector of the phantom. The same protocol was applied to a phantom filled with generator-eluted [^{99m}Tc]TcO$_4^-$.

As regards planar imaging (*Figure 21*), the obtained values for the FWHM in X and Y directions are shown in *Table 22*. For each point source analyzed, FWHM values are all statistically comparable and well within the uncertainties (considering 95% of confidence level), for both X and Y directions, with the reference values of 7.40 ± 0.29 mm and 7.38 ± 0.16 mm respectively obtained with technetium-99m eluted from a molybdenum-99/technetium-99m generator.

As regards the tomographic imaging performance, images show no significant difference between the phantoms filled with cyclotron- and generator-produced technetium-99m in term of noise, spatial resolution, contrast and uniformity (*Figure 22*) quantitatively in accordance with the routine variation of those parameters for generator-obtained ^{99m}Tc-pertechnetate acquisition. The results from the tomographic comparison tests obtained with Jaszczak phantom are reported in *Table 23*.

These results are consistent with the conclusions drown in the recent imaging studies on cyclotron produced technetium-99m from (Hou, et al., 2016 b) and (Selivanova, et al., 2015).

Quantitatively, contrast is consistent with the variability observed in routine acquisitions for clinical quality controls, however further investigations are required as regards the noise evaluation, with this parameter being heavily affected by the presence of impurities (^{9x}Tc isotopes different from ^{99m}Tc). Moreover, the presence of these undesired radioactive contaminants in the final product affect the increase of the injected patient dose. While radionuclidic impurities corresponding to various molybdenum (^{9x}Mo) and niobium (^{9x}Nb) contaminant isotopes can be minimized, thanks to the settled efficient chemical procedures for the separation of radiometals, purification of ^{99m}Tc from others ^{9x}Tc contaminant isotopes is instead unfeasible, since they may not be separated, being basically of the same chemical element. The only way to control their amount is thus limiting their production by increasing (i) as much as possible the ^{100}Mo-enrichment of the target material and (ii) having a

well-established beam irradiation (i.e. optimal energy range/irradiation time) parameters.

Table 22 Average FWHM spatial resolution of Siemens E.CAM gamma camera calculated from the planar grid phantom images. Spatial resolution measured using [^{99m}Tc]TcO4$^-$ eluted from a ^{99}Mo/^{99m}Tc generator is also shown.

Measured FWHM spatial resolution of gamma camera (mm)				
	8 hours after EOB		20 hours after EOB	
Measured point-like source	X direction	Y direction	X direction	Y direction
1	7.43	7.43	7.46	7.42
2	7.35	7.48	7.51	7.38
3	7.28	7.68	7.35	8.04
4	7.24	7.81	7.64	8.07
5	7.65	7.94	7.90	8.31
6	7.72	7.85	7.86	7.97
7	7.44	7.55	7.80	7.82
8	7.62	7.51	7.98	7.52
9	7.41	7.38	7.54	7.77
Overall spatial resolution Cyclotron-^{99m}Tc	7.46 ± 0.17	7.63 ± 0.20	7.67 ± 0.22	7.81 ± 0.32
	X direction		Y direction	
Overall spatial resolution Generator-^{99m}Tc	7.40 ± 0.29		7.38 ± 0.16	

Table 23 comparison between uniformity noise and contrast of tomographic tests obtained with Jaszczak phantom with Tc-99m generator-eluted and cyclotron-produced

	Generator-eluted ^{99m}Tc	Cyclotron-produced ^{99m}Tc
Tomographic Uniformity	15.2%	17.0%
Noise	9.7%	11.6%
Contrast sphere 31.8 mm	68.5%	67.0%
Contrast sphere 25.4 mm	57.0%	52.0%
Contrast sphere 19.1 mm	36.7%	37.9%
Contrast sphere 15.9 mm	30.0%	35.3%
Contrast sphere 12.7 mm	21.8%	19.5%
Contrast sphere 9.5 mm	8.3%	13.7%

In vivo multimodality imaging studies (SPECT-CT) were performed by using both the generator- and accelerator-produced ^{99m}Tc-pertechnetate and the labeled radiopharmaceuticals (RF): HMPAO (CERETC^{TM}) and tetrofosmine (MYOVIEW^{TM}). Molybdenum ^{100}Mo (99.05%) metal targets, were irradiated at JRC-ISPRA (VA, Italy). The energy was chosen in order to test the effectiveness of the chemical separation procedure having a mixture of different Tc-radionuclides yielded. Targets were then treated with the automatic, MEK-based SE method, module system. An aliquot of the final elute was finally added to RF kit, following the standard preparation procedure. The determination of RNP of the 99mTc-eluate was performed by standard γ-spectrometry and the determination of RCP of ^{99m}Tc-pertechnetate, ^{99m}Tc-HMPAO and ^{99m}Tc-tetrofosmine was checked by radio-TLC. WISTAR rats, previously anesthetized, were injected into the jugular vein using generator- and cyclotron-99mTc pertechnetate, HMPAO and tetrofosmine. All the experimental procedure was carried out strictly following the current regulation. Whole-body SPECT-CT biodistribution studies were carried out with the hybrid YAP(S)PET-CT small-animal scanner (Del Guerra, 2006) shown in *Figure 23*.
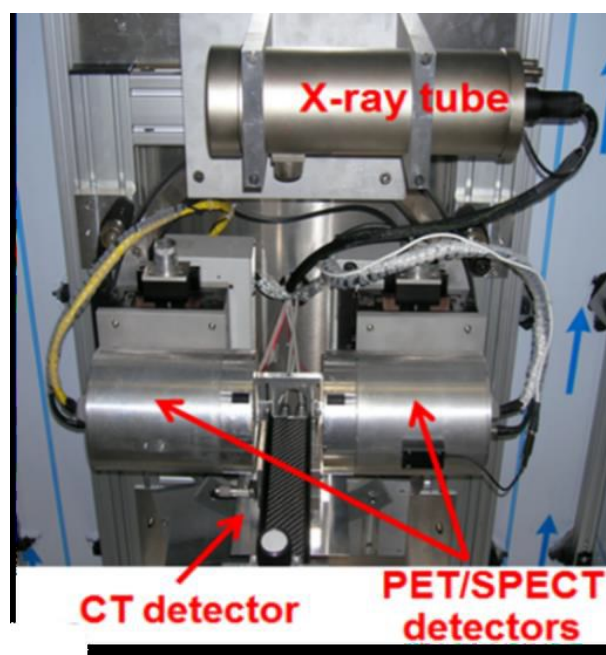
Figure 23 The YAP-(S)PET-CT scanner for small animals.

CT images have been acquired, by using optimized parameters, and corrected for non-uniformity of the beam and detector response (*flat image*), dark current and readout noise (*dark image*). SPECT-images were corrected for injection time, injected activity and reconstructed by using the iterative Expected Maximization-Maximum Likelihood (EM-ML) technique, with the possibility to include scatter correction. In case of accelerator-produced Tc, the scatter contribution due to higher-energy γ-rays emitted in the decay of some Tc-isotopes (shown in *Table 24*), has been corrected by selecting appropriate energy windows. On the other hand, the standard spectral energy range [140-250] keV has been selected to get the imaging reconstruction of the generator ^{99m}Tc-labelled pharmaceutical.

In vivo SPECT-CT preclinical imaging studies in a rat animal model, by using a high-resolution small-animal scanner, confirmed a superimposable biodistribution behavior of heart and brain perfusion of 99mTc-radiopharmaceuticals labeled with both cyclotron- and generator-produced Tc. As an example, one of the preliminary imaging test showing the biodistribution comparison, using the ^{99m}Tc-labelled MYOVIEW pharmaceutical is shown in *Figure 24*.

Table 24 Technetium isotopes detected in the cyclotron produced tc-eluate and decay properties (NuDat, 2.7).

Isotope (half-life)	γ-ray energy [keV] (Int.%)
Tc-99m (6.01 h)	140.511 (89)
Tc-93 (2.75h)	1362.9 (66.2)
Tc-94g (4.88 h)	702.7 (99.6)
	849.7 (95.7)
	871.1 (99.9)
Tc-95g (20.0 h)	765.8 (93.8)
	1073.7 (3.74)
Tc-96g (4.28 d)	778.2 (99.8)
	812.5 (82)
	849.9 (98)
	1126.9 (15.2)
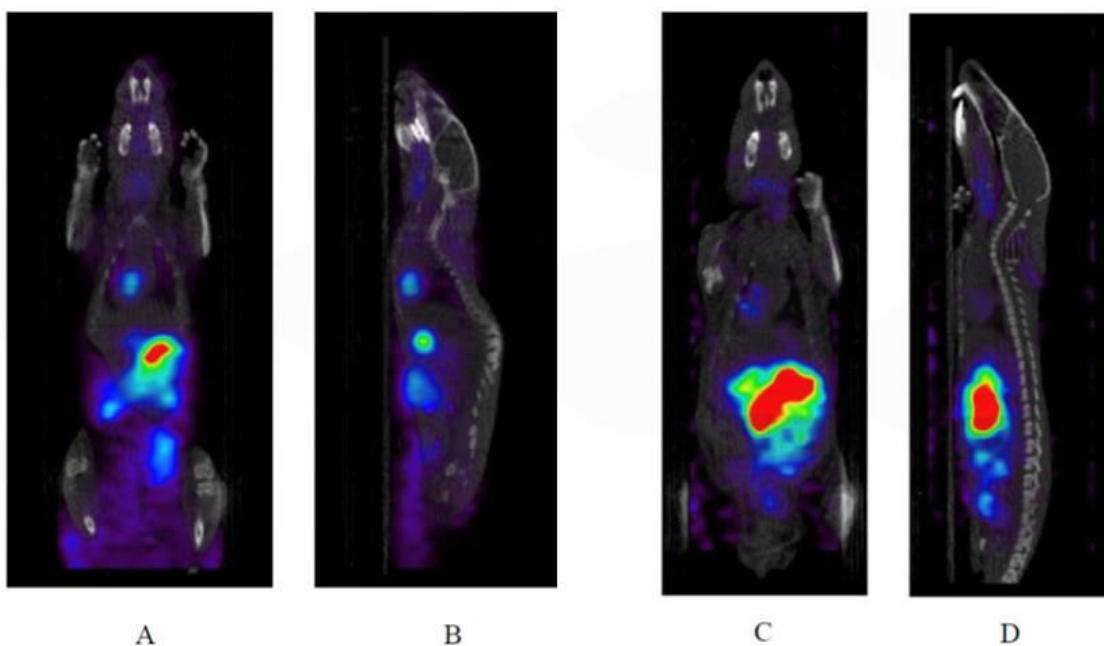
Figure 24 One of the preliminary in-vivo comparison of experimental imaging result studies about the ^{99m}Tc-labelled MYOVIEW radiopharmaceutical. Images marked A and B show the coronal and sagittal sections of SPECT-CT scans of a rat using generator labeled compound. Images C and D show the same scans but using the accelerator-^{9x}Tc instead. (Correction for injection time and activity)

2.7 Target Recovery Studies

The target recovery is a very important step to complete the ^{99m}Tc production cycle. Indeed, the natural abundance of ^{100}Mo (9.63%) and the need for a highly enriched target, to achieve high RNP and IP, makes the target very expensive, thus target recycling is very attractive (Gagnon, et al., 2012). A deep evaluation of the ^{100}Mo recovery strategy needs to be done in order to keep the ^{99m}Tc production costs within affordable limits and the IP and RNP of the final product, from recycled target, within the Pharmacopoeia limits.

No matter which procedure is used for the extraction of ^{99m}Tc from the target, a residual Tc-depleted molybdate alkaline (pH>9) water solution will be the starting point of the recycling process.

This solution may need further purification prior to the reduction in order to remove contaminants (e.g. resin, or organic solvent traces) and impurities (e.g. Nb-, Ru- etc.- radionuclides coming from the irradiation or from decay chain) like pre-reduction SE purification of molybdenum as suggested by (Das, et al., 2016a). Depending on the chemical form of the molybdate, sodium-, potassium- or even

72

ammonium-molybdate, the first step for the target recovery consists in the decomposition of the molybdate anion MoO_4^{2-} into molybdenum trioxide MoO_3 by precipitation-filtration (Kar, et al., 2004), temperature/atmosphere-controlled baking (Gagnon, et al., 2012) or cation exchange chromatography (Benard, et al., 2014a; Hanemaayer, et al., 2014). Once the molybdenum trioxide obtained, in order to achieve the metallic form, a two-step hydrogen reduction is needed. The first step is the exothermic conversion of MoO_3 to MoO_2 with a ramp rate between 500 and 750 °C in low concentration H_2 gas atmosphere, while the second step consists in the reduction of MoO_2 to Mo metal up to 1100 °C in H_2 100% atmosphere (Gagnon, et al., 2012). To evaluate the reduction efficiency and the isotopic composition XRD (X-ray diffraction) and Inductively Coupled Plasma Mass Spectrometry (ICPMS) characterization techniques need to be applied to the recycled sample (Gagnon, et al., 2012; Das, et al., 2016a). Gagnon et al. 2012 reported a complete recovery cycle achieving an overall metal to metal yield of 87%.

Furthermore, the recycled [100]Mo has been used to produce [^{99m}Tc][TcO_4]⁻ with quality parameters comparable to generator-derived [99m]Tc (Gagnon, et al., 2012).

In our experience, the residual alkaline aqueous fraction containing Mo (sodium molybdate and permolybdate), after the extraction of ^{99m}Tc with the automatic module, was chemically processed to recover the enriched Mo material under MoO_3 form. In order to remove the large amount of NaOH from the solution, first, the transformation of sodium permolybdates into molybdic acids and MoO_3 (main product) was realized by refluxing for 8 hours in an excess of HNO_3 (5M) followed by water evaporation. Then, the separation of molybdic acids and MoO_3 from the $NaNO_3$, based on the difference in their water solubility, was performed by repeated dissolution in a small amount of water, followed by centrifugation and separation from mother liquor of the precipitate. When dried in vacuum at 40ºC the precipitate resulted in MoO_3 white powder.

Finally, preliminary experiments on molybdenum recovery have been carried out. We recovered more than 90% of the molybdenum target material in the trioxide chemical form of and we have been spending our effort on getting a refinement of the developed technology. The goal is to recover molybdenum in metal form, with the aim to minimize the final cost per each injected accelerator-^{99m}Tc dose, caused by the expensive staring enriched material.

In the years to come, it would be important to demonstrate how many times the target can be recycled before exceeding the Pharmacopoeia limits for impurities and

to establish at what extent the price of the cyclotron-produced pertechnetate dose can be reduced.

2.8 Project Results

The purpose of this work was the development of a technology able to produce GBq amount of technetium-99m by cyclotron in a local nuclear medicine radiopharmacy and to proof its feasibility. Preliminary investigations pointed out the direct accelerator-^{99m}Tc production via the ^{100}Mo(p,2n) reaction route are favorable for this purpose.

After preliminary theoretical investigation on the most appropriate irradiation conditions, (Esposito, et al., 2013), and the development of an efficient extraction and purification procedure (Martini, et al., 2016), we spent our effort in optimizing all the production aspects in order to fit the Nuclear Medicine Hospital Radiopharmacy needs.

Firstly, a target holder, able to fit different types of target configurations and the solid target station components, has been designed (*Figure 13*). Then, the automated purification procedure previously developed has been adapted to the new target characteristics and optimized for a production scale (*Figure 17*). In particular, the dissolution procedure has been optimized for the treatment of target masses up to 350 mg and different target configurations, such as multiple foils, single coin, or thick/thin film deposited on a backing material with different techniques. All quality controls have been updated to the recently approved monograph on sodium pertechnetate (^{99m}Tc) (accelerator-produced) injection in the European Pharmacopoeia 9.3 (Ph. Eur. , 2017). Labeling and preclinical imaging studies on phantoms have been conducted to assess the equivalence of the image quality obtained with cyclotron and generator ^{99m}Tc-pertechnetate. Finally, in order to shed light and come to a real closed-loop production scheme, the recovery of the ^{100}Mo-enriched moly target material after the extraction/separation procedure has been studied and different steps determined.

The efficiency of such a technology developed has been repeatedly verified through complete production cycles. Molybdenum metal foils approach, produced by lamination technique and clamped together within the target holder in a stack-foil configuration, was assessed first; they were irradiated by a proton beam under

different irradiation conditions and transferred to the reactor of the automatic extraction module for the three step dissolution process, under helium flux at 90°C (Martini, et al., 2016). The main advantage of such a procedure allows to use always fresh pure hydrogen peroxide to react and oxidize the metal target, thus avoiding the passivation of the target surface. The whole procedure, comprehensive of the dissolution step, takes about 60 min (10 minutes less than the previous one (Martini, et al., 2016) and the recovery yield is about 93 ± 3 % decay corrected.

Quality controls on the final product have always demonstrated high purity levels, in compliance with the limits imposed by the Pharmacopoeia. In particular CP and RCP were found to be respectively Al<5ppm and $[^{99m}Tc]TcO_4^-$ > 99%, while RNP, at the end of the purification process, was evaluated being in the range 99.6 - 99.8 %.

In order to test the RCP and stability of cyclotron-produced ^{99m}Tc-RFs, selected commercial kits were used for the preparation of standard clinically used ^{99m}Tc-labeled radiopharmaceuticals. We found that the RCP of cyclotron and generator ^{99m}Tc-RFs were comparable both at the end of the preparation, and at the expiry time (Table 21). With the aim to verify the reproducibility of technetium chemistry with medical-cyclotron-produced technetium-99m, a preliminary experiment on [cyclotron-^{99m}Tc]TcN-DBODC2 compound preparation was carried out. The RCP of the cyclotron and generator produced nitride technetium-99m complex was >95% as determined by chromatographic methods. Both compounds were found to be stable until 6 hours from the preparation.

Moreover, phantom imaging studies were conducted in order to compare image quality obtained with accelerator- and generator-produced $[^{99m}Tc]TcO_4^-$ by using a clinical gamma camera. No significant differences have been found using ^{99m}Tc produced by cyclotron compared ^{99m}Tc generator products. In particular, the spatial resolution in both directions was comparable within experimental errors. Concerning tomographic performance, any variation in spatial resolution, noise, contrast, and uniformity have been found by comparing images of Jaszczak phantoms filled with ^{99m}Tc of different origin. Quantitatively, the contrast is in line with the routine variation of this parameter. Finally, preliminary experiments on molybdenum recovery have been carried out. We recovered more than 90% of the molybdenum target material in the trioxide chemical form.

3 TRIUMF EXPERIENCE ON Tc-99m CYCLOTRON-PRODUCTION

At TRIUMF I had the opportunity to collaborate at the project named "A Trans-regional initiative to achieve large scale production, distribution, supply and commercialization of Tc-99m" by contributing at the optimization and automation of the dissolution and purification procedure of cyclotron-produced ^{99m}Tc. This project has the aim to scale-up and validate an alternative production and purification method for cyclotron-produced Tc-99m.

The Canadian research group holds the world record for the production of Tc-99m by cyclotron (1 TBq after 6h irradiation at 24 MeV and a beam current of 450 µA) (Hoehr, et al., 2017). With a view to the decentralization of the Tc-99m cyclotron-production, they have developed the technology for the complete production cycle for the GE PETtrace 16, TR 19 and TR 24 MeV cyclotrons. The developed technology consists in:

- three target model for the three nominal cyclotrons, in particular Mo-100 deposited by electrophoretic deposition (EPD) on a tantalum backing plate for TR 19 and TR30 (operated at 24 MeV) cyclotrons or pressed, sintered and brased on a copper backing for the GE PETtrace 16MeV cyclotron (Hanemaayer, et al., 2014; Zeisler, et al., 2014);
- extraction and purification of the cyclotron produced ^{99m}TcO$_4^-$ by solid phase extraction (SPE) based on chromatographic columns (Benard, et al., 2014b; Morley, et al., 2012a);
- establish a method for ^{100}Mo recovery and recycling.

In Canada this is a sensitive topic since the imminent shut down, planned for March 2018 (Osborne, 2016), of the Nuclear Reactor NRU in Chalk River (ON, Canada) that was covering over 40% of Mo-99 global market (National Academies of Sciences, 2016). For this reason, some details on the conducted experiments during my stay there, were to be considered confidential and are not presented here.

For this project I was first tasked with the optimization of the dissolution procedure of the especially designed target for a TR30 cyclotron and later for the automation on an IBA Synthera® Extension module of the already optimized separation procedure of Tc from molybdenum target and impurities.

3.1 Target Dissolution

Materials and Methods

The TR30 target consists in electrophoretic deposited molybdenum metal (^{Nat}Mo~1.3 g was used instead of enriched ^{100}Mo for optimization tests) on Tantalum backing plate covering a central rectangular ~ 10cm^2 surface. On the back of the Tantalum plates, some grooves allow a better heat exchange, during the irradiation, thanks to the higher contact surface with the cooling system in the solid target station (*Figure 25*) (Zeisler, et al., 2014; Schaffer, et al., 2015a). The target is originally placed in an aluminum target holder that allow all the connections in the cyclotron solid target station and in the dissolution system once pneumatically transferred in the hot cell.
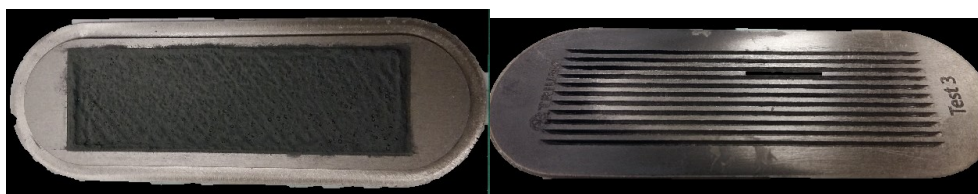
Figure 25 TR30 Target: EPD ^{Nat}Mo on tantalum backing plate (both sides).

In order to simulate the dissolution system in the hot cell, a 3D printed dissolution chamber has been realized with the same dimensions and characteristic of the original one with the addition of a transparent window that allow us to see the evolution of the dissolution process. (*Figure 26*)
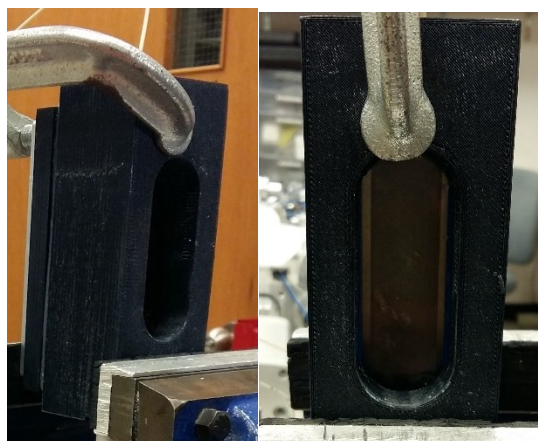
Figure 26 The 3D printed dissolution chamber

The procedure strategy consists in a programmed re-cycle of hydrogen peroxide into the chamber to maximize the dissolution yield and minimize the dissolution time.

In our experiments we tested two different dissolution configurations by changing the collecting point inside the chamber (*Figure 27*):

1. the dissolution chamber is filled with hydrogen peroxide from the bottom and collected from the top cyclically;
2. the dissolution chamber is filled with hydrogen peroxide from the bottom and collected by means of a capillary PEEK tube inserted from the bottom of the chamber and goes up right after the molybdenum deposited surface, cyclically.
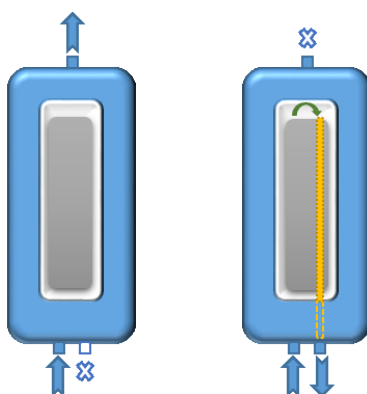
Figure 27 Two dissolution chamber configurations (left: UP-UP [↑↑]; right: UP-DOWN [↑↓]).

A peristaltic pump (WELCO WPX1-S3/32M4-BP model, powered by a tunable voltage power supply) allows the cyclical transfer of the hydrogen peroxide from a vial into the dissolution chamber and back to the same starting vial (see experimental apparatus in *Figure 28*).

Different programmed re-cycles have been tested (see *Experimental* section).
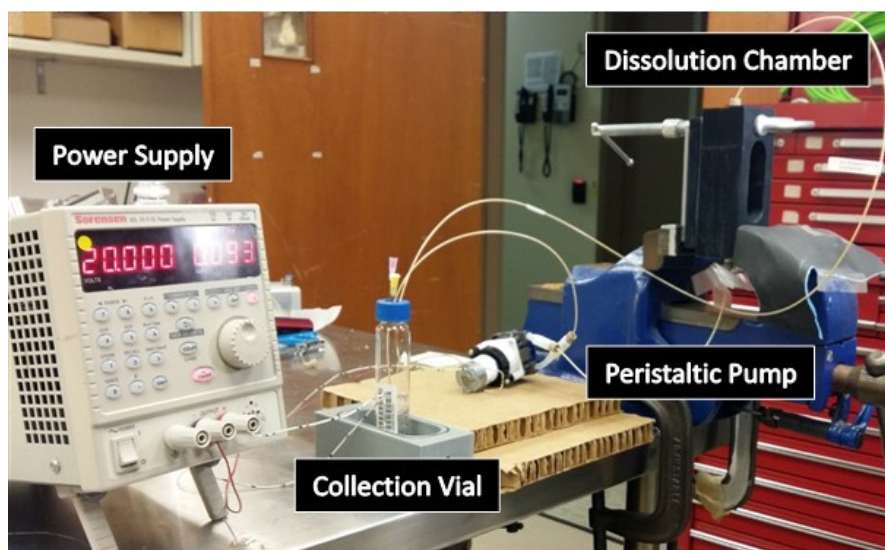
Figure 28 Experimental apparatus

Experimental

Several experiments were conducted to verify if there is any difference in the two dissolution configurations designated as UP-UP and UP-DOWN. 60 ml of fresh diluted Hydrogen peroxide were used and the re-cycle programmed procedure selected was: Pump ON (20 V - 16 rpm, 10 min); Pump OFF (0 V, 10min); Pump ON (20 V - 16 rpm, 10 min) (*Table 25, Figure 29*).

Table 25 Target Characteristics before and after dissolution tests. Instrument sensitivity 0.01 g.

#	configuration	Total Weight Before Dissolution	Total Weight After Dissolution	Weight difference (Moly dissolved)
		[g]	[g]	[g]
1	Up-Up ↑↑	63.52	62.47	1.05
2	Up-Down ↑↓	63.63	62.41	1.22
3	Up-Down ↑↓	53.82	52.57	1.25
4	Up-Up ↑↑	62.39	60.98	1.41

Figure 29 Targets after molybdenum dissolution tests (From left #1 to right #4).

Both configurations dissolved most of the molybdenum from the backing in about 30 min. Visual inspection of the dissolution reaction and of the target backing plate after dissolution did not reveal any substantial difference in the two configurations.

The following tests were conducted in the Up-Up ↑↑ configuration, selected for its geometrical and mechanical simplicity, but changing solvent volume, re-cycle programmed procedure and the plastic target holder component replaced with the original aluminum one in order to optimize dissolution time and yield (*Table 26*).

The new procedure selected includes 38 ml of fresh diluted Hydrogen peroxide and 30 min continuous re-cycle run with Pump ON (20 V – 16 rpm).

Table 26 Dissolution characteristics, percentage of molybdenum dissolved and pictures of targets after the dissolution.

#	Config.	Dissolved Mo %	Photo
5	↑↑	90.6	
6	↑↑	88.7	

Results

The tests described in this report are only some of the tests performed. The experiments not described here were failed for different reasons such 3D printed chamber or fitting leaks and bended tantalum backing plate (once also broken). The failure due to bended tantalum pointed out that tantalum backing plate may not be reusable. In fact, the metal bending may be due to the sintering step after the molybdenum EPD process on a recycled weakened target.

From test #1 to 4 turns out that there is no significant difference between the two dissolution configurations. Initially, a consistent excess of hydrogen peroxide was used for the dissolution tests, once defined the dissolution configuration, the volume was reduced to 38ml.

The final set of experiments pointed out that also with a continuous re-cycle procedure for 30 min, instead of turning the pump on and off twice as in the first 4 tests, the dissolution yield does not seem affected (around 90% yield). The idea of leaving the pump off for 10 min was to give time to hydrogen peroxide to react with molybdenum but, according to tests 5 and 6, the same, and maybe stronger efficacy considering that less H_2O_2 was used, can be reached in the same total time (30 min) with continuous cyclical flow. Moreover, a weak reaction has been noticed in the last test #6 and the dissolution yield confirms it. Our hypothesis is that this could be due to the changing in the target holder component material (aluminum instead of 3D

printed plastic). The hydrogen peroxide reaction with molybdenum metals is an exothermic reaction. When we were using only plastic components the insulating effect of plastic keeps the temperature in the reaction chamber high also under continuous re-cyclic flow of H_2O_2 (the H_2O_2 has time to cool down in the path between the exit and entrance to the dissolution chamber). When changing the plastic component with a metallic one, the heat dissipation decreases the temperature in the reaction chamber reducing also the reaction efficacy. Since the dissolution system placed in the hot cell is metallic, in order to keep the reaction vigorous in the dissolution chamber, the H_2O_2 should be kept warm outside the chamber with a hot plate or water bath.

Finally, as visible in all the pictures reported, the backing tantalum plate after deposition, dissolution and cleaning looks different from a new one. After cleaning, the rectangular area, on which molybdenum was deposited, a material, presumably residual molybdenum, was found. This needs to be proven by other tests or characterization analysis.

3.2 Tc-99m Separation and Purification Module Automation

Since the TRIUMF approach was to apply the already proven Tc-99m cyclotron-production process to different types and sizes of cyclotrons, I was tasked with installing, programming and testing a new purification module that would enable TRIUMF's team to expand and implement their overall process on a new brand of cyclotron, the IBA cyclone 18.

The extraction and purification procedure optimized by the Canadian group is based on solid phase extraction involving a ChemMatrix resin which immobilize the pertechnetate and leave molybdenum to flow through the resin, followed by a cation exchange resin to neutralize any residual base from the first resin in tandem with an alumina column that allow the final elution of pertechnetate in the injectable saline solution (Benard, et al., 2014b; Schaffer, et al., 2015b).

The SPE purification developed at TRIUMF is a three step procedure involving three columns: ChemMatrix (ChM), which immobilizes the pertechnetate and allows the molybdate to flow through into a molybdenum recovery vial; cation exchange to neutralize any residual base from the ChM column and ensure that the

pertechnetate is retained by the alumina. Since the multiplicity of the operations and also for the limited operation allowed by the module itself, only one module was not enough for this purpose. Two IBA Synthera® extension module (E6 and E7) were therefore used for the automation of the complete procedure and the addition of an external peristaltic pump was necessary to speed up and keep under control the big volume liquid transfer on the resins.

Cold and Hot runs were performed in order to test and optimize the automated procedure and verify the purity and yield of the final product.

The automation with Synthera® Extension Modules of cyclotron-produced ^{99m}Tc separation and purification SPE (Solid Phase Extraction) procedure is hereafter described.

Materials and Methods

Module components and accessories provided by IBA:

- Synthera® platform software
- #2 Synthera® Extension modules (E6-E7)
- #2 control box each one related to a module (BoxE6-BoxE7)
- #2 reusable cassettes
- Silicone tubing 1.5 ID / 3 OD (mm)
- PHARMED tubing
- #2 Syringe 5ml (6ml graduations)
- Fittings/ferrules:
- #9 Luer female – barb + ¼-28 mount
- Luer female - barb
- Luer male – barb
- #4 Tee connectors
- #5 Cross connectors

Auxiliary and consumable components:

- Router
- Laptop
- Peristaltic pump WPX1-S3/32S4-BP WELCO connected to the module by means of Power supply and Relè
- Air compressed (-for cold runs, pressurized Nitrogen in the hot run)

- #2 10 ml syringe
- #1 20 ml syringe
- #1 5 ml syringe
- Vials and needles

Chemicals:

- 500 mg ChemMatrix (ChM) Resin previously packed and conditioned with 4M NaOH in an 8 ml reservoir;
- Dionex OnGuard II H 2.5cc cartridge (Thermo) (SCX);
- Sep-Pack® Light Alumina A (Waters Corporation) (Al_2O_3);
- Hydrogen peroxide 30%;
- Sodium hydroxide pellets;
- Natural Molybdenum metal powder 100 mesh;
- 99mTc-pertechnetate saline solution from generator;
- Saline;
- Milli-Q water;
- LaMotte Low range molybdenum kit strip colorimetric test.

Experimental

As first step of the procedure automation, we developed a basic fluidic scheme describing the connection between all components (*Figures 30* and *31*).

The main steps laid down in the first module (E6) are:

- Syringe initialization;
- Columns conditioning: ChemMatrix with 4 ml 4M NaOH rerouted in Residual Moly Vial and SCX cartridge with 4ml Milli-Q H_2O rerouted in Waste through the second module E7;
- Loading of the starting solution (dissolved Molybdenum aqueous sodium hydroxide solution 80 ml), with the aid of a peristaltic pump set to 2ml/min pumping speed, on the top of the ChemMatrix Resin and rerouted in the Residual molybdenum Vessel;
- Rinsing of ChM resin with NaOH 4M 5 ml;
- Pertechnetate elution from ChM resin with H_2O 10ml (in two 5ml steps) rerouted onto SCX cartridge, to module E7, onto Al_2O_3 cartridge and finally into Waste vial.

The main steps laid down in the second module (E7) are:

- Syringe initialization;
- Column conditioning: Al_2O_3 with 4 ml H_2O rerouted in Waste vial;
- Eluted pertechnetate (10 ml H_2O) from module E6 loaded directly onto Al_2O_3 cartridge and rerouted into Waste vial;
- Rinsing of Al_2O_3 with 3 ml H_2O;
- Pertechnetate elution with saline 6ml (in two 3 ml steps) rerouted into product vial.
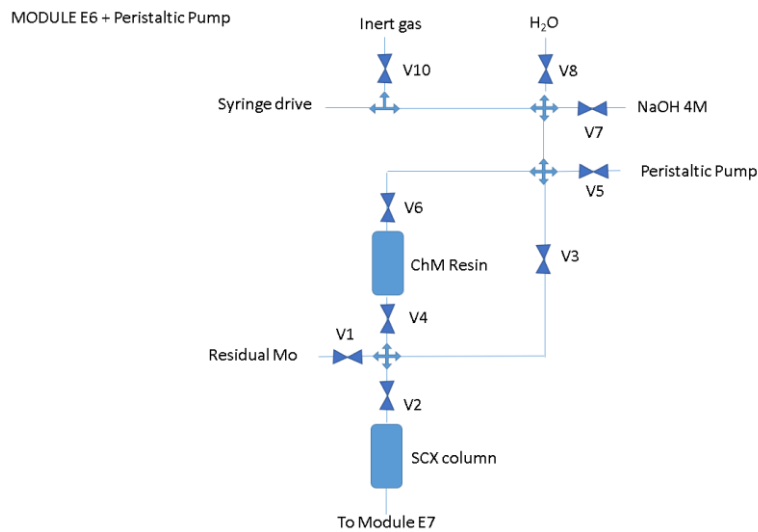
Figure 30 Basic fluidic scheme of Synthera extension module #6.
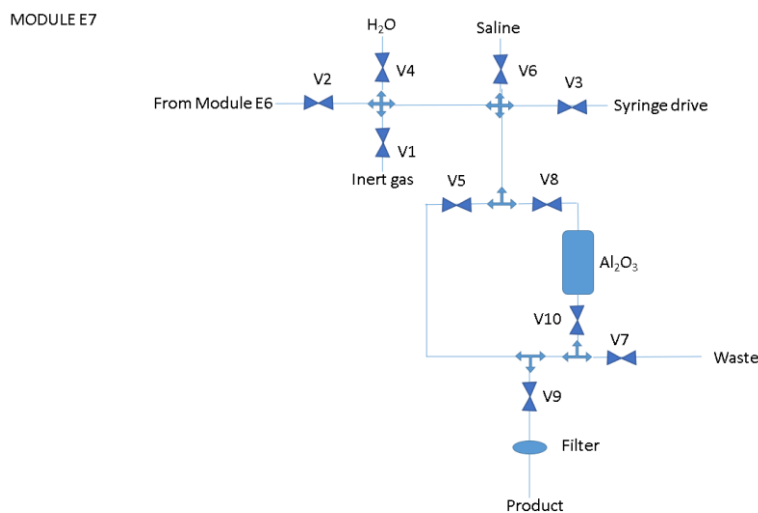
Figure 31 Basic fluidic scheme of Synthera extension module #7.

85

Once defined the basic fluidic schemes (Figures 30 and 31), the cassettes layout drafts have been drawn, the fluidic physical layout has been assembled and applied on the cassettes (*Figure 32*).
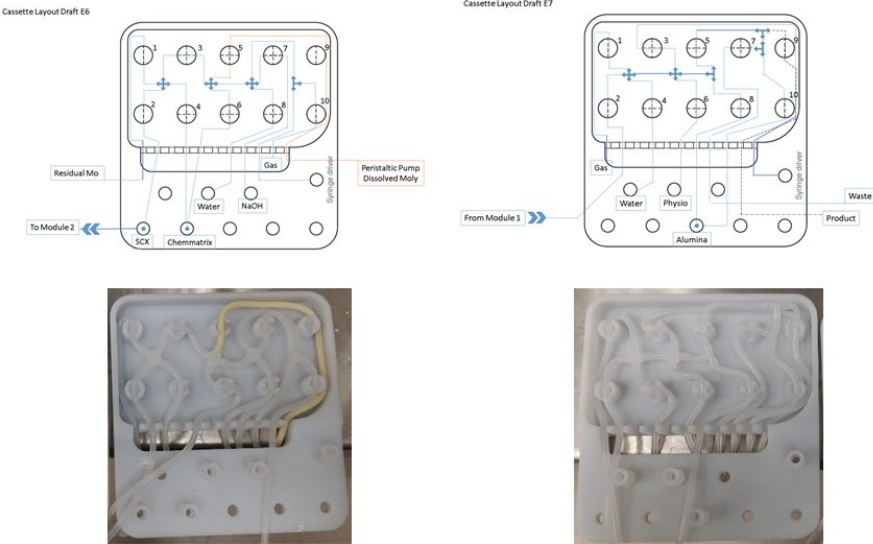
Figure 32 Schemes an pictures of the assembled cassettes, E6 on the left and E7 on the right.

E6 and E7 Fluidic Pathway Scheme (FPS) bitmap (*Figure 33*) have been created on the basis of the fluidic physical layout.
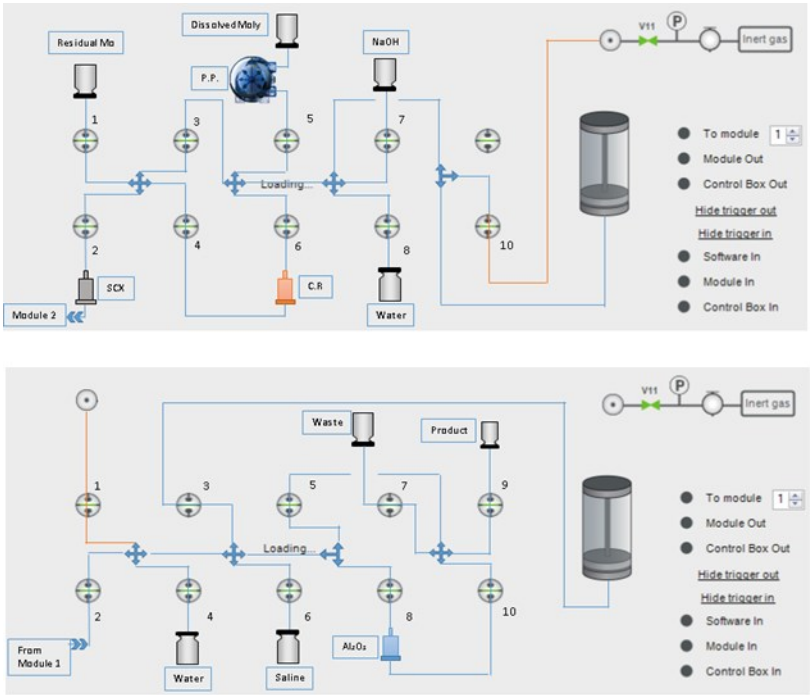
Figure 33 E6 (top) and E7 (bottom) FPS bitmap visible on the software control page.

Operations sequences of E6 and E7 module have been created.

It was necessary to create multiple switches between the two modules in order to allow to operate the purification procedure fluently.

Before each experiment the module preparation consisted of (*Figure 34*):

- Assembly components of module E6:
    - ✓ Empty Syringe 5ml (syringe drive);
    - ✓ 9ml of NaOH 4M in a 10 ml syringe;
    - ✓ 14 ml of Water milliQ in a 20 ml syringe;
    - ✓ 500 mg of ChemMatrix resin paked with NaOH 4M in an 8ml reservoir closed with an adaptor;
    - ✓ SCX cartridge pre-conditioned with 4ml of water;
    - ✓ Starting solution glass bottle 250 ml;
    - ✓ Residual molybdenum plastic bottle 100 ml;
- Assembly components of module E7:
    - ✓ Empty Syringe 5ml (syringe drive);
    - ✓ 6ml of saline in a 6 ml graduations syringe;
    - ✓ 7 ml of Water milliQ in a 10 ml syringe;
    - ✓ Al_2O_3 cartridge pre-conditioned with 4ml of water;
    - ✓ Waste plastic bottle 50 ml;
    - ✓ Product vial 10 ml;
- Peristaltic pump power supply set to 8V (2ml/min pumping speed);
- Open air compressed valve and adjust the pressure with the pressure regulators on the back of the modules in order set gas pressure at 1,2 bar and air compressed at 7,3 bar on the control panel of each module.

Non Radioactive runs were performed in order to optimize the sequences, to define the parameters of its use, were necessary to opt for a peristaltic pump in the loading starting solution step and to evaluate the product's purity.

A last cold run was performed in to emulate the real experiment.

Figure 34 Picture of the assembled IBA module for the extraction and purification of Tc-99m from the molybdenum metal target.

1.1 g of molybdenum metal powder was dissolved in 40 ml diluted H_2O_2 and added to 40 ml of NaOH 4M in a 250 ml bottle.

The module was prepared as described above, the starting molybdenum solution was kept stirred and connected to the peristaltic pump by means of a long needle.

In the recipe management section the two modules have been selected and both FPSs and sequences have been attributed to each module. Once ready, the RUN command has been launched to module E7 and then to E6. The whole procedure was completed in automatic mode in 70 min. The amount of molybdenum in the final product (pertechnetate in saline solution) was estimated to be lower than 0.5 ppm (*Figure 35*).
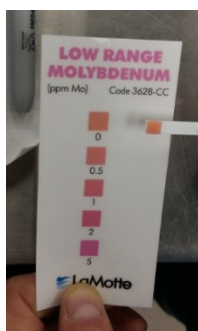
Figure 35 Picture of a strip colorimetric test for the Mo breakthrough determination.

A hot run has been performed in order to evaluate the yield and purity of the final pertechnetate saline solution .

The module and the starting solution were prepared as for the cold run exept for the air compressed that was replaced by nitrogen pressurized for technical and structural reason.

Once everything was ready, an aliquot of ^{99m}Tc-pertechnetate saline solution, obtained from a generator and measured with dose calibrator, was added to the starting molybdenum dissolved solution. The procedure was conducted in automatic mode exept for the second water elution of the ChM resin during which the automatic mode was switched with the manual one. After this step the mode was switched again to the automatic one.

In 80 min the procedure was completed. The activity of the final product and other components were measured with dose calibrator, the final product was then evaluated for the molybdenum content with the colorimentric strip test. The percentage yield have been calculated on decay and volume corrected activity value (*Table 27*).

Table 27 Percentage of ^{99m}Tc activity (decay corrected) in the different components of the automatic module (n=1). Instrument sensitivity 0.01 mCi and 0.01 µCi.

Module component	Acquisition time	Activity	Decay corrected yield
Injected generator eluted pertechnetate	12:03	1.97 mCi	--
Product ^{99m}Tc-pertechnetate	13:32	1.64 mCi	98.63%
Residual Moly (5ml)	13:41	0.00 µCi	0.00%
Waste (5ml)	13:39	0.00 µCi	0.00%
ChM	13:35	0.70 µCi	0.04%
SCX	13:34	1.00 µCi	0.06%
Al_2O_3	13:34	7.46 µCi	0.45%
Water wash	13:46	9.30 µCi	0.57%

Results

The complexity of the three columns purification procedure and the limitations given by the IBA cassette, like two-way valves number and dimension, have immediately highlighted the need to use two Synthera® Extension module in series for the purification of the cyclotron produced Tc-99m from a bulk Mo-100 target solution.The division of labor between the two modules has been evaluated and decided on ChM and SCX resin in module E6 while Al_2O_3 in E7 as shown in the *Experimental* section.

Experiments were performed by using the syringe pump (E6) as loading pump for the starting 80 ml solution. The procedure requires a loading speed of 2 ml/min on the top of the ChM resin of the starting solution. In this condition, and with a 5 ml syringe, at least 16 syringe up-down runs are needed for a total of about 50 min. The presence of air bubbles in the starting solution, coming from the peroxide decomposition, cause an inconsistent flow rate. We have seen experimentally that between 21 and 26 runs were necessary(doubling the transfer time) to complete the solution transfer since each withdrawn volume corresponds to 3-4 ml instead of 5-5.5 ml. Moreover, the purity of the final pertechnetate was likewise not consistent. Indeed, molybdenum breakthrough values were found in the range 0.5-5ppm. This inconsistency in CP values has been evaluated as effect of a cross-contamination in the syringe pump (E6) since in this configuration the syringe is used not only for loading the starting solution, but also to withdraw NaOH for rinsing the ChM resin and water for the elution. The best thing would be to keep separate the starting solution path and the rinsing/eluting solvent path. For that reason, to minimize the molybdenum cross-contamination and to make the starting solution transfer as consistent as possible, we decided to include a peristaltic pump as an auxiliary component of the module.

With the aid of the peristaltic pump the molybdenum breakthrough in the final product was always lower than 0.5 ppm and the transfer time reduced to max 50 min (*Table 28*).

The hot run has shown a good yield and purity of the final product. In about 80 min the module was able to obtain more than 98% of the starting activity and less than 0.5 ppm of molybdenum contamination.

Table 28 Comparison between the two loading device: syringe pump vs peristaltic pump in terms of chemical purity (Mo breakthrough) and loading time.

Loading device	Mo breakthrough	Loading time
Syringe pump	0.5-5 ppm	100 min
Peristaltic pump	<0.5 ppm	Max 50 min

3.3 Comparison Between Tc-99m Separation and Purification Processes

Solvent extraction based modules have been described by (Chattopadhyay, et al., 2010; Chattopadhyay, et al., 2012) and (Martini, et al., 2016). While the first one was created principally for low-medium SA ^{99}Mo/^{99m}Tc decay-extraction process and possibly applicable to cyclotron produced ^{99m}Tc/^{100}Mo extraction with some initial treatment modification, the second one has the advantage of being specially designed for cyclotron-irradiated target processing. Indeed, the automated module, developed during my PhD's work and described in the paper (Martini, et al., 2016) is completely automated with a remote control system in which the dissolution of the target is completely integrated minimizing radioactive manipulation. In particular, the optimized automatic procedure includes: (1) dissolution of the irradiated Mo-100 target in H_2O_2/NaOH, (2) double SE of ^{99m}Tc-pertechnetate from the aqueous alkaline into the MEK organic phase, (3) chromatographic purification of the extracted ^{99m}Tc-pertechnetate onto silica and alumina columns, (4) collection of [^{99m}Tc][TcO$_4$]$^-$ from the alumina column by elution with a saline solution. Solid phase extraction (SPE)-based modules have been developed and described by (Schaffer, et al., 2015b), (Chattopadhyay, et al., 2008), (Das, et al., 2016b) and (Morley, et al., 2012a). Basically, the procedure involves a SPE column, like ABEC-2000^{TM}, ChemMatrix^{TM} or Dowex$^®$ 1x8 resins, that immobilizes the pertechnetate leaving the molybdate flowing through; if an ABEC-2000^{TM} or ChemMatrix^{TM} resin have been used, a cation exchange cartridge is required to ensure eluent neutralization and pertechnetate retention by an alumina column, required in both cases, for the purification of [^{99m}Tc][TcO$_4$]$^-$ from the eluent. The pertechnetate is always eluted with a physiological solution. Among all cited modules, our system (Martini, et al., 2016) and the one described by (Schaffer, et al., 2015b) were realized with commercial components respectively from Eckert and Ziegler (Berlin, Germany) (*Figure 15* and *16*) and Trasis (Ans, Belgium). A comparison between the decay

corrected recovery yields of cyclotron- produced ^{99m}Tc for the described modules is reported in *Table 29*.

Table 29 Comparison between the decay corrected recovery yields of ^{99m}Tc recovery for different extraction procedure.

Extraction method	Yield*	Reference
SPE (Dowex®-1)	80%	(Das, et al., 2016b)
SPE (Dowex®-1)	70±6% (n=7)	(Morley, et al., 2012a)
SPE (ABEC™-2000)	90±5% (n=7)	(Morley, et al., 2012a)
SPE (ChemMatrix™)	78±8% (n=3)	(Schaffer, et al., 2015b)
SE (MEK)	93 ± 3 (n=10)	(Martini, et al., 2016)

* ^{99m}Tc recovery efficiency of the automated separation procedure expressed as percent of the initial activity

Comparing TRIUMF's and our dissolution, extraction and purification system of Tc-99m (*Figure 36*) we first note that their technology results as efficient as our, but more expensive due the technique selected (SPE). Indeed, consumables of cassettes-based modules are quite expensive (about 100€ for each manifold) with single-use while our module is multiple use made of resistant washable materials, moreover, the commercial resins are expensive compared to the common MEK solvent. Reusable manufacturing equipment is permitted by Good Manufacturing Practice (GMP) guidelines (EudraLex, 2015) for pharmaceutical production as long as designed so that it can be easily and thoroughly cleaned adopted to control risk of cross-contamination. It should be cleaned according to detailed and written effective and reproducible cleaning procedures and stored only in a clean and dry environment. For the complete procedure, the Canadian group has developed two separate modules, one for the dissolution and one for the separation. Differently, we provide a single compact device for both dissolution and separation steps reducing operation time, space, costs and the probability of radioactivity loss.
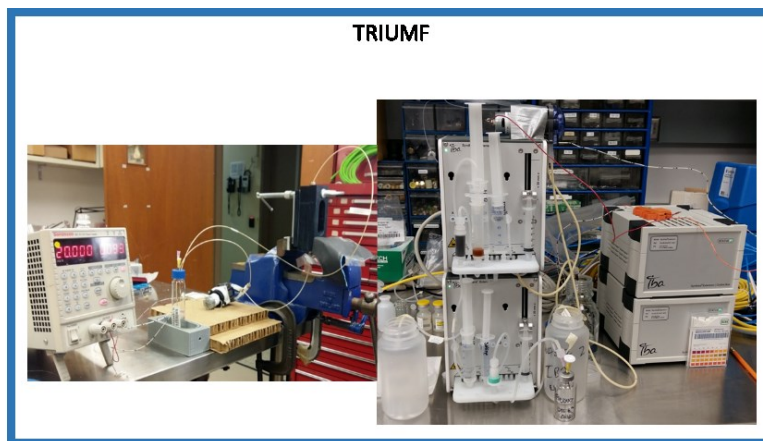
Figure 36 The two developed module under comparison, the SE module developed in Italy with Eckert and Ziegler components on the left, on the right the dissolution system and automatic module developed in Canada with IBA components.

4 COME Project: Cu-67 Production Studies

The radionuclide ^{67}Cu is attracting a considerable interest due to its favorable nuclear properties for theranostics (IAEA, 2015). It decays through the emission of β-particles with mean-energy suitable for therapy (E$_{β-}$=141keV) and γ-radiation (E$_γ$ =185keV) appropriate for diagnostic with standard SPECT or SPECT/CT cameras. Unfortunately, ^{67}Cu production is very challenging due to the very low cross-sections of all potential reactions. ^{67}Cu is tipically produced using a zinc (Zn-68)target by the ^{68}Zn(p,2p)^{67}Cu nuclear reaction which requires high energy (200 MeV), high intensity proton beams and long irradiation times (Medvedev, et al., 2012). Despite its increasing interest, only the amount of one therapeutic dose per month (approximately 100 mCi, i.e. 3.7 GBq) is globally achieved worldwide (Cutler, et al., 2013). For these reasons, the International Atomic Energy Agency (IAEA) has encouraged a selected group of researchers from all around the world to study alternative ^{67}Cu production routes as main goal of the recent Coordinated Research Project (CRP) entitled *Therapeutic Radiopharmaceuticals Labelled with New Emerging Radionuclides (^{67}Cu, ^{186}Re, ^{47}Sc)*, started in September 2016 (IAEA, 2015). The project COME – COpper MEasurement, funded by INFN-CSN3 (Dotazioni-LNL) in 2016 (Pupillo, et al., 2017), aims to directly contribute to the IAEA-CRP by measuring an unexplored nuclear reaction for the ^{67}Cu production. By investigating this cross section, and comparing it to the well-known on Zn-68 targets, we will define the best production route of ^{67}Cu, hopefully finding a way to make this radionuclide available in larger amounts to the scientific community.

A key point of the COME project is the measurement of the co-produced Cu-64 radionuclide. The co-existence of the two radionuclides could be intended as a benefit for theranostics purposes, considering a mixture of $^{64/67}$Cu (Uddin, et al., 2014) (after appropriate dosimetry studies). On the other hand, in order to obtain the purest Cu-67 radionuclide, it is important to minimize the co-production of Cu-64 by considering the best irradiation conditions (energy range, target material and irradiation time). The optimization of these parameters will provide the best activity ratio of Cu-67 and Cu-64 radionuclides at the End Of Bombardment (EOB); taking advantage of the different half-lives (Cu-67 is 61.83 hours, Cu-64 is 12.701 hours) it is possible to evaluate the appropriate decay time to obtain a "pure" Cu-67, i.e. a RNP higher than 99%.

4.1 Evaluation of the ^{70}Zn(p,x)^{67}Cu Reaction

An interesting nuclear reaction for the cyclotron-based production of Cu-67 is the ^{70}Zn(p,x)^{67}Cu, evaluated up to 35 MeV (*Figure 37*) by Levkovskij (1991) and Kastleiner (1999) so far (Kastleiner, et al., 1999; Levkovskij, 1991). No data regarding higher energies can be found on international database (EXFOR database , 2017). Considering the maximum energy available by using compact cyclotrons, as the ones installed at Arronax facility (Haddad, et al., 2008) and at INFN-LNL (SPES project) (Maggiore, et al., 2017), the aim of the COME project was to measure this nuclear reaction up to 70 MeV.
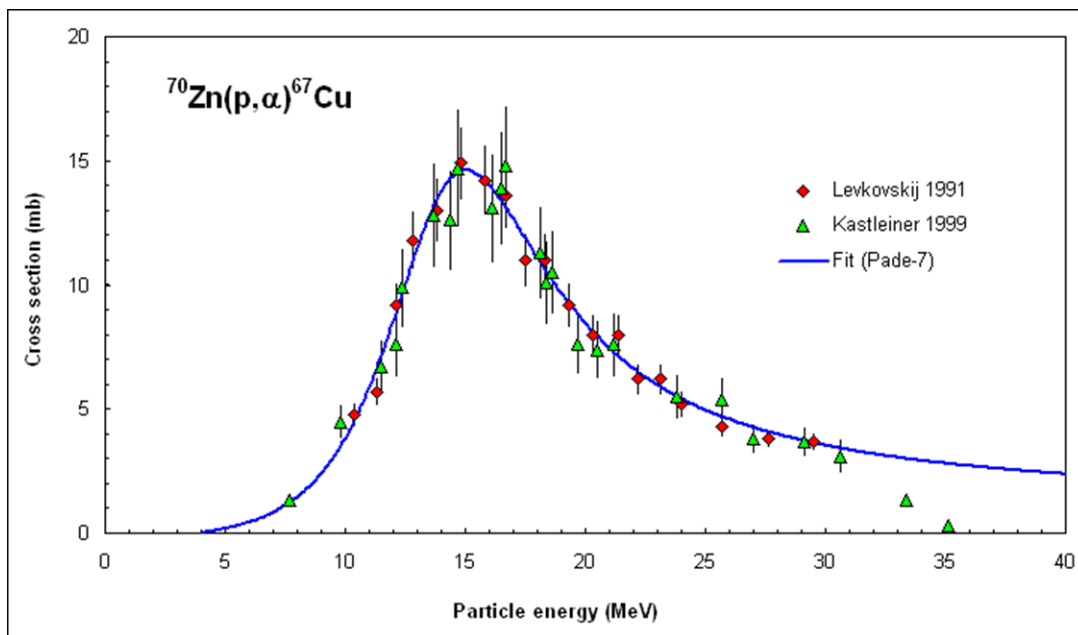
Figure 37 Measurements and evaluation of the ^{70}Zn(p,α)^{67}Cu reaction (IAEA, 2008b).

Preliminary estimations of the cross section trend have been carried out by using two nuclear codes, Talys (Koning & Rochman, 2012) and PACE4, included in LISE++ package (Tarasov, 2003), obtaining contrasting results (*Figure 38*). Estimations with Talys and PACE4 have been both carried out by using default parameters. Moreover, Talys code has also been used with a set of specific parameters that have been previously optimized by comparing simulations with experimental values for many nuclear reactions under the name "Talys*" (Duchemin, et al., 2015).
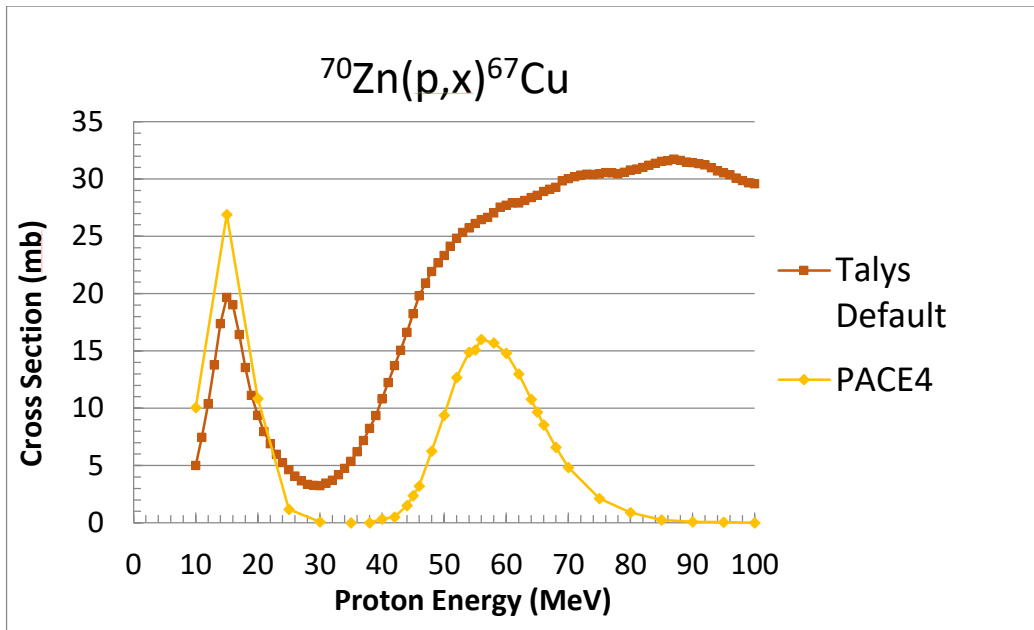
Figure 38 Theoretical estimations of the $^{70}Zn(p,x)^{67}Cu$ reaction, by using PACE4 and Talys code, compared with experimental results up to 35 MeV.

From this plot it appears that the cross section predictions by codes are in agreement only up to 35 MeV, i.e. the explored range (Kastleiner, et al., 1999; Levkovskij, 1991), while, at higher energies, the code-simulations differ from each other. Hence the need for a precise measurement of the $^{70}Zn(p,x)^{67}Cu$ reaction above 35 MeV.

Among the variety of radionuclides produced during the bombardment of a zinc target, the ^{67}Ga (half-life 3.2617 d) is of particular concern: it presents the same γ-lines of ^{67}Cu, since they both decay into ^{67}Zn (*Table 30*) (NuDat, 2.7). Moreover, they have a similar half-life and therefore it is not possible to infer the precise activity of one radionuclide waiting for the decay of the other one. For these reasons, a radiochemical procedure aimed at the separation of copper from gallium elements, is necessary to carry out cross section studies on Cu-67 production.

Table 30 Cu-67 and Ga-67 γ-emission lines (NuDat, 2.7).

γ radiation	Cu-67 (T$_{1/2}$=61.83 h)	Ga-67 (T$_{1/2}$=3.2617 d)
Energy (keV)	Intensity (%)	Intensity (%)
91.266	7.00	3.11
93.311	16.10	38.81
184.577	48.7	21.410
208.951	0.115	2.460
300.219	0.797	16.64
393.529	0.220	4.56

In order to measure the efficiency of the radiochemical separation it is necessary to use tracer radionuclides, i.e. isotopes of copper and gallium elements that present characteristics γ-rays with no interferences with the different γ-lines emitted by all the radionuclides co-produced in the target. In case of gallium, the selected tracer isotope is Ga-66 (half-life 9.49 h), that is directly produced during the proton irradiation of Zn-70 target. In the case of copper elements, it is not possible to use the in-target produced Cu-64, since its 1345.77 keV line has a low intensity (0.475%) (NuDat, 2.7), forcing the need of very long spectra acquisition times. In order to reduce the time of the chemical procedure and spectra acquisition, Cu-61 (3.339 h half-life) was selected as tracer radionuclide of copper elements (*Table 31*); however, Cu-61 should not directly produced into the Zn-70 target in the entire energy-range of interest (*Figure 39*): for this reason, an enriched Cu-63 foil was added to the stacked-target (details in section 4.3) and used as source of Cu-61 (Levkovskij, 1991; McCormick, et al., 1956; Meadows, 1953). By using enriched Cu-63 (and not natural copper foil) the co-production of additional Cu-64 is avoided, thus allowing the measurement of the ^{70}Zn(p,x)^{64}Cu reaction.

Table 31 Cu-61 γ-emission lines (NuDat, 2.7).

γ-emission Energy [keV]	Intensity [%]
283	12.2
656	11
67	4.2
1185.2	3.7
373	2.1
588	1.1
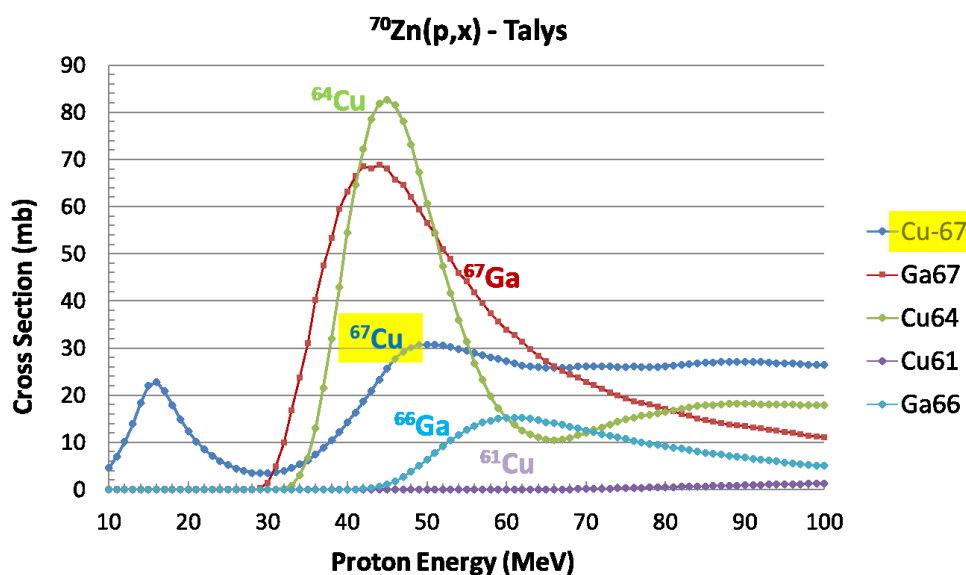
Figure 39 Talys* cross section estimation.

In this graph (*Figure 39*) Zn-70(p,x) cross sections estimation by Talys* are represented. Among the various codes, Talys* has been selected since is the one that best describes the experimental data for the reaction Zn-68(p, 2p)Cu-67 (Pupillo, et al., 2018).

By dissolving the Cu-63 target after irradiation and adding an aliquot of it in the Zn-70 dissolved target before the separation procedure we introduce the tracer for Cu element.

4.2 Development of a High Yield Purification Procedure ^{70}Zn/^{67}Ga/^{67}Cu

Co-production of ^{67}Ga during the production of ^{67}Cu by proton irradiation of natural Zn targets poses a serious issue for the determination of the activity of the final ^{67}Cu because of the co-emission of the same γ-line by the two radionuclides with similar decay constants (Pupillo, et al., 2017). This preclude the possibility of cross section studies without an efficient separation procedure and may hamper the development of a reliable quality control procedure for determining RNP, a crucial parameter to be fixed for ensuring the safe use of a radionuclide in radiopharmaceutical preparations. Since, in principle, the amount of ^{67}Ga impurity cannot be distinguished from ^{67}Cu by γ-spectroscopy, the only solution is to devise a highly efficient procedure for the separation of Ga-isotopes from Cu-isotopes after extraction from the irradiated bulk Zn target.

There are several proven methods for separating Cu-67 from irradiated zinc target. Most of them were described and compared by (Schwarzbach, et al., 1995) and (Smith, et al., 2012): electrodeposition, solvent extraction, ion exchange methods and sublimation. Both solvent extraction with thenoyl-trifluoroacetone in benzene and ion exchange three resins process (described below) reported a high recovery yield of copper (Smith, et al., 2012) but the ion exchange was identified as te most simple and reliable process (Schwarzbach, et al., 1995).

For our purposes, the chemical design of the separation process was accomplished according to the principles of ion-exchange solid phase extraction chromatography since it is a simple, clean method that would allow for automation for use in a hot cell, assuring the reliability and reproducibility of high yield results (Schwarzbach, et al., 1995; Smith, et al., 2012; Medvedev, et al., 2012). The procedure described by (Medvedev, et al., 2012) includes a three step separation with three separation columns: cation exchange resin AG50W-X4, Chelex-100 column and anion exchange resin AG1W-X8 (*Figure 40*).
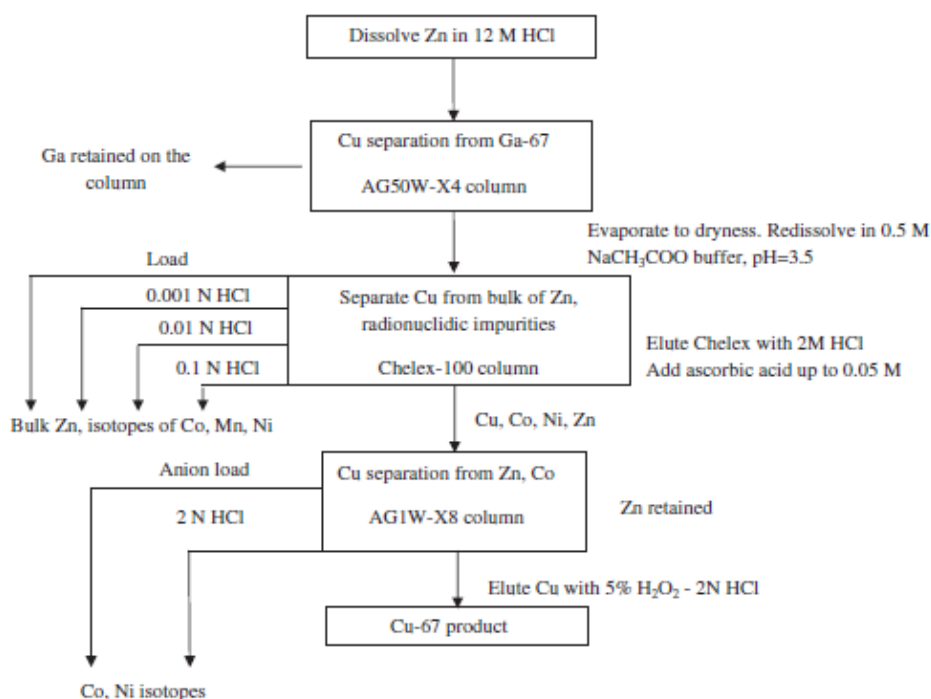
Figure 40 Scheme of the ion exchange method selected from literature.

Materials and Methods

Starting from this method and applying some modifications in order to adapt the procedure to our purpose and our conditions, we developed a two-step separation procedure.

The separation procedure generally comprised the following steps:

(a) removal of Ga isotopes by passing the radioactive solution through a cation exchange resin (AG50W-X4, 100-200 mesh purchased from BioRad packed at the moment in a glass column for chromatography: diameter 1.2 cm, height 20 cm, *Figure 41*);

(b) evaporation of the resulting solution to adjust the HCl concentration by a dedicated evaporation system, designed with acid fumes collector and neutralization (*Figure 42*);

(c) purification of Cu isotopes from bulk zinc by anion exchange resin (AG1-X8, 100-200 mesh purchased by BioRad packed at the moment in a glass column for chromatography: diameter 1.2 cm, height 20 cm, *Figure 41*).
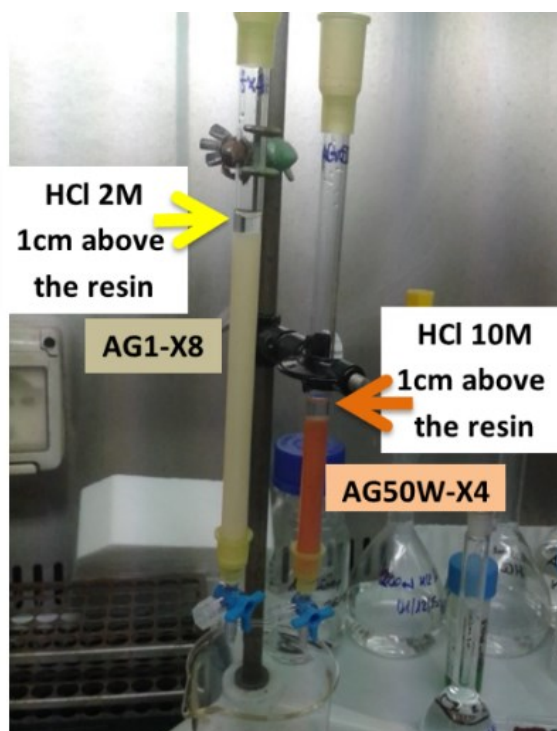
Figure 41 Pictures of the two ion exchange resins involved in the separation procedure.
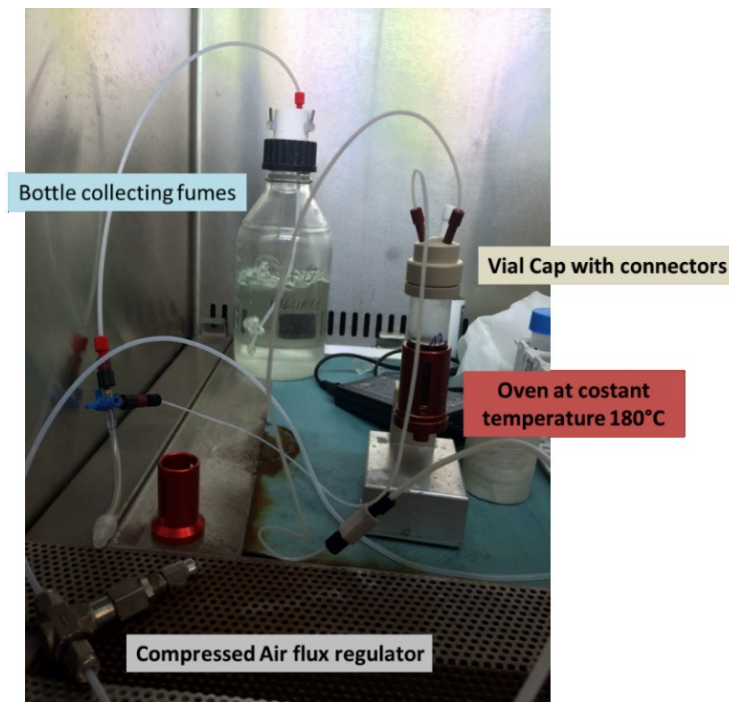
Figure 42 Evaporation system.

In order to develop and optimize the procedure, several simulation experiments have been carried out, in collaboration with the Sant'Orsola Hospital in Bologna, taking into account the following conditions imposed by our final goal, i.e. the cross section measurements:

- Thin target foils of enriched Zn: about 10 mg, Ø=11 mm, 10 µm thickness
- In order to track Cu element by γ-spectrometry, the addition of Cu-61 isotope, produced by the irradiation of a Cu-63 foil is necessary. This means that we need to introduce not a negligible amount of Cu-63 (order of mg) to the starting solution undergoing the purification. In so doing, all volumes and resins amount should be calibrated to this condition. Normally the amount of isotope of interest produced during an irradiation and to be isolated is in the order of nmol. Instead, under these conditions, the amount of Cu to be isolated and purified is in the order of mg.
- Since the final purpose is the estimation of cross section, we don't need to obtain the final solution in an injectable form (i.e. purified from solvent, sterile, pyrogen-free, etc.)
- The elements of interest (Cu-isotopes) have to be separated from the bulk material (zinc target) and Gallium-elements. Other contaminants that do not interfere with the aim of cross section studies (Cobalt, Nickel, etc.) were not considered in the optimization of the procedure.

- The procedure doesn't need to be automated to eliminate time consuming steps, waste volumes and resins amount don't need to be minimized and the procedure can be performed manually.

In order to simulate the real starting conditions, during the preliminary simulation experiments a mock solution of the cold metal ^{nat}Zn was spiked with trace amounts of the radionuclides ^{65}Zn, ^{64}Cu and ^{68}Ga (*Figure 43*) obtained as follow:

- SS1 (Stock Solution): 10 mg Zn-nat metal cold (not irradiated) dissolved in about 500 µl of HCl 10M

- SS2: 70 mg Cu-nat metal target irradiated (for the production of Zn-65 used as tracer of Zn for the yield evaluation) and dissolved in 2ml HNO$_3$ 6N. The solution was evaporated and the residue was dissolved in 1ml HCl 10M (twice). In 150 µl there are about 10 mg of Cu

- SS3: elution of Ga-68 from Ge/Ga generator with 7 ml HCl 0.1 M

- SS4: Cu-64 from the irradiation of Ni-64 target and elution with 4 ml HCl 0.1 M from an extraction and separation automatic module.

MOCK SOLUTION

- **Cu/Zn-65 solution:** 70.9mg Cu-nat metal target irradiated (for the production of Zn-65) and dissolved in 2ml HNO$_3$ 6N. Evaporated and dissolved in 1ml HCl 10M (Twice). In 150µl there are about 10mg of Cu

- **Ga-68 solution:** elution of Ga-68 from Ge/Ga generator: 7ml HCl 0.1M

- **Cu-64 solution:** Cu-64 from the irradiation of Ni-64 target. Elution of Cu-64 from the Extraction and separation automatic module with 4ml HCl 0.1M

- **Zn Solution:** 10mg Zn-nat metal cold (not irradiated) dissolved in about 500µl of HCl 10M

150 µl Cu/Zn-65 sol.
100 µl Ga-68 sol.
100 µl Cu-64 sol.
500 µl Zn sol.

Figure 43 Schematic description of the mock solution composition.

Experimental

The initial 10 M HCl solution was prepared by mixing 500 µl of SS1, 150 µl of SS2, 100 µl of SS3 and 100 µl of SS4.

The first separation step was performed with 7 g of a cation exchange resin (AG50W-X8) conditioned with 10 ml of 10 M HCl. In strong acidic conditions, Ga isotopes are quantitatively retained on the resin as a mixture of the aquo-halogen, monocationic complex [GaCl$_2$(H$_2$O)]$^+$ and the hexa-aquo, tris-cationic complex

$[Ga(H_2O)_6]^{3+}$. After discarding 2 ml of dead volumes of the resin, Cu and Zn isotopes were eluted with HCl (10 M) 12 ml as anionic tetra-halogen complexes $[CuCl_4]^{2-}$ and $[ZnCl_4]^{2-}$ and collected in a glass vial for the subsequent evaporation step. The elution of Ga was performed with 20 ml of Acetone/HCl 0.05 M solution (97.56% of acetone).

The Cu- Zn HCl 10 M solution was evaporated at 180°C in 90 minutes by the evaporation system. The residue was dissolved in 1 ml of HCl 2 M (twice) (*Figure 44*). In these conditions, Zn is presumably still present under the same chemical form of tetra-halogen complex $[ZnCl_4]^{2-}$ whereas Cu is converted into the hexa-aquo dicationic complex $[Cu(H_2O)_6]^{2+}$.
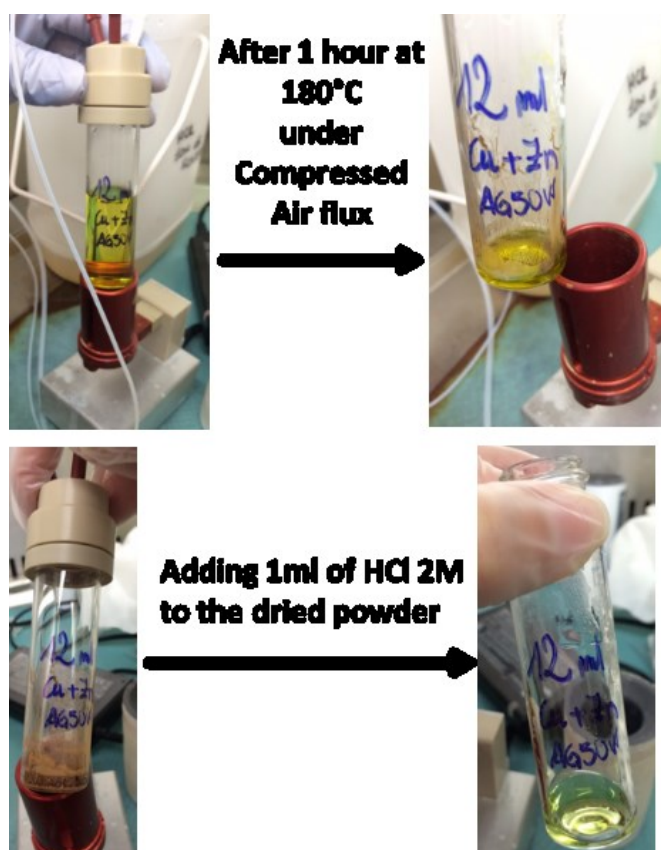
Figure 44 Evaporation steps.

The second step was performed with 7 g of an anion exchange resin (AG1-X8) conditioned with 10 ml of 2 M HCl. The anion exchange resin is able to selectively retain $[ZnCl_4]^{2-}$ and leave $[Cu(H_2O)_6]^{2+}$ to flow through with 20 ml of HCl 2 M, after discarding 2 ml of dead volumes of the resin. Finally, the elution of Zn has been performed with 20 ml of HCl 0.005 M.

The complete procedure lasted approximately 4 hours.

From the three final solutions (*Figure 45*), 20 ml volume each, containing the three separate elements of interest Cu, Zn and Ga, were taken three aliquot of 5 ml each and analyzed by gamma spectrometry for the determination of the separation yields.

Elution profiles of the separation procedure are illustrated in *Figure 46*.
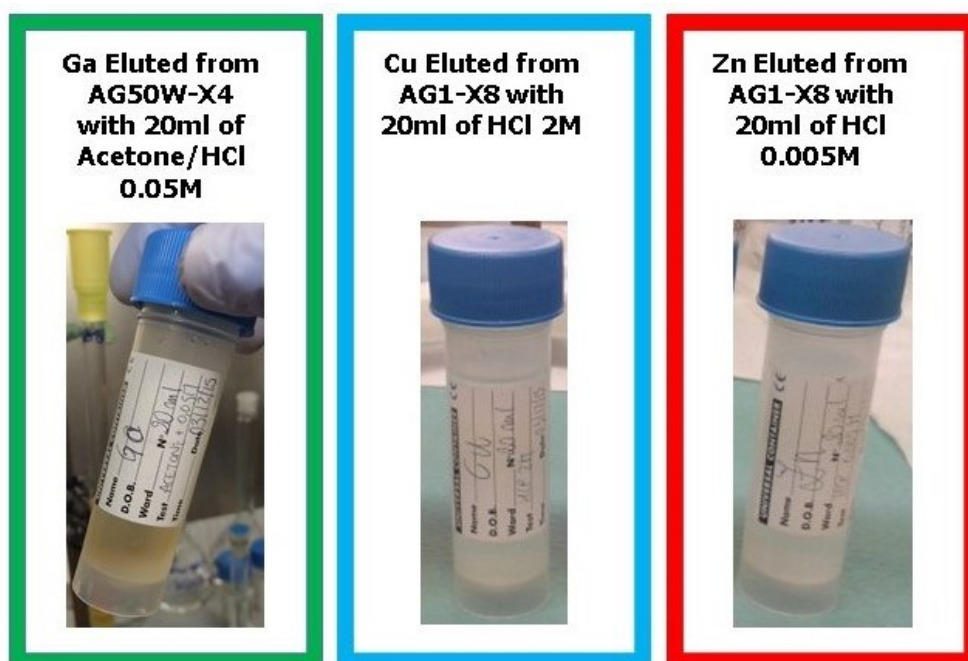
Figure 45 The three final solutions.
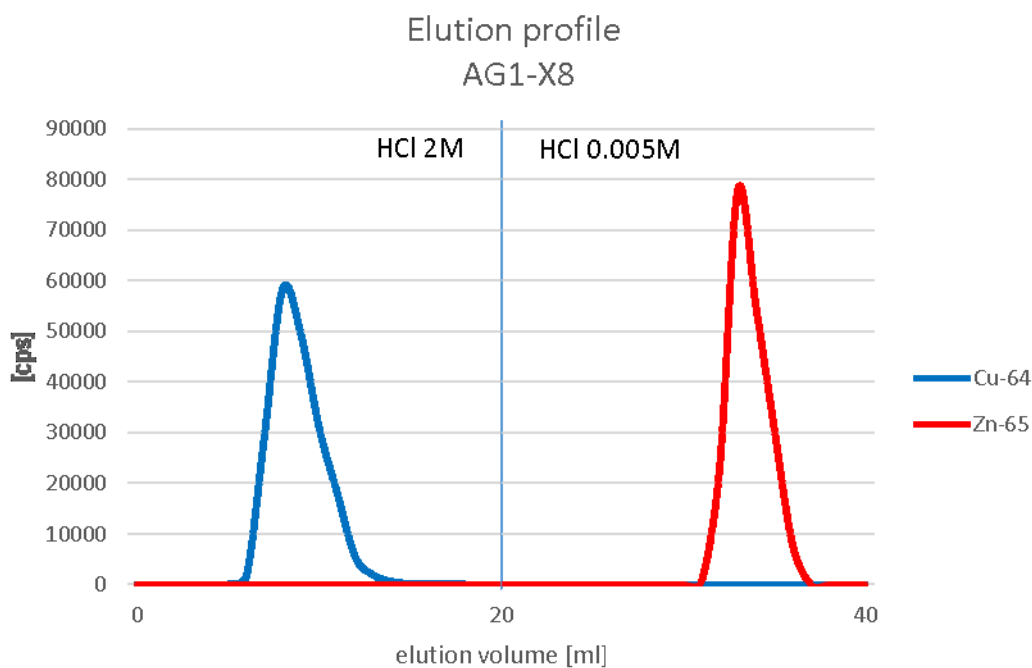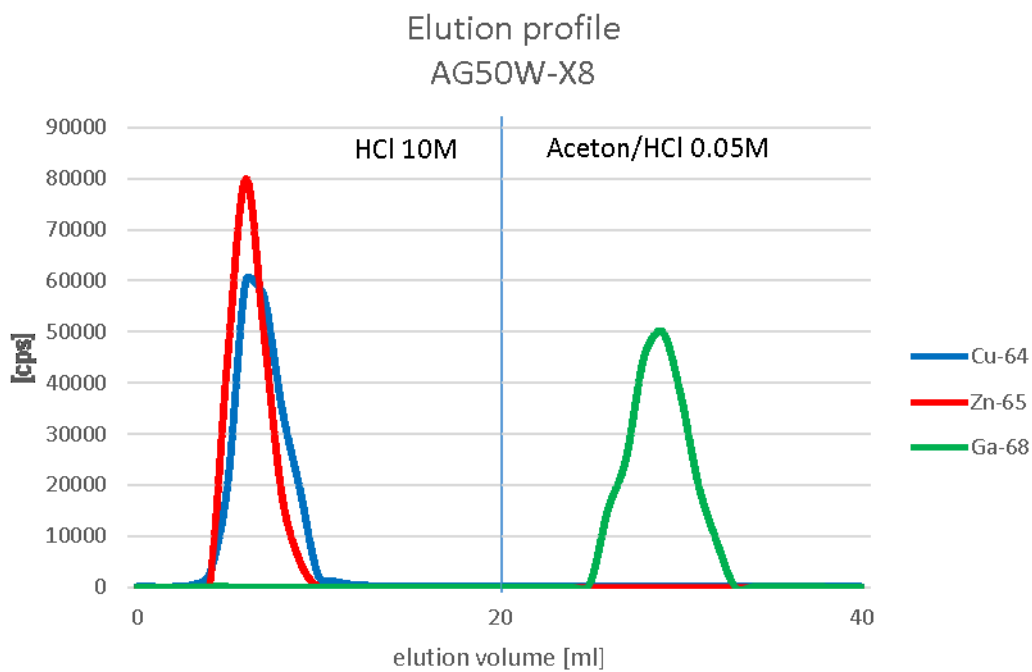
Figure 46 Elution profiles of the separation and purification process, 1ml aliquots collected from the resins and measured by gamma spectrometry. a) Cu-64, Zn-65 and Ga-68 elution profiles on an AG50W-X4 cation exchange resin; b) Cu-64 and Zn-65 elution profiles on an AG1-X8 anion exchange resin.

Results

The experiment was repeated 7 times and a mean separation yield is reported in the table below (*Table 32*).

Table 32 Mean separation percentage yield of Cu, Ga and Zn isotopes in the three final solutions.

%	Gallium Solution	Zinc solution	Copper solution
Ga-68	99.15±0.08	0.61±0.06	0.24±0.04
Zn-65	0.06±0.02	99.91±0.02	0.04±0.01
Cu-64	0.24±0.02	0.33±0.04	99.43±0.06

This new separation procedure, schematically represented in *Figure 47*, allowed a quantitative separation of the elements Cu, Zn and Ga based on the ion exchange resins. It is worth noting that this procedure can be easily automated and remotely controlled to ensure an effective operator's radioprotection and to maximize the reproducibility of the separation process. Furthermore, it can be potentially translated to the production of pharmaceutical ^{67}Cu solutions having characteristics suitable for preclinical and clinical applications.
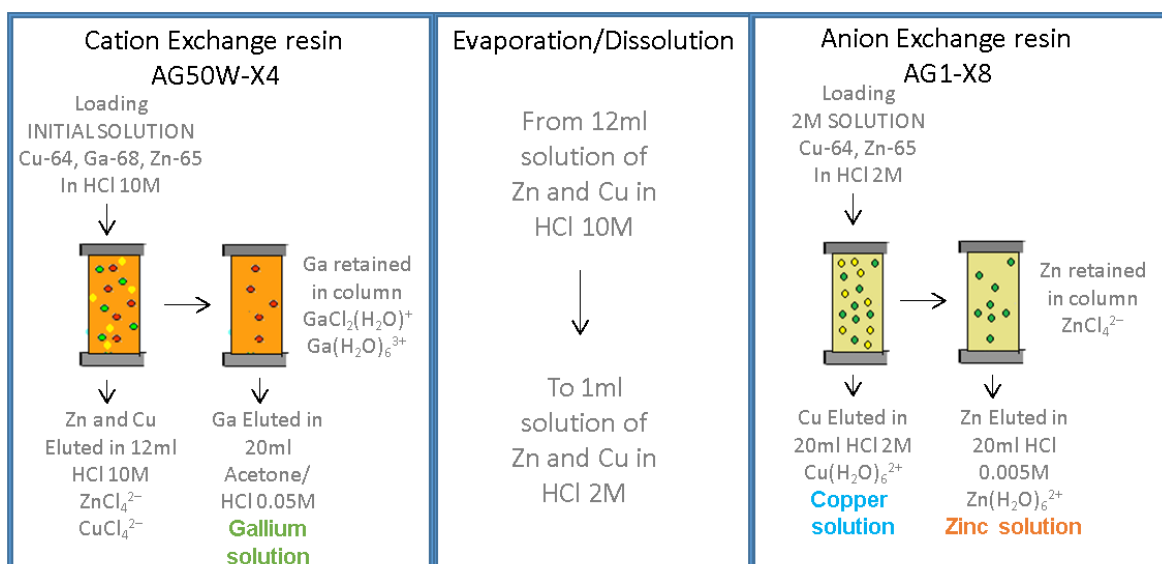
Figure 47 Shows a scheme of the process developed for the separation of Cu, Ga and Zn.

Once optimized, the procedure for ^{67}Cu extraction was applied after six irradiation runs performed by proton bombardment of a Zn-70 metallic targets as described in the following section. The yield of the chemical process was checked, by gamma spectrometry, for each irradiated target foil by considering the activity of tracer radionuclides (^{61}Cu, ^{66}Ga, ^{65}Zn) before and after application of the chemical procedure.

4.3 Irradiation Tests at ARRONAX Facility

Six irradiation runs have been performed in the past two years at ARRONAX facility by using the proton beam with a tunable energy of 35-70 MeV (*Table 33*). The first two irradiation runs will not be considered in the final cross section measurement as they were preliminary experiments for testing and upgrading the methodology.

For simplicity the final step by step experimental procedure is hereafter described.

For each run a stacked-foils target (*Figure 48*) has been irradiated containing (Pupillo, et al., 2014):

- two target foils of ^{70}Zn (about 10 μm thick) produced by lamination from highly pure enriched powder purchased by TRACE (enrichment: Zn-70=95.42%, Zn-64<0.02%, Zn-66<0.02%, Zn-67=0.13, Zn-68=4.45) and by Chemotrade (enrichment: Zn-70=95.47%, Zn-64=0.05%, Zn-66=0.27%, Zn-67=0.07, Zn-68=4.14) (Znx1 and Znx2);
- two aluminum monitor-catcher foils (Nickel in the run #5) (about 20 μm thick) placed right after each Zn foil (Alx1 and Alx2); Al monitor foils used to measure the effective beam flux by considering the well-known ^{27}Al(p,x)^{22}Na reference reaction recommended by the International Atomic Energy Agency (IAEA, 2007b);
- an aluminum foil (about 2 mm thick) placed among the first Al-monitor and the second Zn-target (Al) works as energy degrader;
- a ^{63}Cu foil (99.7% ia) for the production of the Cu element tracer ^{61}Cu (Cux1) (as described above, *section 4.1*);
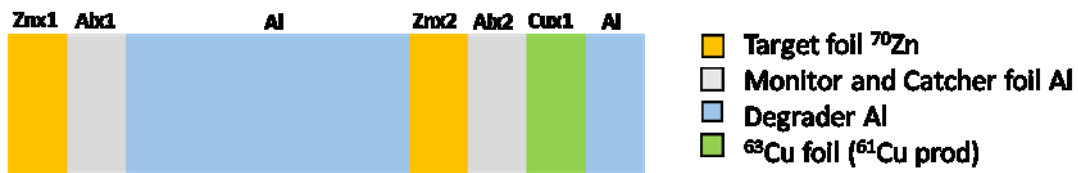
Figure 48 Graphical representation of the staked foil target configuration.

Table 33 Irradiation parameters and target characteristics of irradiation runs performed at ARRONAX facility (Nantes, Francia). §purchased by TRACE; ¤purchased by Chemotrade

Irradiation #	Proton Energy (MeV)	Irradiation time (s)	Mean current (nA)	Zn Target 1	Zn Target 2
1	70.3	5390	98.8	Zn11 §	Zn12 §
2	56.0	5396	100.4	Zn21 §	Zn22 §
3	61.0	4895	110.5	Zn31 §	Zn32 ¤
4	68.0	5406	100.7	Zn41 §	-
5	48.0	7270	102.5	Zn51 ¤	Zn52 §
6	56.0	5400	100.4	Zn61 ¤	Zn62 §

All Al and Ni foils have been purchased by Alfa Aesar and Goodfellow respectively, while all enriched metals, Zn-70 and Cu-63, have been produced by lamination in the target laboratory at INFN-LNL. All foils have been cut in circular shape of 12 mm diameter and the mean thickness calculated by knowing the diameter and the mass of each foil, weighted by using a precision scale. In *Figure 49* a sample of target foils used in the 5th irradiation.
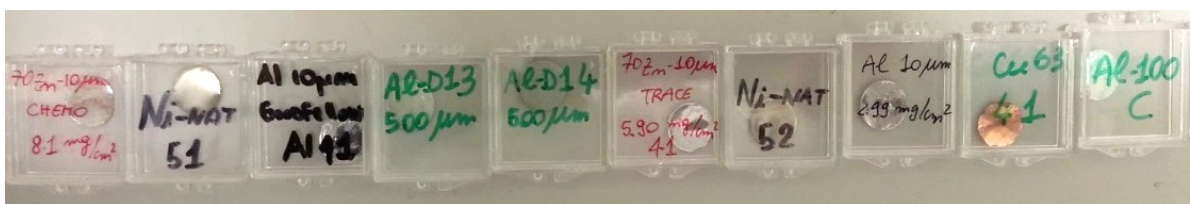
Figure 49 Picture of target foils used in the 5th irradiation run.

A dedicated target holder for these experiments has been designed and realized at INFN-LNL (*Figure 50*) This device is able to fit the target station of the research beam-line at our disposal at ARRONAX facility and it is optimized for the small

dimensions of the enriched and costly materials that have been used during these experiments (Zn-70 and Cu-63).

Figure 50 Picture of the dedicated target holder built at INFN-LNL.

A dedicated collimator in graphite (cylinder with hole diameter 9 mm, length 4 cm) and its plastic support were also designed and built at INFN-LNL. Before each irradiation run the target holder and the collimator have been aligned on the beam line (*Figure 51*).
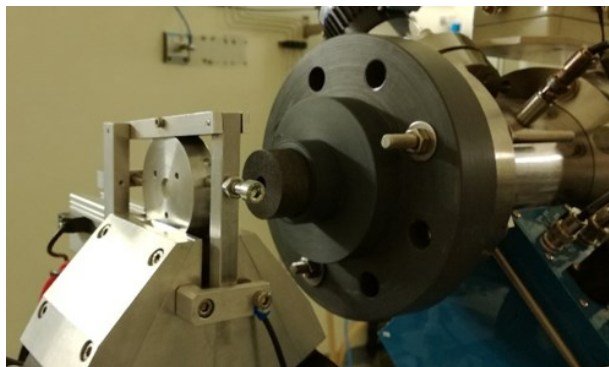
Figure 51 Picture of the dedicated beam-line at ARRONAX facility, with target holder and collimator installed before the irradiation run.

The separation material was prepared and the evaporation setup was assembled, taking into account that two targets have to be treated simultaneously. Two 10 ml evaporation glass vials were placed on a hot plate in an aluminum vials holder and connected to the evaporation system by means of a peek cap with three connectors (purchased by Radius): one was sealed, one was connected to air compressed line

and the last was connected to the bottle collecting fumes with a 200 ml basic solution for the neutralization of acid fumes. The following solvent have been prepared:

- HCl 10 M
- HCl 2 M
- HCl 0.005 M
- Acetone/HCl 0.05 M solution (97.56% of acetone)
- HNO$_3$ 6 N.

The vials listed below (*Table 34*) were named and weighted in order to make the proper volumes correction of the aliquot solutions.

Table 34 List of the vials involved in the procedure. The name of each vial describe: what is collected inside (i.e. Ga stands for gallium solution, MIX stands for starting solution containing all the isotopes,); the first number represent the irradiation number; the second number represent the position of the target in the stacked foils configuration (i.e. 1 for the first target impinged by the beam and 2 for the second);the type of vial (i.e.vials named "gamma" represent the 5 ml vial specific for gamma spectrometry made of PE and with PP cap while vials named "20 ml" are 40 ml PP vessels in which the eluted element (Cu or Zn) is collected in a 20 ml solution at the end of the separation procedure). Unlike the others, the collecting vial for the 20 ml Ga eluate is an 80 ml glass bottle: in fact, the elution of Gallium is made with a two phases mixture (aqueous-organic mixture) and it is important to stir vigorously the sample before aliquoting it, in order to obtain an as much as possible homogeneous distribution of the activity in the sample, avoiding phase separation and activity concentration in one of the two phases..

MIX-31 gamma	Cu31 gamma
MIX-32 gamma	Cu32 gamma
Ga31 20 ml (glass)	Zn31 20 ml
Ga32 20 ml (glass)	Zn32 20 ml
Ga31 gamma	Zn31 gamma
Ga32 gamma	Zn32 gamma
Cu31 20 ml	Al31 gamma
Cu32 20 ml	Al32 gamma

The target disassembly and the separation procedure was always performed the day after the irradiation.

Once disassembled the target, each solid foil spectrum was acquired by HPGe starting from ^{63}Cu-x1, Zn-x1 and Zn-x2 of about 30 min each. Meanwhile, two columns for each resin (2 AG50W-X4 and 2 AG1-X8) have been prepared by conditioning the resin in the proper solvent (as described above, 4.2).

For a better understanding, in *Figure 52* the main steps of the procedure are described by pictures. The elution profile of the separation procedure and a schematic representation of the purification process are also described in *Figure 46 and 47*, respectively (4.2 section).

At the end of the ^{63}Cu-x1 acquisition, the foil was inserted in a glass evaporation vial, 0.5 ml of HNO$_3$ 6 N were added to the foil and then placed on the hot plate set at 180°C and connected to the evaporation system under air compressed flux (Figure 42 in Materials and Methods section). The target was dissolved and evaporated. The residue was dissolved in 1 ml HCl 10 M and evaporated again. Finally, the residual was dissolved again in 1 ml of HCl 10M and left to cool. In this way, the irradiated Cu-63 target was dissolved and brought to the chloride form (anionic tetra-halogen complexes [CuCl$_4$]$^{2-}$) by the two evaporation step and dissolution in concentrated hydrochloric acid.

Once ready, the first Zn-x1 metal target was transferred into the "MIX-x1 gamma" vial and 4.5ml of HCl 10 M have been added for the Zn dissolution. 0.5 ml of the ^{63}Cu solution in HCl 10M was added. γ-spectrometry was carried out on this sample for 1 h before starting the separation process.

The same procedure was performed for Zn-x2 in "MIX-x2 gamma" vial.

After γ-spectrometry, the MIX samples were ready to be treated with the already described separation procedure almost simultaneously.

Briefly, the MIX solution was injected in the cation exchange resin and collected, after discarding the first 2 ml of dead volume of the column, in a glass evaporation vial by the elution with 12 ml of HCl 10 M. The so far obtained solution, containing copper and zinc, were transferred to the evaporation system and left for about 40 min to dry. In the meantime, the retained gallium on the column was eluted in "Ga-xy 20ml" glass bottle with 20 ml of the acetone/HCl solution and weighted. The Ga

solution was vigorously stirred by a mechanical vortex and a 5 ml homogeneous aliquot was transferred in "Ga-xy gamma" spectrometry vial, ready to be weighted and analyzed (1h of acquisition).

After the complete evaporation of the Cu-Zn solution, the residue was dissolved in 1ml of HCl 2M and evaporated and dissolved again with 1ml of HCl 2M.

This solution was injected into the second resin, the anion exchange one, discarding the first 2 ml, then eluted copper with 20 ml of HCl 2M and collected in "Cu-xy 20ml" vial. The solution was weighted, stirred and a 5ml aliquot transferred in "Cu-xy gamma" spectrometry vial, ready for the 2h spectrometry acquisition.

The Zn retained on the column was eluted in "Zn-xy 20ml" vial with 20 ml of HCl 0.005 M, weighted, stirred, aliquoted and analyzed by γ-spectrometry for 1h.

Finally, Al monitor foils, already acquired by γ-spectrometry in solid configuration, were dissolved directly in the "Al-xy gamma" spectrometry vial by adding 5 ml of HCl 10 M. Then, weighted and acquired again in liquid configuration for all the night long. Similarly, the same procedure has been adopted for Ni monitor foils, in run #5.
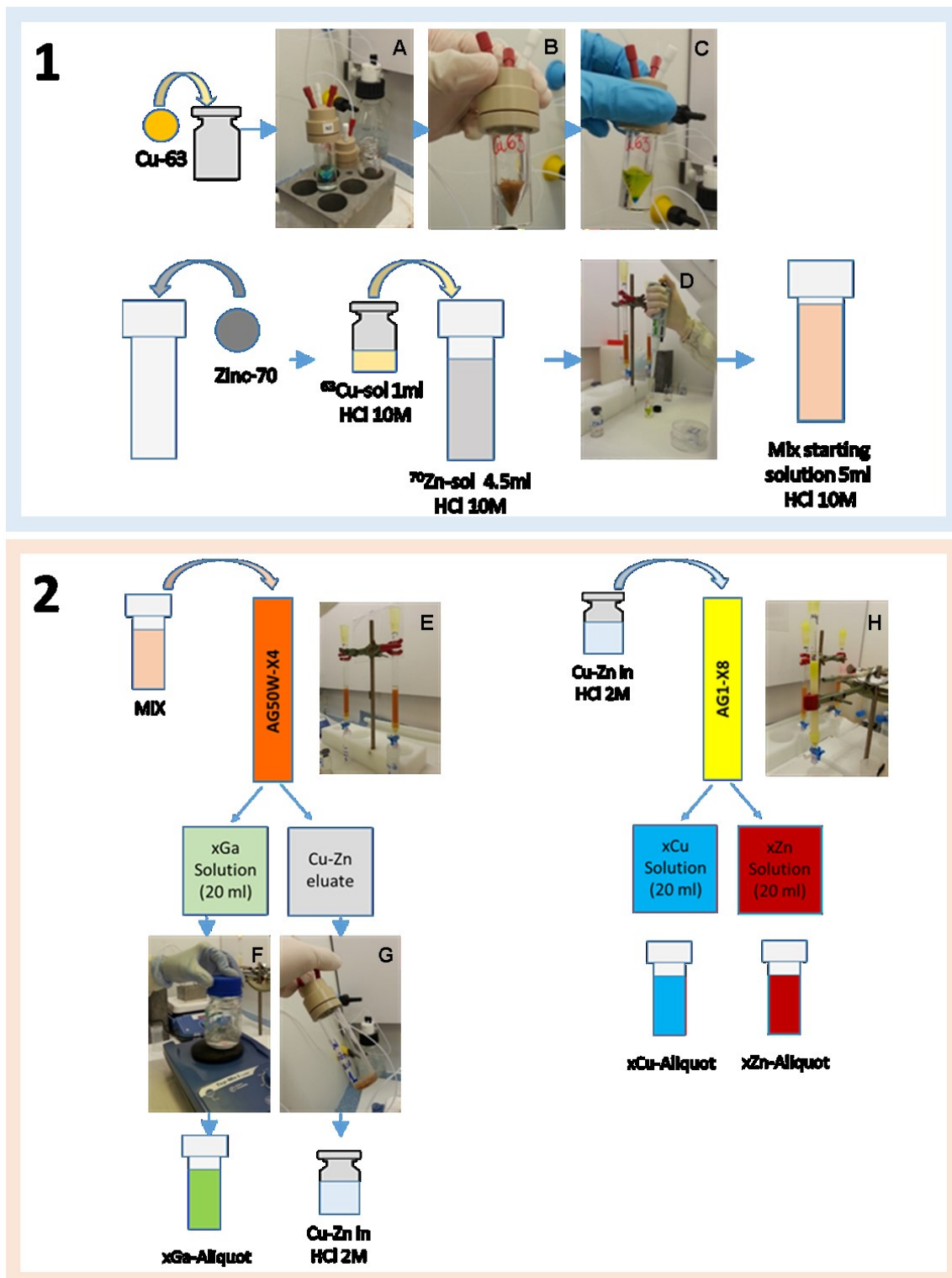
Figure 52 Schematic representation with pictures of main steps of the separation procedure applied to all the targets used in all the irradiation runs (11 times in total). Box n.1 on the top represents the preparation of the starting solution from the irradiated targets: **A, B, C and D**: Dissolution of Cu-63 in HNO$_3$ 6 M and consequent evaporation, dissolution in HCl 10 M (repeated twice); dissolution of the Zn-70 target in HCl 10M and addition of a 0.5ml Cu-63 aliquot to the dissolved zinc thus becoming the MIX solution containing all Cu, Ga and Zn isotopes.

Box n.**2** on the bottom represents the separation steps by means of two ion exchange resins: **E**. Simultaneous treatment of MIX solution by the cation exchange resin in which gallium isotopes are retained (Ga-66 e Ga-67) while Cu and Zn isotopes are left to flow through the resin; **F**. The "xGa" solution eluted from the cation exchange resin under stirring by means of a mechanical vortex to ensure the homogeneity of the solution before aliquoting (xGa-Aliquot 5ml); **G**. The eluted Cu-Zn solution under evaporation before dilution in HCl 2 M (repeated twice); **H**. Simultaneous treatment of Cu-Zn 2 M HCl solution by the anion exchange resin in which Zn isotopes are retained (Zn-62, Zn-65, Zn-69 and Zn-nat) while Cu isotopes are left to flow through the resin (Cu-61, Cu-64 e Cu-67) in the final "xCu" solution; "xZn" solution is then obtained by eluting the colum with HCl 0.005M. Both solutions were aliquoted for gamma spectrometry analysis (xCu- and xZn-Aliquot 5 ml each).

All γ-spectrometry analysis were performed by a HPGe detector available at ARRONAX facility (*Figure 53*), by using two different geometries: sample at 19 cm distance from the detector, such as for the MIX solution acquisition, and sample in contact with the detector, such as for xCu, xZn, xGa and monitor foils acquisition. For both geometries the detector efficiency was measured by using a certified reference solution (source).
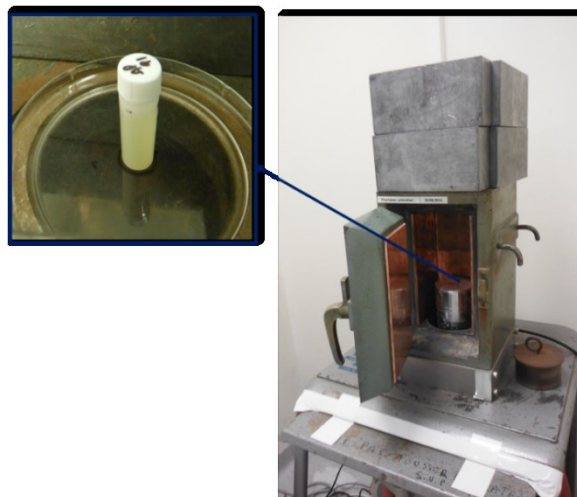
Figure 53 Picture the HPGe detector involved in the γ-spectrometry measurements of our samples.

Some examples of spectra acquired are showed in *Figure 54*. Even with a visual inspection of the spectra it is possible to notice qualitatively that the separation procedure was able to separate the three elements of interest, considering the different shape of the spectra, the absence of characteristics lines etc..
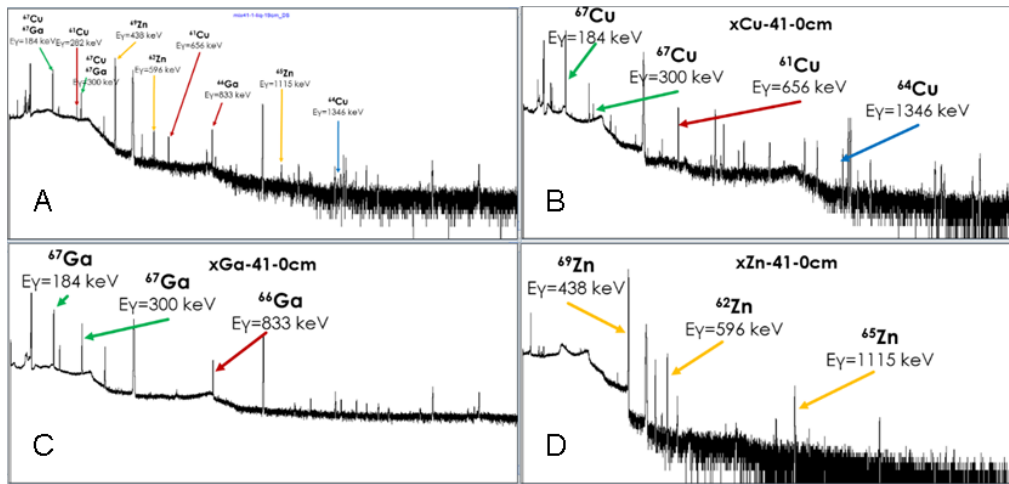
Figure 54 Some spectra example of MIX solution (A), xCu (B), xGa (C) and xZn (D) solutions after the separation procedure.

By using the tracer radionuclides, Cu-61 for Cu-isotopes (Cu-67 and -64) and Ga-66 for Ga-isotopes (Ga-67), it was possible to calculate the separation yield and therefore to deduce the activity of the radionuclides before the separation ($Act^I_{nuclide}$) by means of the following *Equation 4*:

$$Act^I_{tracer} : Act^I_{nuclide} = Act^F_{tracer} : Act^F_{nuclide} \rightarrow Act^I_{nuclide} = Act^F_{nuclide} \cdot \frac{Act^I_{tracer}}{Act^F_{tracer}}$$

Equation 4

The activity determination from the γ-spectra, acquired by HPGe detectors, was performed as follow:

once identified the corresponding peaks for each element tracer is possible to calculate the radionuclide activity *A* (*Equation 5*), in Becquerel,

$$A = \frac{A_n}{t \cdot \varepsilon(E) \cdot y(E)}$$

Equation 5

where A_n represent the net area of the peak, *t* the acquisition time, *ε(E)* the detector efficiency at the energy value of the peack, *y(E)* the abundance of the γ-emission at the energy peack.

When the nuclides of interest present two or more γ-lines with no interference, a weighted mean value of the corresponding activities *A** has been calculated, by using *Equation 6*:

116

$$A^* = \frac{\sum A_i/\sigma_i^2}{\sum 1/\sigma_i^2} \qquad \sigma(A^*) = \sqrt{\frac{1}{\sum 1/\sigma_i^2}}$$

Equation 6

Where $\sigma(A^*)$ is the resulting uncertainty related to A^* and σ_i is the uncertainty associated to each value A_i.

4.4 Project Preliminary Results

Firsts results from the spectra analysis revealed a mean separation yield based on the last 4 irradiation runs (therefore, on 7 target foils). The recovery yield of each tracer in its solution are listed in *Table 35*.

Table 35 Mean purification yield evaluated on all eleven samples expressed in percentage. ND= Not Determinable since isotopes characteristic peaks have not been observed in the spectra (peaks assessed below the minimum detectable activity).

%	Gallium solution	Copper solution	Zinc solution
Ga-66	79 ± 11	2 ± 1	ND
Cu-61	ND	95 ± 2	ND
Zn-69	ND	ND	84 ± 2

While Cu is all recovered in the Cu solution and no Cu trace have been found in the other samples, a small amount of Ga-66 has been found in the Cu solution and precisely the 2 ± 1 % of the total Ga-66 activity present in the MIX solution before the separation procedure. This means that the first cation exchange resin did not trap efficiently Ga, in agreement with standard chromatographic technology efficiency.

This percentage of Ga-67 into the copper solution has to be taken into account when elaborating the data for cross section determination. Data analysis are still ongoing, we expect to accomplish this study within few months.

In addition to this, the recoil effect has to be considered during activity estimation. In fact, some atoms are recoiled from the foil were they are produced into the

following; this effect is particularly evident in thin foils (thickness in the order of 10 μm) and light atoms (as Na-24) such as those used in these experiments (*Figure 55*)
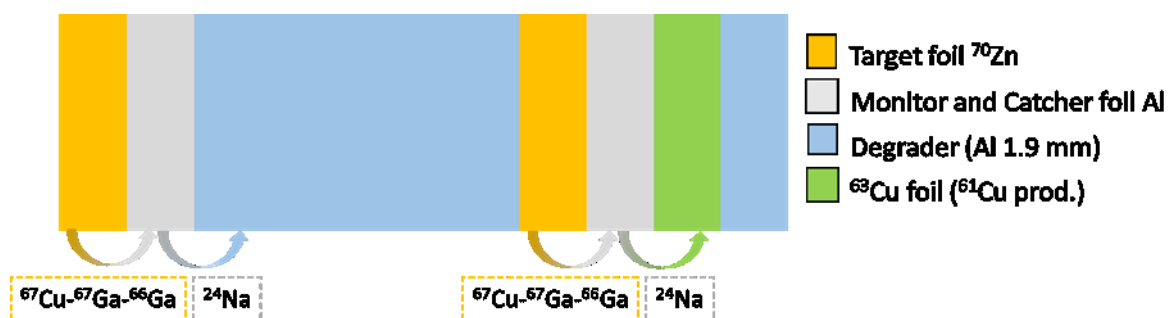
Figure 55 Graphical representation of the Recoil effect in a typcal stacked-foils target.

The proper procedure, described above, was optimized based on the experience gained during the first two experiments. In the following a list of issues and solution experienced:

- During the first run the starting solution was prepared in a glass vial and then transferred to the first resin for starting the separation procedure without acquiring a spectrum of the whole starting solution, missing in this way a reference of the starting activity.

- In the second run we decided to acquire the spectrum of the whole starting solution by transferring it from the glass vial in which it was prepared into the "MIX-xy gamma" vial. That time we found that the total activity was underestimated for a factor of about 50%. The glass vial in which the starting solution was prepared, also if empty, was still active. Acquiring a rough spectrum of the vial, also if not calibrated for that geometry, it was found that part of the gallium isotopes was still in the vial, but no other elements (copper or zinc). Indeed, it is known in literature (Baum & Rösch, 2012; Sampson, 1994) that gallium "wets" glass, whereby the adsorption of gallium on the glass wall of the vials occurs through intermolecular interaction and adhesive force. It was also proved that this effect does not happen if gallium is in the chloride complex form. We also experienced the same since gallium at 10 M HCl concentration is in the cationic hydrate form and adhere at the glass vial,

instead, when eluting Ga in the chloride anionic form in the glass vial this was not retained on the glass walls.

- The Ga solution eluted in a glass bottle was vigorously stirred before the aliquot sampling. We adopted this technique since we have found gallium in the final separated solution illustrating the heterogeneity of the aliquot taken as reference for the whole sample. An experiment (4th irradiation run) also dedicated to the measurement of solution's homogeneity, confirmed that it is possible to analyze with γ-spectrometry an aliquot of the solution and apply the result to the whole solution, once the volume ratio is taken into consideration.

5 Ga-68 PRODUCTION STUDIES FROM LIQUID TARGET AT TRIUMF

^{68}Ga ($T_{1/2}$ = 68 min) is a positron emitting radioisotope currently produced by a germanium-68 (^{68}Ge; $T_{1/2}$ = 270.95 d) ^{68}Ge/^{68}Ga generator. Radiometal production by liquid target on a small medical cyclotron could be an alternative and inexpensive method since it could be done in the already existing infrastructure and device routinely in use for F-18 and others PET isotopes production (Oehlke, et al., 2015; Pandey, et al., 2014 a; Degrado, et al., 2011). This technique will improve the availability of Ga-68 in hospitals housing an appropriate cyclotron by making hospitals independent self-producers (Oehlke, et al., 2015; Pandey, et al., 2014 b).

TRIUMF and others are investigating the liquid target cyclotron production of several radiometals such as technetium-94m (Hoehr, et al., 2012), scandium-44 (Hoehr, et al., 2014), yttrium-86, zirconium-89, copper-61 and gallium-68 (Oehlke, et al., 2015; Pandey, et al., 2014 a; Degrado, et al., 2011). The liquid target Ga-68 cyclotron production by the ^{68}Zn(p,n)^{68}Ga nuclear reaction has been previously investigated and published for irradiation condition optimizations such as nitric acid concentration and target body materials (Oehlke, et al., 2015).

In order to obtain a final product comparable with the generator eluate, a purification procedure has been developed. Since the sensitivity of the DOTA-TOC radiolabeling to the quality of the Ga-68 used, the procedure particularly focuses on the high quality of the final product in terms of CP to enable radiolabeling and in-vivo imaging studies.

5.1 Liquid Target Preparation and Irradiation

The liquid target material used for the experiments was a ^{68}Zn nitrate solution prepared right before the irradiation. Enriched zinc oxide ^{68}ZnO (99.9%) was purchased from Isoflex (Ward Hill, MA, USA), ultrapure nitric acid (TraceMetal™ grade) was obtained from Fisher Scientific (Ottawa, Ontario, Canada). 0.5 g of zinc oxide were dissolved in 0.5M nitric acid solution and stirred for 1 or 2 hours. The solution was then evaporated to dryness and other 0.5M nitric acid has been added (about 6 ml).

The TR19 cyclotron installed at the BC Cancer Agency (BCCA) in Vancouver and a niobium-body target (6.6 ml target volume, ASCI, Richmond, Canada) have been

used for irradiation runs. As beam window an Havar® 30 μm thick foil (Hamilton Precision, Lancaster, PA, USA) were used.

The irradiation conditions and expected activity production are listed in *Table 36*. At the end of each irradiation, the liquid target was transferred by pressurized helium and collected into a vial in the hot cell.

Table 36 ^{68}Zn(p,n)^{68}Ga production yields from 13.8 MeV proton bombardment in liquid target on a TR19 cyclotron.

Beam time [min]	123 ± 26
Dose [μA.min]	2105 ± 166
Number of runs	5
Beam current [μA]	17.6 ± 3
Beam time [min]	123 ± 26
EOB Yield [MBq]	3564 ± 608
Saturated Yield [MBq/μA]	288 ± 25

In addition to co-produced isotopes by alternative nuclear reaction channels on the Zn target, contaminants coming from the liquid body-target degradation since the corrosivity of the liquid target nitric acid solution, such as iron from the Havar beam-window foil, are present in solution.

5.2 Separation Procedure ^{68}Zn/^{68}Ga

Materials and Methods

Preliminary purification optimization experiments were conducted by preparing a cold mock natural-Zn nitrate solution simulating the liquid target characteristics described in the previous paragraph, and by adding a small amount of generator eluted Ga-68 0.6M HCl solution (about 0.36 GBq eluted by an iThemba ^{68}Ge/^{68}Ga Generator, South Africa). This solution was then spiked with iron (III) chloride (0.145 mg) to reproduce possible impurity conditions post irradiation.

Once a purification procedure was established it was then performed on liquid target cyclotron-produced Ga-68.

For the purification, nitric acid and hydrochloric acid (TraceMetal™ grade) were obtained from Fisher Scientific (Ottawa, Ontario, Canada), AG50W-X8 resin was purchased from BioRad (Hercules, California, USA), DGA and LN resins were purchased from Triskem International (Bruz France). For the automation of the procedure three peristaltic pumps used for the semi-automated system was purchased from Welco, model number WPX1-P1/16S4-BP (Tokyo, Japan).

For the determination of the CP, iron test strips with a detection sensitivity range from 0-5 mg/L were purchased from Hach (London, Ontario, Canada), Quantofix Zinc test strips from Macherey-Nagal and Potassium thiocyanate ACS reagent ($\geq$ 98.5%) were purchased from Sigma (Oakville, Ontario, Canada).

Experimental

Different resins combinations were tested in order to find the proper procedure that allowed to obtain a high pure Ga-68 product. The resins were always conditioned and manually packed in empty polypropylene reservoirs of different volumes capped by PTFE frits:

- DGA resin was packed between two 10 µm polyethylene frits in a 1 mL reservoir and conditioned with 7 M HCl;
- LN resin was first incubated with H_2O for 20 min to swell, packed into a 1 or 4 mL reservoir between two frits and then conditioned with 7 M HCl;
- AG50W-X8 resin was incubated in 10 M HCl for at least 20 min and subsequently packed on top of one frit in a 15 mL reservoir.

The purification system used for the experiments (procedure 1) consisted of DGA (100 mg), LN (1000g) and DGA (50 mg) (*Figure 55*). According to (Horwitz, et al., 2005), the DGA resin should not retain Zn^{2+} at any HCl or HNO_3 concentration while Ga^{3+} should be well retained in HCl 7-12M. LN resin retains both Ga^{3+} and Fe^{3+} at HCl concentration between 5 to 7 M while decreasing the HCl concentration to 0.5-1 M should cause Ga to be eluted from the resin, while Fe should still be retained. The last DGA resin has been used to concentrate the Ga^{3+} by first retention on the resin and then elution in a small volume of water. The so called procedure 1 is schematically described in the diagram below (*Figure 56*)
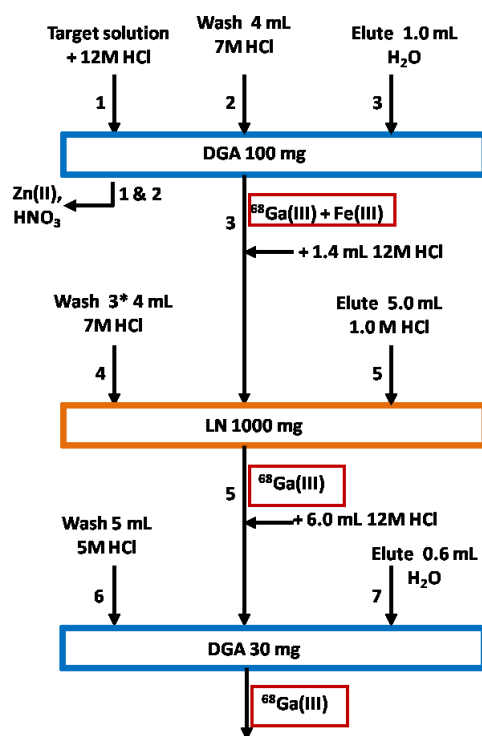
Figure 56 Purification schematic (procedure 1) with DGA, LN resins and DGA.

The purification procedure takes about 48 ± 11 min and is able to recover 69±5% (Decay Corrected, DC) of the starting activity (n=5). Given that the samples to be analyzed for chemical purity determination were radioactive, the fastest and easiest tests enabling to avoid instrument contamination were selected. In particular, the determination of Zn in the final solution has been conducted by colorimetric strip test while the iron amount determination in the final product has been conducted by using potassium thiocyanate. This last assay forms a pink-red colored complex $FeSCN^{2+}$ even at ppm quantities of Fe^{3+}. Higher concentrations of Fe^{3+} in the solution will produce a more intense color. By preparing standard solutions with an increasing known amount of Fe^{3+}, we can create our own color gradation scale. We have prepared 5 standard solutions in the range of 0.5 ppm to 2.5 ppm by increasing steps of 0.5 ppm of Fe^{3+} and by adding 4 drops of KSCN 1M to each.

The Zinc and Iron (III) amount in the final product have been found <100 ppm and >2 ppm respectively (Oehlke, et al., 2015; Pandey, et al., 2014 b). Since the poor quality of the so far obtained final isolated product, low radiolabeling yield (<20%) of DOTA-TOC were always obtained. Indeed, as demonstrated by Oehlke et al., the radiolabeling yield can be affected by a reduction of 20% if an excess of Fe^{3+} is

present in the solution (iron to ligand ratio of 1) (Oehlke, et al., 2013; Oehlke, et al., 2016).

For that reason, some changes have been introduced to the original procedure in order to maximize the final CP of Ga-68.

In particular, the first resin has been replaced by an AG50W-X8 (3.5 g) cation exchange resin followed by the LN (1000 mg) and DGA (30 mg) (*Figure 57*). Other changes affected the resins amount and elution volumes ad concentrations.
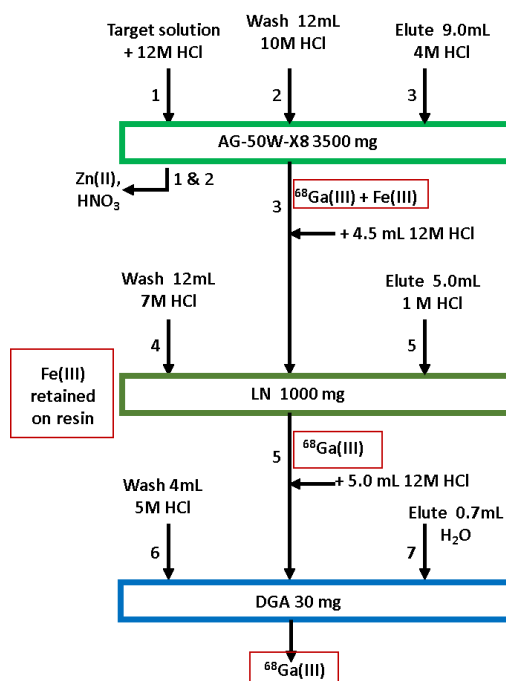
Figure 57 Purification schematic (procedure 2) utilizing AG50W-X8, LN and DGA resins for improved ^{68}Ga purification from Zn^{2+} and Fe^{3+}.

The manual procedure takes place in 110±5 min and allows to recover 67±8% (n=3, DC) of the starting Ga-68 activity. The Zn and Iron amount have been evaluated being <2 ppm and <0.5 ppm respectively.

The procedure includes (see also illustrated gallium activity distribution in *Figure 60* for a better understanding):

- Dilution of starting solution (mock Zn solution in nitric acid spiked by generator eluted Ga-68 and Iron (III) chloride) in 24ml of HCl 12M in order to obtain a 10M HCl solution of about 30 ml;

- Loading of the 10 M HCl solution onto AG50W-X8 resin and collecting the eluate in a waste vial, Ga^{3+} and Fe^{3+} should be retained on the column while Zn should flow through the resin;
- Washing the resin with 12ml of HCl 10M and collecting the eluate in a washing/waste vial;
- Eluting Gallium from the resin with 9 ml of HCl 4M and collecting the eluate in a vial after discarding 2 first ml of dead volume of the resin.
- Adding to the Ga-68 eluate 4.5 ml of HCl 12 M in order to bring the HCl concentration in solution up to 7M;
- Loading the obtained 7M solution on the top of the LN resin and collecting the eluate in a waste vial, both Ga^{3+} and Fe^{3+} should be retained on the resin;
- Washing the LN resin with 12 ml of HCl 7M and collecting the eluate in a washing/waste vial;
- Eluting Gallium from the resin with 5 ml of HCl 1M in a vial after discarding the first ml of dead volume of the resin while Fe3+ should still be retained by the resin;
- Adding 5ml of HCl 12 M to the eluted Gallium to bring the HCl concentration up to 6M;
- Loading the 6M gallium solution into the DGA resin and collecting the eluate in a waste vial, gallium should be retained on the resin;
- Washing the DGA with 4ml of HCl 5M and collecting the eluate in a washing/waste vial;
- Eluting Gallium with 0.7ml of H_2O (final product).

Once the optimal purification method was established, a semi-automated system was devised to decrease the operators dose. The automatic procedure has been firstly developed by using only one peristaltic pump as liquid transfer mechanism (*Figure 58*). Separation of ^{68}Ga from Zn^{2+} and Fe^{3+} contaminants using one peristaltic pump for all three resins was not effective. When this module was used for the purification test a cross contamination of elements caused a decrease in the final purity of the product. Indeed, all solutions (loading, washing or elution solvents) were passing through the same pump leaving traces of metals on the tubing walls that were unfortunately not removed by the washing steps. Zn and Fe traces have been found > 100 ppm and > 2 ppm respectively in the final solution.
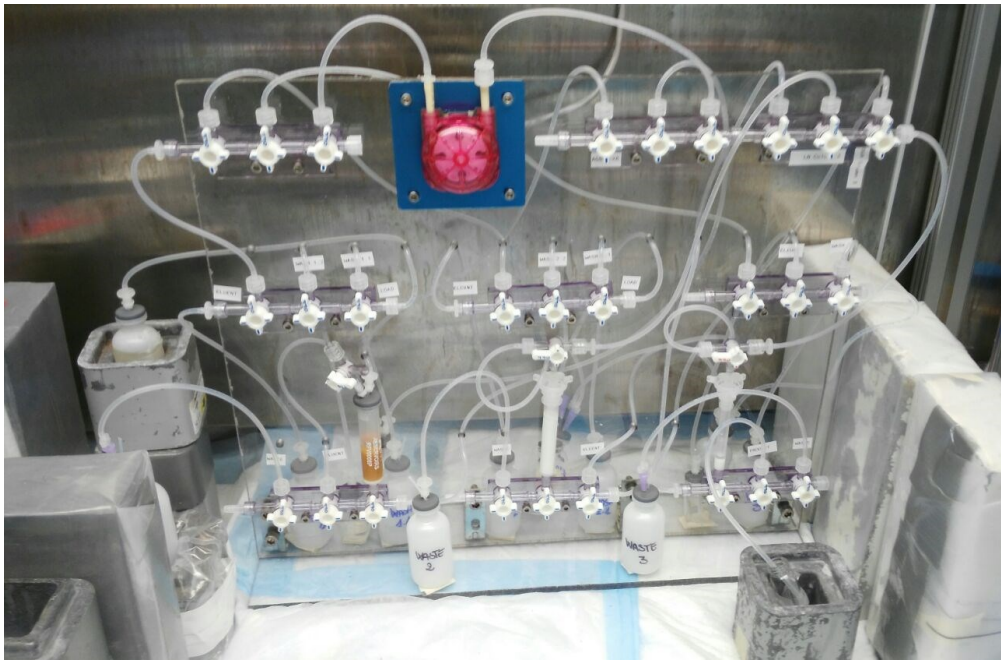
Figure 58 One pump semi-automatic module.

To solve this problem, a new semi-automatic module based on three peristaltic pumps, one for each resin, have been realized (*Figure 59*) preventing the spread of metal impurities during the purification.

Figure 59 Three pumps semi-automatic module.
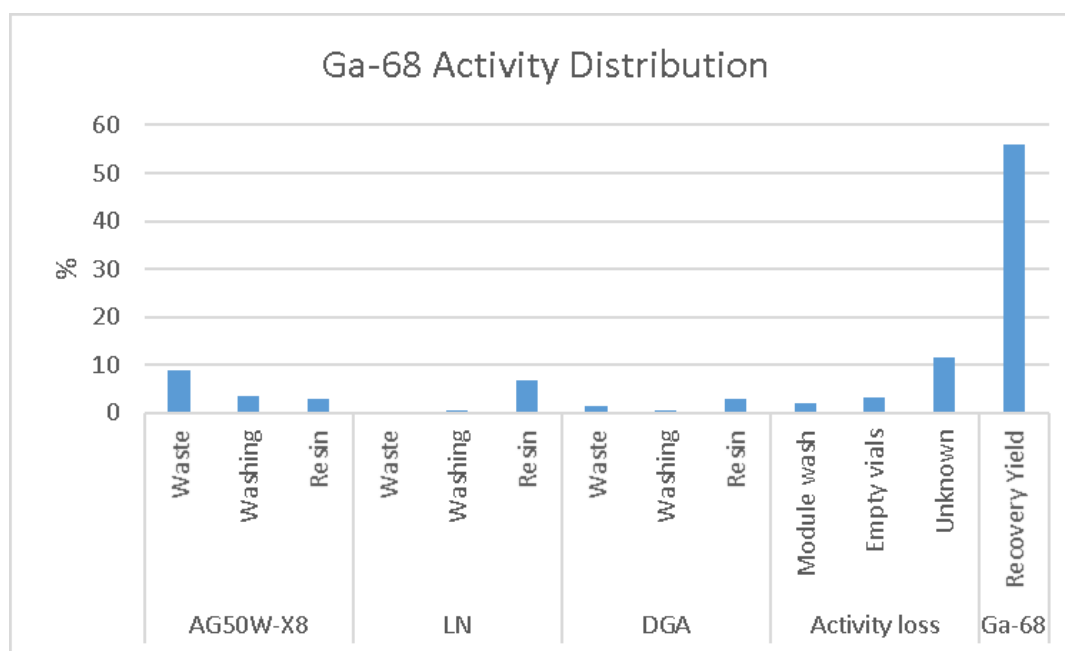
Figure 60 Ga-68 activity distribution in the three step separation/purification procedure. Ga-activity measured for different samples (Waste, Washing, Resins, empty vials) and in the final product (recovery yield), expressed in terms of percentage (average of n= 4 experiments). Estimated activity loss, not measured (Unknown) are also reported in the graph.

Results

All tests, from an irradiated liquid Zn target and processed by the three pumps semi-automatic module, resulted in a high pure gallium solution (Zn<5 ppm and Fe<0.5 ppm) at the expense of the time required to complete the procedure and the recovery yield. Indeed, in 90 ± 10 min the 55 ± 10 % (n = 4, DC) of the starting activity were recovered at the end of the procedure (*Figure 60*). However, the lengthy procedure is not ideal for ^{68}Ga purification we think that by developing a fully automated system we could reduce the time necessary for the purification, increase the recovery yield and maintain the high purity of the final product. However, despite the lower purification yield, Ga-68-DOTA-TOC radiolabeling yield were consistent at 91 ± 6% (n = 4).

5.3 Radiolabeling of DOTATOC

Using the method described in the previous section, cyclotron-produced $^{68}GaCl_3$ (380 MBq in 0.7ml H_2O) was added to 25μg of DOTATOC (Advanced Biochemical Compounds, Radeberg, Germany) in HEPES buffer solution (0.7ml, 2M, pH=5) and heated up in a microwave for 90 sec. The purification of ^{68}Ga-DOTATOC from unlabeled DOTATOC and free gallium has been performed by HPLC (high performance liquid chromatography, Agilent™ system equipped with a UV and NaI scintillation detectors) by using a C-18 semi-preparative column (Phenomenex C18, 5 μm, 250 x 10mm) and with 79% PBS buffer and 21% acetonitrile (MeCN) at a 4.5mL/min flow rate.

C18 Sep-Pak cartridges (1cc, 50 mg) were obtained from Waters Corporation (Milford, MA) and conditioned with 5 mL 100% ethanol and 10 mL 0.05 M ammonium formate. Quality control and SA determination of the radiolabeled ^{68}Ga-DOTATOC was conducted on a C-18 analytical column (Phenomenex C18, 5 μm, 250 x 4.6 mm). Only labeled ^{68}Ga-DOTATOC was collected from the HPLC and the radiochemical yield was so determined. The ^{68}Ga-DOTATOC was then diluted with 50 ml of ammonium formate 0.05M solution and loaded on a C18 light Sep-Pak cartridge.

The final product was eluted from the cartridge with ethanol (100%) and formulated in PBS for animal studies (ethanol concentration less than 10% in PBS). An aliquot of the final radiopharmaceutical has been analyzed for purity and SA determination by HPLC on a C18 column with 79% PBS and 21% acetonitrile at a flow rate of 2 ml/min (isocratic).

The same procedure has been adopted for generator eluted Ga-68 DOTATOC preparation (297 MBq starting activity).

Both generator and cyclotron produced radiopharmaceuticals, involved in the animal studies (n=1 each), yielded a RCP >98%. Radiolabeling yield was found of 96% for the generator and 94% for the cyclotron produced Ga-68-DOTATOC. SA was calculated as 115 MBq/nmol for ^{68}Ga-gen-DOTATOC and 443 MBq/nmol for ^{68}Ga-cyclo-DOTATOC.

5.4 Imaging and Biodistribution Studies

Twelve female mice (25g NSG mice) were implanted with ZR75-1 cells in matrigel on the right shoulder; BD Biosciences, San Jose, CA, USA) were used in this study performed at the BCCRC (BC Cancer Research Centre) Animal Resource Centre in accordance with the guidelines of the Animal Care Committee at UBS (University of British Columbia, Vancouver, BC, Canada).

Six mice were involved for imaging studies (three injected with generator- and three with cyclotron-^{68}Ga-DOTATOC) with a Simens Inveon Small animal PET scanner (Siemens Medical Solutions, Knoxville, TN, USA). These six and the remaining six mice were all involved for biodistribution studies 1h post injection (six injected with generator-^{68}Ga-DOTATOC and six with cyclotron-^{68}Ga-DOTATOC).All mice were anaesthetized with isoflurane (2% O2) prior to the radiopharmaceutical injection.

Generator (4.6±0.2 MBq) or cyclotron (5.0±0.5 MBq) ^{68}Ga-DOTATOC were injected via intravenous tail vein to six mice for PET imaging studies. About 45 min post injection the mouse was placed in the scanner bed and the acquisition started. Each mouse underwent a CT scan (10 minutes- total body in three times) followed by a PET acquisition (10 minutes) (*Figure 61*). Images were reconstructed using the 3-dimensional ordered-subsets expectation maximization (OSEM3D, 2 iterations) followed by a fast maximum a priori algorithm (FastMAP: 18 iterations) and corrected for attenuation based on the CT image.

The remaining six mice were injected with with 1.6±0.3 MBq gen-^{68}Ga-DOTATOC or 1.5±0.4 MBq of cyclo-^{68}Ga-DOTATOC. These six mice and those involved in imaging studies were euthanized by inhalation of isoflurane followed by CO_2 1-hour post injection and biodistribution studies were conducted on all mice.

Blood was withdrawn by intra-cardiac puncture and all organs were harvested, washed in PBS, weighed and the activity measured by a gamma counter. The activity uptake was expressed as a percentage of the injected dose per gram of tissue (%ID/g) (*Table 37*).
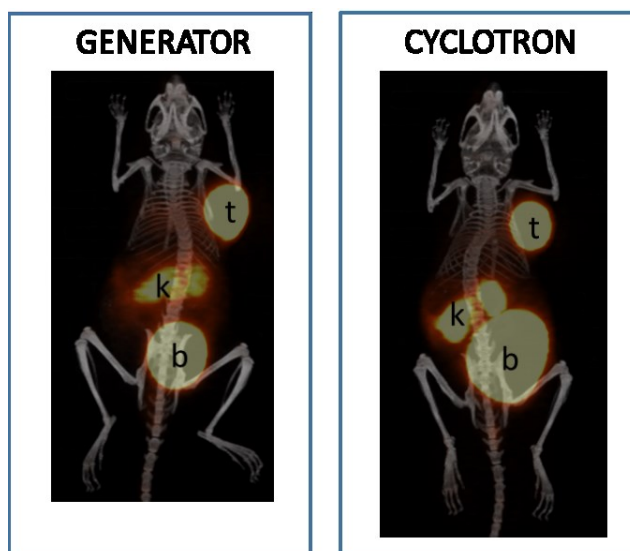
Figure 61 Representative PET/CT images at 1 hour post injection of DOTATOC radiolabeled with ^{68}Ga either from the generator (left) or the cyclotron (right). ZR75-1 tumours (t) are visible on the right shoulder as well as kidney (k) uptake and bladder (b).

Table 37 Biodistribution data (mean ± SD %ID/g, n=6 for each category) 1 hour after injection of gen-^{68}Ga- DOTATOC or cyclo-^{68}Ga- DOTATOC in mice bearing ZR75-1tumours.

Organs	%DI/g	
	Generator	Cyclotron
Blood	0,5 ± 0,2	0,8 ± 0,2
Fat	0,19 ± 0,07	0,4 ± 0,2
Ovaries	0,8 ± 0,3	0,9 ± 0,2
Uterus	0,6 ± 0,2	0,9 ± 0,1
Intestine	2,1 ± 0,8	2,2 ± 0,9
Spleen	0,5 ± 0,2	0,7 ± 0,2
Pancreas	11 ± 3	12 ± 3
Stomach	2 ± 1	3 ± 2
Liver	0,6 ± 0,1	0,7 ± 0,1
Adrenals	5 ± 2	6 ± 3
Kidney	11 ± 1	14 ± 3
Heart	0,3 ± 0,1	0,4 ± 0,1
Lungs	11 ± 6	8 ± 4
Tumour	18 ± 3	18 ± 6
Muscle	0,2 ± 0,1	0,2 ± 0,1
Bone	0,4 ± 0,2	0,5 ± 0,1
Brain	0,04 ± 0,01	0,06 ± 0,01
Tail	1,1 ± 0,4	0,9 ± 0,2

5.5 Project Results

We have developed a method for the purification of cyclotron-produced ^{68}Ga that permitted radiolabeling of the sensitive DOTATOC by minimizing the presence of iron and zinc contaminants, a process that until now resulted in poor radiolabeling yields. The purification from zinc excess was carried out by the cation exchange resin AG50W-X8 while the use of LN resin significantly reduced the iron content. The automation of the purification procedure was performed by assembling valves, tubing and peristaltic pumps on a Plexiglas thick sheet. The conversion from 1 pump to 3 pumps, one pump dedicated to each resin was necessary to avoid metal contamination of the final product reducing its CP. These resin combinations and semi-automated procedure resulted in successful radiolabeling of DOTATOC, with high radiochemical yield. Comparative radiolabeling, imaging and biodistribution studies have been conducted between generator-^{68}Ga and liquid target cyclotron-produced ^{68}Ga labelled DOTATOC.

Radiolabeling yields were found to be comparable between cyclotron and generator produced ^{68}Ga-DOTATOC, respectively 94% and 96%.

μPET-CT images (1 h post-injection, *Figure 61*) showed similar high uptake of the ^{68}Ga-DOTATOC within the ZR75-1 tumours also confirmed by the biodistribution data 18 ± 3 and 18 ± 6 % injected dose per gram for the generator and liquid target cyclotron-produced Ga-68, respectively (*Table 37*).

For both ^{68}Ga-*gen* and ^{68}Ga-*cyclo*, a typical biodistribution profile of ^{68}Ga-DOTATOC was observed with high kidney and bladder uptake, an expected result due to the high expression of somatostatin receptors in these organs; all other organs showed no statistical differences in absolute uptake (t-test, p values < 0.05 were considered statistically significant).

CONCLUSIONS AND PERSPECTIVES

Radiometals are widely used in all nuclear medicine branch, SPECT/PET diagnostic, therapy and theranostics. Their employment is regulated by the physical characteristic such as half-life, radiation emission type (γ, β^+, β^-, auger, α), by the associated emission energy and the chemical ability to coordinate with ligands forming a wide range of radiopharmaceuticals for different purposes.

Medical isotopes are commonly produced by nuclear reactors and cyclotrons. In particular the announced permanent shutdown of some nuclear reactors (e.g. NRU Chalk River (Osborne, 2016)), has accelerated the research on alternative accelerator-based production routes, that can result in a complete, safe, cost-effective, efficient technology able to prevent further medical radionuclide shortages.

Supporting this theory, a wide international interest of research groups and, even more important, companies, demonstrated on the development of the technology for radiometals cyclotron production, such as targets, targets processing modules etc., and for expanding the radiometals availability for medical applications.

Also the Italian scientific community has demonstrated its involvement in this research topic in particular by the foundation of an at the vanguard research facility under construction nowadays.

Indeed, at Legnaro National Laboratories of the National Institute of Nuclear Physics (LNL-INFN) a high performance cyclotron has been installed in the SPES (Selective Production of Exotic Species) project context. LARAMED (LAboratoty of Radioisotopes for MEDicine) is a branch of SPES aimed at the study and production of medical radionuclides by means of cyclotron. Even if the cyclotron is still not in operation the LARAMED team started working on the cyclotron production of conventional radionuclides such as Tc-99m (APOTEMA, and TECHN-OSP projects), emerging radionuclides such as Cu-67 (COME project), Sc-47 (PASTA project) and Mn-52 (just approved METRICS project) and on the development of high power target (TERABIO premium-project). The collaboration with Nuclear Medicine radiopharmacies holding a PET cyclotron (e.g. Sant'Orsola Hospital, Bologna, IT), national and international research institute such as JRC-ISPRA (Varese, IT) and ARRONAX (Nantes, FR) respectively made all this possible.

In this work, in the framework of LARAMED project, the TECHN-OSP and COME project have been described. The emphasis was on post irradiation target processing: the development and optimization of radiochemical separation and purification of the desired product from the activated target and the automation of the procedure as final step.

Moreover, my collaboration experience at TRIUMF (Vancouve, CA) with the Life Sciences division on two more projects (i.e. Tc-99m cyclotron production and Ga-68 liquid-target cyclotron-production) has been here described as well.

The purpose of TECHN-OSP project was the development of a proper technology able to produce GBq amount of technetium-99m by medical cyclotron, through the (p,2n) nuclear reaction on a Mo-100 enriched metal target, and to afford routine supply of the most used radiometal in diagnostic applications in case of shortages. To achieve this aim: (1) a specific target assembly, suitable for a standard solid target station in medical cyclotron, has been designed; (2) a remotely controlled module for high yield pertechnetate extraction/purification has been developed and (3) a molybdenum target recovery process has been studied and determined.

In order to validate such a technology, several production tests have been performed in a nuclear medicine department (Sant'Orsola Hospital, Bologna, IT) equipped with a 16 MeV cyclotron by irradiating ^{100}Mo-enriched molybdenum metallic targets. Quality control procedures on the final products, radiolabeling and phantom imaging studies with a clinical gamma camera, have been conducted as well.

The developed technology allowed to obtain cyclotron-produced $[^{99m}Tc]TcO_4^-$ suitable for clinical application with a Quality Assurance (QA) process in compliance with the European Pharmacopoeia recently issued.

Labeling, on phantom and in vivo imaging studies performed have demonstrated that no substantial differences in radiopharmaceuticals stability, images quality and biodistribution, respectively, between generator- and cyclotron- produced technetium-99m may be found. In particular, the presence of other Tc isotopes in the final product does not affect significantly the image definition, if using conventional gamma-cameras in standard energy window, nor the equivalence of imaging parameters and biodistribution between cyclotron- and generator-derived

^{99m}Tc preparations (Selivanova, et al., 2017; Guérin, et al., 2010; Martini, et al., 2015; Pupillo, et al., 2016).

In conclusion, local nuclear medicine departments equipped by medical cyclotrons and our technology will be able to self-produce sufficient amount of technetium-99m for their daily diagnostics needs.

With the aim to scale-up and validate an alternative Tc-99m production and purification method, the TRIUMF research group is also working on Tc-99m cyclotron-production. When I was there, I had the opportunity to collaborate at the project named "A Trans-regional initiative to achieve large scale production, distribution, supply and commercialization of Tc-99m" by contributing at the optimization and automation of molybdenum target dissolution and purification procedure of cyclotron-produced ^{99m}Tc.

With regards to the dissolution, an experimental setup has been installed to performed the dissolution experiments of electrophoretic deposited molybdenum TR30 targets. The 30 min procedure optimized allowed for the recovery of more than 90% of the molybdenum from the tantalum backing. The efficiency resulted slightly temperature and solvent flow dependent.

Furthermore, the automation of the separation and purification procedure with an IBA Synthera® extension customizable module was a key point for applying the already proven Tc-99m cyclotron-production process to different types and sizes of commercial cyclotrons, such as the IBA Cyclone® 18 cyclotron. The procedure based on ChemMatrix and ion exchange resins have been automatized by means of two Synthera® Extension module connected in series. Moreover, a peristaltic pump has also been included as auxiliary component of the module in order to minimize the molybdenum cross-contamination, due to the syringe pump multi-operation, and to make the starting solution transfer as consistent as possible.

In about 80 min the module was able to obtain more than 98% of the starting Tc-99m activity and less than 0.5 ppm of molybdenum contamination have been found in the product.

The two automatic separation module of Tc-99m that I have developed, in the framework of TECHN-OSP and during my experience at TRIUMF, are comparable in efficiency and product quality.

As regard COME projects, we have set ourselves the aim to define the best production route of ^{67}Cu working on unknown cross-section measurement of nuclear reactions on a Zn-70 target (35-70MeV energy range), hopefully finding a way to make this radionuclide available in larger amount for therapeutic and/or theranostics application in nuclear medicine.

Essential for this project was the development and optimization of a high yield separation and purification procedure of Cu-67 from the Zn-70 bulk and the co-produced Ga-67 contaminants that, having the same γ-lines of Cu-67 (both decay to Zn-67 with similar half-lives), poses a serious issue for the determination of the activity of the final ^{67}Cu. Cross-section analysis are still under elaboration while preliminary separation and recovery yield results have demonstrated the high efficiency of the optimized procedure.

Finally, in the framework of a cyclotron production study of the PET radiometal Ga-68 under investigation at TRIUMF starting from a zinc liquid target, I optimized an already existing ion exchange based separation and purification procedure of Ga-68 from Zn and Fe contaminants in order to obtain a final product suitable for medical use and to enable radiolabeling and in-vivo imaging studies with cyclotron produced ^{68}Ga-DOTATOC. A semi-automatic module was also developed to minimize the operator radiation exposure during experiments and the reproducibility of the results. The combination of three resins, AG50W-X8, LN, DGA and the semi-automated procedure resulted in a high pure cyclotron-produced Ga-68 allowing successful radiolabeling of DOTATOC, with high radiochemical yield. Comparative radiolabeling, imaging and biodistribution studies have also been conducted between generator-^{68}Ga and liquid target cyclotron-produced ^{68}Ga labelled DOTATOC demonstrating the equivalence in image quality and biodistribution profile.

More projects are actually underway in the framework of LARAMED and the involvement of the target processing after irradiation is always required:

- PASTA project, Production with Accelerator of Sc-47 for Theranostic Applications (started in 2016): Sc-47 cyclotron production studies based on the investigation of ^{48}Ti(p,2p)^{47}Sc and ^{50}Ti(p,x)^{47}Sc nuclear reactions.
- METRICS project, Multimodal pET/mRi Imaging with Cyclotron-produced 52/51Mn (β+emitter/paramagnetic) iSotopes (approved in 2017): Mn-52

cyclotron production studies by $^{Nat}Cr(p,xn)^{52}Mn$ reactions. This radiometal is particularly important in nuclear medicine for its application in multimodality PET/MRI imaging.

- TERABIO premium-project (2017-2019): based on the study and development of high power targets for the production of medical radionuclides by cyclotron.

The approval and financing of all these new projects underline the importance and interest of the scientific world in the radiometals cyclotron-production for medicine. In this context LARAMED will be an at vanguard laboratory for the study and production of medical radionuclides by cyclotron, and the target processing after the irradiation will always be the link between physics studies and medical applications making the so far produced radionuclides suitable for injection in patients.

Bibliography

Ambrosini, V., Campana, D. & Bodei, L., 2010. Ga-68-DOTA-NOC PET/CT clinical impact in patients with neuroendocrine tumors. *J Nucl Med,* Volume 51, pp. 669-673.

Antunes, P., Ginj, M. & Zhang, H., 2007. Are radiogallium labeled DOTA-conjugated somatostatin analogs superior to those labeled with other radiometals?. *Eur J Nucl Med Mol Imaging,* Volume 34, pp. 982-993.

ARRONAX, s.d. [Online]
Available at: http://www.cyclotron-nantes.fr/spip.php?rubrique84
[Consultato il giorno 27 11 2017].

Banerjee, S. & Pomper, M., 2013. Clinical Applications of Gallium-68. *Appl Radiat Isot,* Volume 0, p. 2–13.

Baum, R. P. & Rösch, F., 2012. *Theranostics, Gallium-68, and Other Radionuclides: A Pathway to Personalized Diagnosis and Treatment.* s.l.:Springer Science & Business Media.

Beaver, J. E. & Hupf, H. B., 1971. Production of Tc-99m on a medicalcyclotron: a feasibility study. *J Nucl Med,* Volume 12, p. 739–741.

Benard, F., Buckley, K. R. & Ruth, T. J., 2014a. Implementation of multi-curie production of Tc-99m by conventional medical cyclotrons. *J Nucl Med,* Volume 55, p. 1017–1022.

Benard, F. et al., 2014b. Cross-Linked Polyethylene Clycol Beads to Separate 99mTc-Pertechnetate from Low-Specific-Acitvity Molybdenum. *J Nucl Med,* Volume 55, pp. 1910-1914.

Boschi, A. et al., 2012. Rhenium(V) and technetium(V) nitrido complexes with mixed tridentate p-donor and monodentate p-acceptor ligands. *Inorg Chem ,* Volume 51, p. 3130–3137.

Boschi, A., Martini, P., Pasquali, M. & Uccelli, L., 2017. Recent achievements in Tc-99m radiopharmaceutical direct production by medical cyclotrons. *Drug Development and Industrial Pharmacy,* p. DOI:10.1080/03639045.2017.1323911.

Boschi, A. et al., 2013. Mixed tridentate p-donor and monodentate p-acceptor ligands as chelating systems for rhenium-188 and technetium-99m nitride radiopharmaceuticals. *Curr Radiopharm,* Volume 6.

Boyd, R., 1987. Technetium Generators: Status and Prospects. *Radiochim Acta,* Volume 41, p. 59−64.

Bushburg, J., 2002. *The Essential Physics of Medical Imaging.* s.l.:Lippincott Williams & Wilkins.

Celler, A., Hou, X., Benard, F. & Ruth, T., 2011. Theoretical modeling of yields for protoninduced reactions on natural and enriched molybdenum targets. *Phys Med Biol ,* Volume 56, p. 5469–84.

Chattopadhyay, S. et al., 2012. A computerized compact module for separation of Tc-99m radionuclide from molybdenum. *Appl Radiat Isot ,* Volume 70, pp. 2631-2637.

Chattopadhyay, S., Das, S. & Das, M. K., 2008. Recovery of 99mTc from Na2[99Mo]MoO4 solution obtained from reactor-produced (n,gamma)Mo-99 using a tiny Dowex-1 column in tandem with a small alumina column. *Appl Radiat Isot,* Volume 66, p. 1814–1817.

Chattopadhyay, S., Das, S. S. & Barua, L., 2010. A simple and rapid technique for recovery of Tc-99m from low specific activity (n,γ)Mo-99 based on solvent extraction and column chromatography. *Appl Radiat Isot,* Volume 68, p. 1−4.

Cicoria, G., Corazza, A. & Zagni, F., 2016. Preliminary assessment of radionuclidic purity of cyclotron produced Tc-99m. *Physica Medica,* Volume 32, p. 102.

Cutler, C. S. et al., 2013. Radiometals for Combined Imaging and Therapy. Chemical Review. *Nuclear Chemistry,* Volume 113, p. 858−883.

Dallali, N. et al., 2007. Liquid-liquid extraction of ultra trace amounts of technetium produced by Mo-100(p, 2n)Tc-99m nuclear reaction in cyclotron.. *Indian J Chem,* Volume 46A, p. 1615−1617.

Dash, A., Knapp, F. J. & Pillai, M. R. A., 2013. Mo-99/Tc-99m separation: An assessment of technology options. *Nuclear Medicine and Bology,* Volume 40, p. 167–176.

Das, M. K., Das, S. S. & Madhusmita, 2016a. Separation of Mo from Nb, Zr and Y: applicability in the purification of the recovered enriched Mo-100 used in the direct production of Tc-99m in cyclotrons. *J Radioanal Nucl Chem,* Volume 311, p. 643–647.

Das, M. K., Madhusmita & Chattopadhyay, S., 2016b. Production and separation of Tc-99m from cyclotron irradiated Mo-100/natural targets: a new automated module for separation of Tc-99m from molybdenum targets. *J Radioanal Nucl Chem,* Volume 310, p. 423–432.

Degrado, T. et al., 2011. A solution target approach for cyclotron production of 89Zr: understanding and coping in-target electrolysis. *J Label Compd ,* Volume 54, p. S248.

Del Guerra, A., 2006. Performance evaluation of the fully engineered YAP-(S)PETscanner for small animal imaging.. *IEEE Transactions on Nuclear Science,* 53(3), pp. 1078-1083.

Dougherty, G., 2009. *Digital Image Processing for Medical Applications.* s.l.:Cambridge University Press, ISBN 978-0-521-86085-7.

Duchemin, C. et al., 2015. Production of medical isotopes from a thorium target irradiated by light charged particles up to 70 MeV. *Phys Med Biol,* Volume 60, p. 931–946.

Eckelman, W. C., 2009. Unparalleled Contribution of Technetium-99m to Medicine Over 5 Decades. *JACC: Cardiovascular Imaging,* 2(3).

Esposito, E., Boschi, A. & Ravani, L., 2015. Biodistribution of nanostructured lipid carriers: A tomographic study. *Eur J Pharm Biopharm,* Volume 89, p. 145–156.

Esposito, J., 2011. *APOTEMA project proposal.* Legnaro, Padova: LNL-INFN.

Esposito, J. et al., 2013. Evaluation of Mo-99 and Tc-99m Productions Based on a High-Performance Cyclotron. *Sci Technol Nucl Ins,* pp. 1-14.

EudraLex, 2015. *EudraLex - Volume 4 - Good Manufacturing Practice (GMP) guidelines.* [Online]
Available at: https://ec.europa.eu/health/documents/eudralex/vol-4_en
[Consultato il giorno 26 01 2018].

EXFOR database , 2017. *Experimental Nuclear Reaction Data (EXFOR).* [Online]
Available at: http://www.nndc.bnl.gov/exfor/exfor.htm.
[Consultato il giorno 28 11 2017].

Gagnon, K. et al., 2017. *Cyclotron production and automated new 2-column processingof [Ga-68]GaCl3,* Vienna: EANM 2017.

Gagnon, K., Wilson, J. S. & Holt, C. M. B., 2012. Cyclotron production of Tc-99m: recycling of enriched Mo-100 metal targets. *Appl Radiat Isot,* Volume 70, p. 1685–1690.

Graves, A. et al., 2015 . Novel Preparation Methods of 52Mn for ImmunoPET Imaging. *Bioconjugate Chem,* 26 (10), p. 2118–2124.

Guérin, B., Tremblay, S. & Rodrigue, S., 2010. Cyclotron production of Tc-99m: an approach to the medical isotope crisis. *J Nucl Med,* Volume 51, p. 13N–16N.

Haddad, F. et al., 2008. ARRONAX, a high-energy and high-intensity cyclotron for nuclear medicine. *European Journal of Nuclear Medicine and Molecular Imaging,* Volume 35, pp. 1377-1387.

Hanemaayer, V., Benard, F. & Buckley, K. R., 2014. Solid targets for Tc-99m production on medical cyclotrons. *J Radioanal Nucl Chem,* Volume 299, p. 1007–1011.

Hanemaayer, V., Benard, F. & R., B. K., 2014. Solid targets for Tc-99m production on medical cyclotrons. *J Radioanal Nucl Chem,* Volume 299, p. 1007–1011.

Hoehr, C. et al., 2017. Medical isotope production at TRIUMF – from imaging to treatment. *Physics Procedia Conference on the Application of Accelerators in Research and Industry, CAARI 2016, 30 October– 4 November 2016, Ft. Worth, TX, USA,* Volume 90 , p. 200 – 208.

Hoehr, C. et al., 2012. Radiometals from liquid targets: Tc-94m production using a standard water target on a 13 MeV cyclotron. *Appl Radiat Isot ,* Volume 70, p. 2308–12.

Hoehr, C. et al., 2014 . Sc-44g production using a water target on a 13 MeV cyclotron. *Nuclear Medicine and Biology ,* Volume 41 , p. 401–406 .

Hofmann, M., Maecke, H. & Borner, A., 2001. Biokinetics and imaging with the somatostatinreceptor PET radioligand Ga-68-DOTATOC: preliminary data. *Eur J Nucl Med Mol Imaging,* Volume 28, pp. 1751-1757.

Horwitz, E. P., McAlister, D. R., Bond, A. H. & Barrans, R. E., 2005. Novel extraction of chromatographic resins based on tetraalkyldiglycolamides: Characterization and potential applications. *Solvent Extr Ion Exc ,* Volume 23, pp. 319-44.

Hou, X., Celler, A. & Grimes, J., 2012. Theoretical dosimetry estimations for radioisotopes produced by proton-induced reactions on natural and enriched molybdenum targets. *Phys Med Biol,* Volume 57, p. 1499–1515.

Hou, X., Tanguay, J. & Buckley, K. R., 2016 a. Molybdenum target specifications for cyclotron production of Tc-99m based on patient dose estimates. *Phys Med Biol,* Volume 61, p. 542–553.

Hou, X. et al., 2016 b. Imaging study of using radiopharmaceuticals labeled with cyclotron-produced Tc-99m. *Phys Med Biol,* Volume 61, p. 8199–8213.

Huclier-Markai, S., Sabatie, A. & Kubicek, V., 2011. Chemical and biological evaluation of scandium (III)-polyamino-polycarboxylate complexes as potential PET agent and radiopharmaceutical. *Radiochim Acta ,* Volume 99, p. 653–662.

IAEA, 2003. *Manual for Reactor Produced Radioisotopes.* Vienna : IAEA-TECDOC-1340.

IAEA, 2004. *Development of Generator Technologies for Therapeutic Radionuclides, Rep. Research Coordination Meeting (333-F2-RC-958).* Vienna, IAEA.

IAEA, 2007a. *Trends in Radiopharmaceuticals (ISTR-2005). Proceedings of an International Symposium. Vol. 1:14–18.* Vienna, IAEA.

IAEA, 2007b. *IAEA, International Atomic Energy Agency. Monitor Reactions.* [Online]
Available at: https://www-nds.iaea.org/medical/monitor_reactions.html.
[Consultato il giorno 28 11 2017].

IAEA, 2008a. *Cyclotron produced radionuclides: Principles and Practice,* Vienna, Austria: IAEA Technical Reports Series No. 465.

IAEA, 2008b. *Emerging isotopes: Recommended cross sections for Zn-70(p,a)Cu-67 reaction.* [Online]
Available at: https://www-nds.iaea.org/radionuclides/zn067cu0.html
[Consultato il giorno 28 11 2017].

IAEA, 2009a. *Cyclotron Produced Radionuclides: Physical Characteristics and Production Methods,* Vienna, Austria: IAEA Technical Report No. 468.

IAEA, 2009b. *Directory of Cyclotrons used for Radionuclide Production in Member States 2006 Update,* Vienna, Austria: IAEA Technical Report IAEA-DCRP/2006.

IAEA, 2009c. No. 6. Quality Assurance for SPECT Systems. In: *IAEA Human Health Series.* Vienna: IAEA.

IAEA, 2010. *Production and Supply of Molybdenum-99 - NTR2010 Supplement.* Vienna, 54th IAEA General Conference (2010) Documents.

IAEA, 2015. *Therapeutic Radiopharmaceuticals Labelled with New Emerging Radionuclides (Cu-67, Re-186, Sc-47) Coordinated Research Project open for proposals.* [Online]
Available at: http://cra.iaea.org/cra/stories/2015-09-30-F22053-New_Emerging_Radionuclides.html
[Consultato il giorno 27 11 2017].

ISOFLEX, 2015. *Stable isotopes of molybdenum available from ISOFLEX. San Francisco (CA).* [Online]
Available at: http://www.isoflex.com/molybdenum-mo
[Consultato il giorno 27 11 2017].

Jauw, Y. et al., 2016. Immuno-Positron Emission Tomography with Zirconium-89-Labeled Monoclonal Antibodies in Oncology: What Can We Learn from Initial Clinical Trials?. *Front Pharmacol,* Volume 7, p. 131.

Kar, B. B., Datta, P. & Misra, V. N., 2004. Spent catalyst: secondary source for molybdenum recovery. *Hydrometall,* Volume 72, p. 87–92.

Kastleiner, S., Coenen, H. H. & M., Q. S., 1999. Possibility of production of 67-Cu at a small-sized cyclotron via the (p,α) reaction on enriched 70-Zn. *Radiochimica Acta,* Volume 84, p. 107.

Kesch, C. et al., 2018. Ga-68 or F-18 for Prostate Cancer Imaging?. *J Nucl Med,* Volume DOI: 10.2967/jnumed.117.190157.

Knapp, F. F. j. et al., 1999. Production of Medical Radioisotopes in the ORNL High Flux Isotope Reactor (HFIR) for Cancer Treatment and Arterial Restenosis Therapy after PTCA. *Czech J Physics,* 49(Suppl.S1).

Knapp, F. F. j., Mirzadeh, S. & Beets, A. L., 1996. Reactor Production and Processing of Therapeutic Radioisotopes for Applications in Nuclear Medicine. *J Radioanalyt Nucl Chem Lett,* Volume 205, p. 93.

Knapp, F. F. j., Mirzadeh, S., Beets, A. L. & Du, M., 2005. Production of Therapeutic Radioisotopes in the ORNL High Flux Isotope Reactor for Applications in Nuclear Medicine, Oncology and Interventional Cardiology. *J Radioanalyt Nuc Chem,* Volume 263, p. 503.

Koning, A. J. & Rochman, D., 2012. Modern nuclear data evaluation with the TALYS code system. *Nuclear Data Sheets,* Volume 113, p. 2841.

Kovalsky, R. J. & Falen, S. W., 2004. Radiopharmaceuticals in Nuclear Pharmacy and Nuclear medicine. *Ed. Appleton and Lange.*

Levkovskij, V., 1991. *Cross sections of medium mass nuclide activation (A=40-100) by medium energy protons and alpha-particles (E=10-50 MeV.* Moscow : s.n.

Levkovskij, V. N., 1991. Middle mass nuclides (A=40+-100) Activation cross sections by medium energy (E=10+-50 MeV) protons and a-particles (experiment and systematics).. *Inter-Vesi, Moscow.*

LNL-INFN, SPES facility. *Galleria_Fotografie_Gli Accelleratori.* [Online] Available at: http://www.lnl.infn.it/index.php/it/2014-05-02-12-58-46/2014-05-14-08-51-28/gli-acceleratori
[Consultato il giorno 27 11 2017].

MacKee, G. M., 1921. *X-rays and Radium in the Treatment of Diseases of the Skin.* New York: Lea & Febiger.

Maggiore, M. et al., 2017. SPES: A new cyclotron-based facility for research and applications with high-intensity beams. *Modern Physics Letters A,* 32(17), p. 16.

Manenti, S. et al., 2014. The excitation functions of Mo-100(p,x)Mo-99 and Mo-100(p,2n)Tc-99m. *Appl Radiat Isot,* Volume 94, pp. 344-348.

Martini, P. et al., 2016. A solvent-extraction module for cyclotron production of high-purity technetium-99m. *Appl Radiat Isot,* Volume 118, p. 302–307.

Martini, P., Pupillo, G. & Boschi, A., 2015. *First Accelerator-Based Tc-99m GBq Production Levels and in-vivo Imaging Tests for APOTEMA Experiment,* Legnaro, Padova: INFN-LNL Annual Report 2014.

Matei, L., McRae, G. & Galea, R., 2014. *A new approach for manufacturing and processing targets used to produce Tc-99m with cyclotrons.* Prague, CZ, 15th Int. Workshop on Targetry and Target Chemistry WTTC15.

McCormick, G., Blosser, H., Cohen, B. & Newman, E., 1956. (p,He3) and (p,t) Cross-Section Measurements. *Journal of Inorganic and Nuclear Chemistry,* Volume 2, p. 269.

Meadows, J., 1953. Excitation Functions For Proton-Induced Reactions With Copper. *Physical Review,* Volume 91, p. 885.

Medvedev, D., F., M. L. & Srivastava, S. C., 2011. Irradiation of strontium chloride targets at proton energies above 35 MeV to produce PET radioisotope Y-86. *Radiochim Acta ,* Volume 99, p. 755–761 .

Medvedev, D. J., Mausner, L. F. & Meinken, G. E., 2012. Development of large scale production of Cu-67 from Zn-68 at the high energy accelerator: closing the Zn-68 cycle. *Int J Appl Radiat Isot,* Volume 70, p. 423–429.

Metello, L., 2015. 99mTc-tecnetium shortage: old problems asking for new solutions. *J Med Imag Radiat Sci,* Volume 46, p. 256–261.

Mikolajeszak, R. & Parus, J. L., 2005. Reactor Produced Beta-Emitting Nuclides for Nuclear Medicine. *World J Nucl Med,* Volume 4, p. 184.

Milton, B. F., 1996. *Commercial Compact Cyclotrons in the 90's.* s.l., 14th International Conference on Cyclotrons, World Scientific Pulblishing Co..

Mirzadeh, S., Mausner, L. F. & Garland, M., 2003. Reactor-Produced Medical Radioisotopes, Volume 4, Chapter 3. In: K. A. Publishers, a cura di *Handbook of Nuclear Chemistry.* Amsterdam: A. Vertes, N. S. Klencsar, p. 1– 46.

Morley, T. J. et al., 2012a. An automated module for the separation and purification of cyclotron-produced 99mTcO4-. *Nucl Med Biol,* Volume 39, pp. 551-559.

Morley, T. J., Penner, L. & Schaffer, P., 2012b. The deposition of smooth metallic molybdenum from aqueous electrolytes containing molybdate ions. *Electrochem Commun,* Volume 15, p. 78–80.

National Academies of Sciences, 2016. Chapter 3.3.1 Reactors shutdown. In: *Molybdenum-99 for medical imaging. Committee on State of Molybdenum-99 Production and Utilization and Progress Toward Eliminating Use of Highly Enriched Uranium.* Washington, DC: The National Academies Press, p. 74.

Noronha, O. P. D., 1986. Solvent extraction technology of Mo-99/Tc-99m generator system. An Indian experience: process design considerations. *Isotopenpraxis,* Volume 22, p. 53−57.

Novak, J. & Fajgelj, A., 1983. Tc-99m extraction generator. *Vestn Slov Kem Drus,* Volume 30, p. 1−7.

NuDat, 2.7. *NuDat 2.7 selected evaluated nuclear structure data Database at the US NNDC.* [Online]
Available at: http://www.nndc.bnl.gov/nudat2/
[Consultato il giorno 27 11 2017].

Oehlke, E. et al., 2015. Production of Y-86 and other radiometals for research purposes using a solution target system. *Nuclear Medicine and Biology,* 42(11), pp. 842-849.

Oehlke, E. et al., 2016. The role of additives in moderating the influence of Fe(III) and Cu(II) on the radiochemical yield of [Ga-68(DOTATATE)]. *Appl Radiat Isotopes ,* Volume 107, pp. 13-6.

Oehlke, E. et al., 2013. Influence of metal ions on the Ga-68-labeling of DOTATATE. *Appl Radiat Isotopes,* Volume 82:, pp. 232-8.

Osborne, J., 2016. *NRU Mo-99 Production. Presentation to Mo-99 2016 Topical Meeting.* s.l.:Atomic Energy of Canada Limited (AECL).

Pandey, M. et al., 2014 a. Production of 89Zr via the 89Y(p, n)89Zr reaction in aqueous solution: effect of solution composition on in-target chemistry. *Nucl Med Biol,* Volume 41, p. 309–16.

Pandey, M. K., Byrne, J. F., Jiang, H. P. A. B. & DeGrado, T. R., 2014 b. Cyclotron production of 68Ga via the Zn-68(p,n)Ga-68 reaction in aqueous solution. *Am J Nucl med mol imaging,* 4(4), pp. 303-310.

Pascali, C., Bogni, A., Crippa , F. & Bombardieri , E., 1999. *Concetti Generali sulla produzione di radiofarmaci emettitori di positroni.* Milano: Aretré.

Perkins, A. C. & Vivian, G., 2009. Molybdenum supplies and nuclear medicine services. *Nucl Med Commun,* 30(9), pp. 657-659.

Ph. Eur. , 2016a. Sodium pertechnetate (Tc-99m) injection (fission).. In: *European Pharmacopoeia 8.8.* s.l.:s.n., p. 1090.

Ph. Eur. , 2017. Sodium Pertechnetate (Tc-99m) injection (accelerator-produced). In: *European Pharmacopoeia 9.0.* s.l.:s.n., pp. 4801-4803.

Ph. Eur., 2016b. Sodium pertechnetate (Tc-99m) injection (non-fission). In: *European Pharmacopoeia 8.8.* s.l.:s.n., p. 1091.

Ph. Eur., 2016c. Residual solvents (5.4.). In: *European Pharmacopoeia 8.8.* s.l.:s.n., p. 5967.

Pillai, M., Dash , A. & Knapp , F. J., 2013. Sustained availability of 99mTc: possible paths forward. *J Nucl Med,* Volume 54, p. 313–323.

Proescher, F., 1913. The Intravenous Injection of Soluble Radium Salts in Man. *Radium ,* Volume 1, pp. 9-10.

PubMed, 2017. *US National Library of Medicine.* [Online] Available at: PubMed.gov [Consultato il giorno 27 11 2017].

Pupillo, G. et al., 2014. Experimental cross section evaluation for innovative Mo-99. *J Radioanal Nucl Chem,* Issue DOI 10.1007/s10967-014-3321-9..

Pupillo, G. et al., 2017. *COME – COpper MEasurement project,,* Legnaro, Padova: INFN-LN_ Annual eport 2016.

Pupillo, G. et al., 2018. New production cross sections for the theranostic radionuclide 67Cu. *Nuclear Inst and Methods in Physics Research B ,* Volume 415 , p. 41–47.

Pupillo, G., Zagni, F. & Corazza, A., 2016. *Imaging tests with accelerator-produced Tc-99m by conventional medical cyclotron,* Legnaro, Padova: INFN-LNL Annual Report 2015.

Qaim, S., 2001. Nuclear data for medical applications: an overview.. *Radiocimica Acta, 89,* pp. 189-196.

Qaim, S., 2012. The present and future of medical radionuclide production .. *Radiochimica Acta,* Volume 100, pp. 635-651.

Qaim, S., 2015. Nuclear data for medical radionuclides. *J Radioanal Nucl Chem,* Volume 305, p. 233–245.

Qaim, S. M., 2008. *Role of Radiochemistry in Nuclear Data Research and the Cyclotron Production of Medical Radionuclides.* Loughborough, UK: Lecture at the "Seminar on Production, Use and Disposal of Radioisotopes in Medicine" RSC's Radiochemistry Group .

Qaim, S. M., Tarkanyi, F. & Capote, R., 2011. *Nulcear data for the production of therapeutic radionuclides,* Vienna, Austria: IAEA.

RadDecay, 2005. *Radiation Decay V4 Database.* s.l.:s.n.

Rahmim, A. & Zaidai, H., 2008. PET versus SPECT: Strengths, Limitations and Challenges. *Nuclear Medicine Communications,* Volume 29, p. 193–207.

Roesch, F. & Filosofov, D., 2010. Production, radiochemical processing and quality evaluation of Ge-68. Chapter 2. In: *Production of long lived parent radionuclides for generators: Ge-68, Sr-82, Sr-90 and W-188.* Vienna: International Atomic Energy Agency (IAEA).

Roesch, F. & Knapp, F. j., 2003. Radionuclide Generators, Volume 4, Chapter 3. In: *Handbook of Nuclear Chemistry.* Amsterdam: A. Vertes, N.S. Klencsar, Publishers: Kluwer Academic, pp. 81-118.

Ruth, T., 2009. Accelerating production of medical radioisotopes. *Nature,* Volume 437, p. 536–537.

Ruth, T., 2014. The medical isotope crisis: how we got here and where we are going.. *J Nucl Med Technol,* Volume 42, p. 245–248.

Sampson, C. B., 1994 . *Textbook of Radiopharmacy: theory and practice.* s.l.:CRC Press.

Schaffer, P., Benard, F. & Bernstein, A., 2015b. Direct Production of Tc-99m via Mo-100(p,2n) on Small Medical Cyclotrons. *Phys Procedia,* Volume 66, p. 383–395.

Schaffer, P., Buckley, K. R. & Celler, A., 2015a. A tale of three targets: Direct, multi-Curie production of Tc-99m on three different cyclotrons. *J Nucl Med,* Volume 56, p. 164.

Schmor, P. W., 2010. *Review of cyclotrons used in the production of radioisotopes for biomedical applications, AAPS Inc., TRIUMF.* Lanzhou, China, Proceedings of CYCLOTRONS.

Scholten, B., Lambrecht, R. & Cogneau, M., 1999. Excitation functions for the cyclotron production of 99mTc and 99Mo. *App Radiat Isot,* Volume 51, p. 69–80.

Schwarzbach, R. et al., 1995. Development of a Simple and Selective Separation of Cu-67 from Irradiated Zinc for use in Antibody Labelling: A Comparison of Methods. *Appl Radiat Isot,* 46(5), pp. 329-336.

Selivanova, S. V., Lavallée, É. & Senta, H., 2015. Radioisotopic purity of sodium pertechnetate Tc-99m produced with a medium-energy cyclotron: implications for internal radiation dose, image quality, and release specidication. *J Nucl Med,* Volume 56, p. 1600–1680.

Selivanova, S. V. et al., 2017. Clinical trial using sodium pertechnetate Tc-99m produced with medium-energy cyclotron: biodistribution and safety assessment in patients with abnormal thyroid function. *J Nucl Med,* Volume 58, p. 791–798.

Siliari, M., 2010. *Radionuclide Production. African school of physics.* CERN, Ginevra: s.n.

Skuridin, V. S. & Chibisov, E. V., 2010. Development of a small-size extractor for separation of the Mo-99/Tc-99m couple. *Radiochemistry,* Volume 52, p. 90−94.

Smith, N. A., Bowers, D. L. & Ehst, D. A., 2012. The production, separation, and use of 67Cu for radioimmunotherapy: A review. *Appl Radiat Isot ,* Volume 70 , pp. 2377-2383.

Srivastava, S. C., 2010. Theragnostic radiometals: getting closer to personalized medicine. In: *Mazzi U et al. Technetium and other radiometals in chemistry and nuclear medicine.* Padova: SG Editoriali, p. 553–568.

Srivastava, S. C., 2011. Paving the way to personalized medicine: production of some theragnostic radionuclides at Brookhaven National Laboratory. *Radiochim Acta ,* Volume 99, p. 635–640.

Srivastava, S. C. & Mausner, L. F., 2013. Therapeutic radionuclides: production, physical characteristics and applications. In: *Therapeutic Nuclear Medicine, Medical Radiology. Radiation Oncology.* Verlag Berlin Heidelberg: R. P. Baum, Springer.

Tachimori, S., Amano, H. & Nakamura, H., 1971. Preparation of Tc-99m by direct adsorption from organic solution. *J Nucl Sci Technol,* Volume 8, p. 357−362.

Tarasov, B., 2003. PACE4 code. *Nucl Instrum Meth B,* Volume 204, pp. 174-178.

Taskaev, E., Taskaeva, M. & Nikolov, P., 1995. Extraction generator for [Tc-99m] sodium pertechnetate production. *Appl Radiat Isot,* Volume 46, p. 13−16.

TENDL, 2012. *TENDL-2012: TALYS-based evaluated nuclear data library.* [Online] Available at: ftp://ftp.nrg.eu/pub/www/talys/tendl2012/tendl2012.html [Consultato il giorno 27 11 2017].

Thomas, B., Wilson, J. & Gagnon, K., 2014. *Solid Mo-100 target preparation using cold rolling and diffusion bonding.* Prague, CZ, 15th Int. Workshop on Targetry and Target Chemistry WTTC15 .

TRIUMF, a. *TRIUMF Overview/Profile.* [Online] Available at: http://www.triumf.ca/home/about-triumf/about-us/overview-profile [Consultato il giorno 27 11 2017].

TRIUMF, b. *About CycloMed99.* [Online] Available at: http://www.triumf.ca/cyclomed99 [Consultato il giorno 27 11 2017].

TRIUMF, c. *Positron Emission Tomography.* [Online] Available at: http://www.triumf.ca/positron-emission-tomography [Consultato il giorno 27 11 2017].

TRIUMF, d. *Main Cyclotron and Beam Lines.* [Online] Available at: http://www.triumf.ca/research-program/research-facilities/main-cyclotron-beam-lines [Consultato il giorno 27 11 2017].

TRIUMF, e. *TRIUMF Maps.* [Online] Available at: http://www.triumf.ca/home/contact-us/maps-triumf [Consultato il giorno 27 11 2017].

TR-RCM2, I., 2013. *Report on the 2nd Research Coordination Meeting on Accelerator-based Alternatives to Non-HEU Production of Mo-99/Tc-99m,* Legnaro, Padova : IAEA.

Uccelli, L. et al., 2013. Influence of the Generator in-Growth Time on the Final Radiochemical Purity and Stability of Tc-99m Radiopharmaceuticals. *Sci Technol Nucl Ins,* pp. 1-7.

Uddin, S., Rumman-uz-Zaman, Hossain, S. M. & Qaim, S. M., 2014. Radiochemical measurement of neutron-spectrum averaged cross sections for the formation of Cu-64 and Cu-67 via the (n,p) reaction at a TRIGA Mark-Feasibility of simultaneous production of the theragnostic pair Cu-64/Cu-67.. *Radiochimica Acta,* 102(6), pp. 473-480.

van der Marck, S., Koning, A. & Charlton, K., 2010. The options for the future production of the medical isotope 99Mo. *Eur J Nucl Med Mol Imag,* Volume 37, p. 1817–1820.

Wild, D., Macke, H., Waser, B. & Reubi, J., 2005. Ga-68-DOTANOC: a first compound for PET imaging with high affinity for somatostatin receptor subtypes 2 and 5. *Eur J Nucl Med Mol Imaging,* Volume 32, pp. 724-724.

Yeong, C.-H., Cheng, M.-h. & NG, K.-H., 2014. Therapeutic radionuclides in nuclear medicine: current and future prospects. *Journal of Zhejiang University-SCIENCE B (Biomedicine & Biotechnology),* 15(10), pp. 845-863.

Zaitseva, N. G. & Dmitriev, S. N., 1999 . Radiochemical separation methods for preparation of biomedical cyclotron radionuclides. *Czechoslovak Journal of Physics,* 49(Suppl. S1).

Zeisler, S. K., Hanemaayer & Buckley, K. R., 2014. *High power Targets for Cyclotron Production of Tc-99m.* Prague, CZ, 15th Int. Workshop on Targetry and Target Chemistry WTTC15.

Zykov, M. P. et al., 2001. Use of extraction generator for preparing a Tc-99m radiopharmaceutical. *Radiochemistry,* Volume 43, p. 297−300.

Figure Captions

Dichiarazione di Conformità con Embargo

Sezioni

UNIVERSITÀ DEGLI STUDI DI FERRARA
· EX LABORE FRUCTUS ·

Dottorati di ricerca

Il tuo indirizzo e-mail

mrtptr1@unife.it

Oggetto:

Dichiarazione di conformità della tesi di Dottorato

Io sottoscritto Dott. (Cognome e Nome)

MARTINI PETRA

Nato a:

Zevio

Provincia:

Verona

Il giorno:

21 Dicembre 1988

Avendo frequentato il Dottorato di Ricerca in:

FISICA

Ciclo di Dottorato

30

Titolo della tesi:

High-Yield Cyclotron Production of Metallic Radioisotopes for Nuclear Medicine

Titolo della tesi (traduzione):

Produzione da Ciclotrone in Alta Resa di Radioisotopi Metallici per la Medicina Nucleare

Tutore: Prof. (Cognome e Nome)

Palmieri Vincenzo

Settore Scientifico Disciplinare (S.S.D.)

FIS/03

Parole chiave della tesi (max 10):

Radiometals, Cyclotron production, Tc-99m, Cu-67, Ga-68, Separation and Purification Techniques, Radiopharmaceuticals, Nuclear Medicine, Theranostic

Consapevole, dichiara

CONSAPEVOLE: (1) del fatto che in caso di dichiarazioni mendaci, oltre alle sanzioni previste dal codice penale e dalle Leggi speciali per l'ipotesi di falsità in atti ed uso di atti falsi, decade fin dall'inizio e senza necessità di alcuna formalità dai benefici conseguenti al provvedimento emanato sulla base di tali dichiarazioni; (2) dell'obbligo per l'Università di provvedere al deposito di legge delle tesi di dottorato al fine di assicurarne la conservazione e la consultabilità da parte di terzi; (3) della procedura adottata dall'Università di Ferrara ove si richiede che la tesi sia consegnata dal dottorando in 2 copie, di cui una in formato cartaceo e una in formato pdf non modificabile su idonei supporti (CD-ROM, DVD) secondo le istruzioni pubblicate sul sito: http://www.unife.it/studenti/dottorato alla voce ESAME FINALE – disposizioni e modulistica; (4) del

163

DICHIARO SOTTO LA MIA RESPONSABILITA': (1) che la copia della tesi depositata presso l'Università di Ferrara in formato cartaceo è del tutto identica a quella presentata in formato elettronico (CD-ROM, DVD), a quelle da inviare ai Commissari di esame finale e alla copia che produrrà in seduta d'esame finale. Di conseguenza va esclusa qualsiasi responsabilità dell'Ateneo stesso per quanto riguarda eventuali errori, imprecisioni o omissioni nei contenuti della tesi; (2) di prendere atto che la tesi in formato cartaceo è l'unica alla quale farà riferimento l'Università per rilasciare, a mia richiesta, la dichiarazione di conformità di eventuali copie. PER ACCETTAZIONE DI QUANTO SOPRA RIPORTATO

Dichiarazione per embargo

12 mesi

Richiesta motivata embargo

5. Tutela della proprietà intellettuale

Liberatoria consultazione dati Eprints

Consapevole del fatto che attraverso l'Archivio istituzionale ad accesso aperto "EPRINTS.unife.it" saranno comunque accessibili i metadati relativi alla tesi (titolo, autore, abstract, ecc.)

Firma del dottorando

Ferrara, li 06 Febbraio 2018 MARTINI PETRA Firma del Dottorando _____

Firma del Tutore

Visto: Il Tutore Prof. PALMIERI VINCENZO Si approva Firma del Tutore

164